Dual function of Langerhans cells in skin TSLP-promoted TFH differentiation in mouse atopic dermatitis

Pierre Marschall, Ruicheng Wei, Justine Segaud, Wenjin Yao, Pierre Hener, Beatriz Falcon German, Pierre Meyer, Cecile Hugel, Grace Ada da Silva, Reinhard Braun, et al.

Title:

Dual function of Langerhans cells in skin TSLP-promoted Tfh cell differentiation in mouse atopic dermatitis

Pierre Marschall, PhD,[a] Ruicheng Wei, PhD,[a]* Justine Segaud, MS,[a]* Wenjin Yao, PhD,[a] Pierre Hener, MS,[a] Beatriz Falcon German, MS,[a] Pierre Meyer, MS,[a] Cecile Hugel, MS,[a] Grace Ada Da Silva, PhD,[a] Reinhard Braun, MS,[b], Daniel H. Kaplan, MD, PhD,[c,d] and Mei Li, PhD [a]

[a] Institut de Génétique et de Biologie Moléculaire et Cellulaire, CNRS UMR 7104 - Inserm U 1258 – Université de Strasboug, Illkirch, France

[b] PANTEC Biosolutions AG, Ruggell, Liechtenstein

[c] Department of Dermatology and [d] Department of Immunology, University of Pittsburgh School of Medicine, Pittsburgh, Pennsylvania, USA.

*, equal contribution

Disclosure of potential conflict of interest: The authors declare that they have no relevant conflicts of interest.

Corresponding author

Mei Li

Institut de Génétique et de Biologie Moléculaire et Cellulaire, CNRS UMR 7104 - Inserm U 1258 – Université de Strasboug,

1 Rue Laurent Fries, 67404, Illkirch, France

Telephone: +33 3 88 65 35 71

Fax: +33 3 88 65 32 01

Email: mei@igbmc.fr

Key words: Atopic dermatitis; TSLP; Dendritic cells; Langerhans cells; Tfh; Th2; allergen sensitization; mouse

Abbreviations used:

AD: atopic dermatitis

BAL: Bronchoalveolar lavage

CT: Wild-type Control

DC: Dendritic cell

DEG: Differentially expressed genes

DT: Diphtheria toxin

DTR: Diphtheria toxin receptor

EDLN: Ear-draining lymph node

GC: Germinal center

H&E: Hematoxylin and eosin

IHC: Immunohistochemistry

Ig: Immunoglobulin

i.n.: Intranasal

i.p.: Intraperitoneal

LC: Langerhans cell

LMP: laser-assisted skin microporation

LN: Lymph node

NT: Non-treated

PAS: Periodic Acid Schiff

PCA: Principle component analysis

Tfh: T follicular helper

Th2: T helper type 2

ELISA: Enzyme-linked immunosorbent assay

TS: Tape stripping

TSLP: Thymic stromal lymphopoietin

Key messages:

- TSLP is critically involved in mounting Tfh/GC response in mouse AD driven by MC903 or OVA-sensitization.
- LCs promote Tfh/GC response in MC903-induced AD.
- LCs suppress Tfh/GC response and Th2 skin inflammation in OVA sensitization-induced AD.

Abstract

Background: Atopic dermatitis (AD) is one of the most common chronic inflammatory skin diseases, usually occurring early in life, and often preceding other atopic diseases like asthma. Th2 cell has been believed to play a crucial role in cellular and humoral response in AD, but accumulating evidences have shown that T follicular helper (Tfh) cell, a critical player in humoral immunity, is associated with disease severity and plays an important role in AD pathogenesis.

Objectives: We aimed at investigating how Tfh cells are generated during the pathogenesis of AD, particularly what is the role of keratinocyte-derived cytokine TSLP and Langerhans cells (LCs).

Methods: We employed two experimental AD mouse models, triggered by the overproduction of TSLP through topical application of MC903, or induced by epicutaneous allergen ovalbumin (OVA) sensitization.

Results: We demonstrated that the development of Tfh cells and GC response were crucially dependent on TSLP in MC903 model and OVA sensitization model. Moreover, we found that LCs promoted Tfh cell differentiation and GC response in MC903 model, and the depletion of Langerin$^+$ DCs or selective depletion of LCs diminished the Tfh/GC response. By contrast, in the model with OVA sensitization, LCs inhibited Tfh/GC response and suppressed Th2 skin inflammation and the subsequent asthma. Transcriptomic analysis of Langerin$^+$ and Langerin$^-$ migratory DCs revealed that Langerin$^+$ DCs became activated in MC903 model, whereas these cells remained inactivated in OVA sensitization model.

Conclusion: Together, these studies revealed a dual functionality of LCs in TSLP-promoted Tfh and Th2 cell differentiation in AD pathogenesis.

Capsule Summary

This study demonstrates that keratinocyte-derived cytokine TSLP plays a critical role in promoting not only Th2 but also Tfh/GC response in the pathogenesis of atopic dermatitis, which implicates a dual function of epidermal Langerhans cells.

Introduction

Atopic dermatitis (AD) is one of the most common chronic inflammatory skin diseases which affects up to 20% of children and 3% of adults worldwide, with increasing prevalence in the industrialized countries during the last 30 years [1]. AD is characterized by chronic cutaneous inflammation, T helper type 2 (Th2) response and hyper immunoglobulin IgE. Patients suffering from AD often present genetic risk factors in the form of mutations affecting the skin barrier structure or the immune system [2]. Onset of AD usually occurs early in life and may lead to allergen sensitization, which can trigger the progression from AD to other atopic diseases such as asthma/allergic rhinitis, in a process called "atopic march" [3, 4].

It has been recognized that Th2 cell response is critically implicated in the pathogenesis of AD. Previous studies from us and others using mouse models have established a central role of the cytokine thymic stromal lymphopoietin (TSLP) expressed by epidermal keratinocytes in promoting Th2 cell response and driving the pathogenesis of AD [5-8]. In addition to Th2 cell response, humoral immune response is another key feature of AD, with increased serum IgE and IgG1 levels associated with AD, which contribute to AD pathology and the atopic march [9, 10]. For a long time, Th2 cell has been believed to play a crucial role both in cellular response and humoral response, e.g. helping B cells to produce Igs. However, such knowledge has been challenged with the identification of T follicular helper (Tfh) cell, which emerges to be a critical player in humoral immunity and T cell memory [11].

In lymphoid organs, Tfh cell differentiation process is believed to begin with an initial dendritic cell (DC) priming of naive $CD4^+$ T cells, which undergo a cell-fate decision with the acquisition of master transcription factor Bcl6 expression and chemokine receptor CXCR5 expressed on cell surface to become early Tfh cells, of which CXCR5 promotes their migration

126 from T cell zone to the B cell follicles [12, 13]. The full differentiation and maintenance of Tfh
127 cells implicate the Tfh cell-B cell interaction, leading to GC Tfh cells which are phenotypically
128 defined by their high expression of CXCR5 and PD-1 [14]. It has been shown that Tfh cells
129 coordinate generation of the GC, initiate help for antigen-specific B cells, and promote selection
130 of high-affinity B cells and differentiation into either memory B cells or long-lived plasma cells
131 [15]. Recent studies have identified Tfh cells as an important source of IL-4, a master regulator in
132 type 2 immunity which was previously thought to be produced by Th2 cells, for providing
133 critical B-cell help by its anti-apoptotic and IgE and IgG1 class switch effects [16]. In addition, it
134 was reported that Tfh cells produce IL-4 in a GATA3-independent manner [17], suggesting
135 distinct mechanisms employed by Tfh and Th2 cells in the regulation of IL-4.

136 Since their initial identification, the biological functions of Tfh cells and their mechanisms
137 of action in the onset and development of diseases have been studied in autoimmuity, infectious
138 diseases, immunodeficiencies and vaccination [18]. Less is known on Tfh cells in the context of
139 AD and other atopic diseases, but more and more evidences have suggested that Tfh cells are
140 associated with disease severity and Tfh cells play an important role in the pathogenesis [19-21].
141 In human, alteration of circulating Tfh cells is correlated with severity of the disease in children
142 with AD [22], or with the comorbid association of allergic rhinitis with asthma [23], and allergen-
143 specific T follicular helper cell counts are correlated with specific IgE levels and efficacy of
144 allergen immunotherapy [24]. In mice, it has been reported that Tfh cells are important for house
145 dust mite-induced asthma [25] or peanut allergy [26].

146 Despite of these accumulating evidences showing the importance of Tfh cells in atopic
147 diseases, how Tfh cells and humoral responses are generated and regulated in AD remained to
148 be investigated. In this study, by employing two experimental AD mouse models, one triggered
149 by the overexpression of TSLP in mouse skin through topical application of MC903 [6, 7, 27], and
150 the other one induced by epicutaneous allergen ovalbumin (OVA) sensitization, we

151 demonstrated that skin TSLP plays a crucial role in driving/promoting Tfh cell differentiation
152 and GC response, in addition to its recognized role in promoting Th2 cell response. Moreover,
153 we investigated the role of skin DCs in mediating the Tfh cell differentiation. We uncovered a
154 dual functionality of epidermal langerhans cells (LCs) in TSLP-promoted Tfh/Th2 cell
155 differentiation in AD pathogenesis, and further explored the molecular insights by
156 transcriptomic analyses, thus shedding new light onto the long-standing controversy of LCs in
157 skin immunity.
158

Methods

Details on the methods used in this study are described in the Methods section in this article's Online Repository, including Experimental mice; MC903 topical application; Epicutaneous OVA sensitization and airway challenge; Depletion of Langerin$^+$ DCs or LCs in mice; Cell preparation for flow cytometry analyses; Surface staining for flow cytometry analyses; LN cell culture and antigen stimulation; RNA sequencing; BAL cell analyses; ELISA; Histopathology; IHC staining; RNA in situ hybridization and Statistics.

Results

Topical MC903 treatment induces TSLP-dependent Tfh cell differentiation and GC response

We have previously reported that topical treatment with MC903, a low calcemic analog of vitamin D3, induces the overproduction of TSLP (TSLP^{over}) and the pathogenesis of AD [6, 7]. To examine the Tfh cell differentiation and GC response in MC903-induced AD model, Balb/c wildtype (WT) mouse ears were topically treated every other day from day (D) 0 to D10 with MC903 and ear-draining lymph nodes (EDLN) were analyzed at D0, D7 and D11 (**Fig 1A**). Results showed that the frequency and number of CXCR5$^+$ PD-1$^+$ Tfh cells were both increased in MC903-treated WT mice at D7 and further augmented at D11 (**Fig 1B**). We next examined the expression of IL-4, a key signal provided by Tfh cells to sustain B cell maturation, by taking use of *Il4*/*Il13* dual reporter 4C13R$^{Tg/0}$ mice, in which AmCyan and dsRed are expressed under the control of IL-4 and IL-13 regulatory elements, respectively [28]. In agreement with a previous report [29], CXCR5$^+$ PD-1$^+$ Tfh cells in EDLNs express IL-4 (AmCyan) but not IL-13 (dsRed) (**Fig E1A**), and the IL-4 expression by Tfh cells was augmented in MC903-treated 4C13R$^{Tg/0}$ mice at both D7 and D11 (**Fig 1C**).

Together, MC903 treatment induces not only Tfh cell differentiation but also the production of IL-4 by Tfh cells.

To examine whether the induction of Tfh cells in MC903 model is triggered by TSLP, mice lacking TSLP (*Tslp*$^{-/-}$) [6] were subjected to MC903 treatment. Results showed that these mice exhibited highly diminished Tfh cell frequency and number at D7 and D11, compared to WT mice (**Fig 1B**). By breeding *Tslp*$^{-/-}$ with 4C13R$^{Tg/0}$ to generate *Tslp*$^{-/-}$/4C13R$^{Tg/0}$ mice, we showed that MC903-induced IL-4 expression in Tfh cells was abrogated in the absence of TSLP (**Fig 1C**). In agreement with the recognized role of TSLP in Th2 cell differentiation, we showed that the MC903-induced IL-4- or IL-13-expressing CXCR5^{-} CD4^{+} non-Tfh cells (representing Th2 cells) were also abrogated in *Tslp*$^{-/-}$ mice (**Fig E1B**). These results indicate that the overproduction of TSLP triggers not only Th2 cell differentiation, but also Tfh cell differentiation and IL-4 expression by these cells.

Next, we examined the GC response in MC903-treated Balb/c WT mice. The number of GC B cells, identified as GL-7^{+} CD95^{+} B cells, exhibited an increase in MC903-treated WT mice at D11, but not at D7 (**Fig 1D**). Such increase was abrogated in MC903-treated *Tslp*$^{-/-}$ mice (**Fig 1D**). This was confirmed by immunofluorescence (IF) staining for GCs (**Fig E2A**). In addition, both IgG1^{+} and IgE^{+} B cells exhibited an increase in their numbers in MC903-treated WT mice at D11, which was also abrogated in MC903-treated *Tslp*$^{-/-}$ mice (**Fig 1E**). Of note, we observed that most of the IgG1^{+} B cells were GL-7^{+} CD95^{+} (**Fig E1C**), suggesting that these cells harbor a GC phenotype; however, this was not the case for IgE^{+} B cells (**Fig E1C**).

Taken together, these data indicate that the overproduction of TSLP triggers Tfh cell differentiation and GC response.

Depletion of Langerin$^+$ DCs or LCs diminishes the TSLP^{over}-triggered Tfh/GC response

LCs reside in the epidermis as a dense network of immune system sentinels, in close proximity to keratinocytes. We then asked whether LCs mediate the TSLP^{over}-triggered Tfh/GC response. To this aim, we first employed Langerin-DTR knock-in mice (Lang^{DTR}) in which Langerin$^+$ cells, including LCs and Langerin$^+$ dermal DCs, express the human diphtheria toxin receptor (DTR) and can thus be depleted upon injection of diphtheria toxin (DT) [30]. Lang^{DTR} mice and their wildtype control littermates were intraperitoneally (*i.p.*) injected with DT at D-2, D0 and every 4 days to maintain the depletion of Langerin$^+$ cells (named Lang^{DEP} and CT respectively), and were subjected to topical MC903 treatment (**Fig 2A**). Results showed that the TSLP^{over}-triggered Tfh cell differentiation was largely diminished in Lang^{DEP} mice (**Fig 2B**). The expression of IL-4 (AmCyan) by Tfh cells was also reduced in Lang^{DEP}/4C13R$^{Tg/0}$ mice (**Fig 2C**). Accordingly, GC B cell number was lower and IgG1$^+$ (however not in IgE$^+$) B cell number was significantly decreased (**Fig 2D**). Therefore, these results indicate that Langerin$^+$ DCs play an important role in mediating the TSLP^{over}-induced Tfh/GC response.

As LCs and Langerin$^+$ cDC1s were both depleted in Lang^{DEP} mice, we next examined whether LCs mediate Tfh cell differentiation by depleting selectively LCs using two strategies: one took use of the differential recovery time between LCs and Langerin$^+$ cDC1s after DT-induced depletion as previously reported [31] (**Fig E3A-B**), and the other one employed human Langerin-DTR (huLang^{DTR}) mice in which DT injection efficiently depletes LCs but not Langerin$^+$ cDC1s [32] (**Fig E3C-D**). In both cases, we showed that the selective depletion of LCs led to a decrease in frequency and number of Tfh cells, suggesting an important role for LCs in TSLP^{over}-triggered Tfh cell differentiation.

Epicutaneous OVA sensitization induces a TSLP-dependent Tfh cell differentiation and GC response

We have previously reported that TSLP plays a crucial role for promoting skin sensitization to allergens, using an experimental mouse protocol in which OVA sensitization through tape-stripped (TS) skin leads to an allergic AD inflammation, accompanied by Th2 cell response, and an increased production of OVA-specific IgG1 and IgE in sera [33]. Here, we developed a novel experimental protocol, in which Precise Laser Epidermal System (P.L.E.A.S.E.®) [34] was used to disrupt skin barrier and to generate patterned micropores in mouse skin. This protocol allowed us to deliver allergens to micropores at precise depths of the epidermis, thereby achieving a higher efficiency and reproducibility of allergen sensitization through the skin compared with experiments based on TS. We showed that micropores at a depth of 30μm (30μm-LMP) on Balb/c WT mouse ears reached basal layer of ear epidermis (**Fig 3A**). ELISA analyses indicated that the protein level of TSLP increased at 48 hours after treatment (**Fig 3B**), in agreement with the previous studies showing that barrier disruption induces TSLP production in mouse [33] and human skin [35]. Notably, such level of TSLP was comparable to our previously reported TSLP level in TS skin [33], although it was much lower compared to that of MC903-treated skin (**Fig 3B; see also Fig E13B**). The administration of OVA did not further induce the TSLP level (**Fig 3B**). *In situ* hybridization showed that TSLP RNA expression was restricted to epidermal keratinocytes in LMP skin (**Fig 3C**).

As expected, OVA treatment on LMP ears (named "LMP/OVA"; **Fig 3D**) induced a Th2-type skin inflammation in TSLP-dependent manner, showing that OVA sensitization-induced infiltration of eosinophils and basophils (**Fig E4A-B**), Th2 cytokines (IL-4 and IL-13) expression by T cells in the skin (**Fig E4C**) and by $CXCR5^{-}CD4^{+}$ cells in EDLNs (**Fig E4D**), were all abolished in mice lacking TSLP. Examination of EDLNs revealed that both

frequency and number of Tfh cells were increased in LMP/OVA- compared to LMP/PBS-treated WT mice, and such increase was largely diminished in *Tslp*$^{-/-}$ mice (**Fig 3E**). Note that LMP/PBS was not sufficient to induce Tfh cell differentiation (despite of the induction of TSLP), but LMP plus OVA together promoted Tfh/GC response which was TSLP-dependent (**Fig 3E**). Moreover, IL-4 production by Tfh cells was augmented in LMP/OVA-treated *Tslp*$^{+/+}$/4C13R$^{Tg/0}$ mice but not *Tslp*$^{-/-}$/4C13R$^{Tg/0}$ mice (**Fig 3F**). GC B cell number analyzed by flow cytometry (**Fig 3G**) and GC size analyzed by immunofluorescence (**Fig E2B**) both showed an increase in LMP/OVA-treated WT mice, and this increase was abrogated in the absence of TSLP. IgG1$^+$ and IgE$^+$ B cell numbers were also increased in LMP/OVA-treated WT mice, and they were much lower in LMP/OVA-treated *Tslp*$^{-/-}$ mice (**Fig 3G**). Accordingly, serum levels of OVA-IgG1 and OVA-IgE were decreased in *Tslp*$^{-/-}$ mice compared to WT mice upon LMP/OVA treatment (**Fig 3H**). Together, these results demonstrate that TSLP is crucially required for epicutaneous OVA sensitization-induced Th2 and Tfh/GC responses.

Depletion of Langerin$^+$ DCs or LCs augments the Tfh/GC response induced by epicutaneous OVA sensitization

Based on the above data from MC903-induced AD, we had expected that Langerin$^+$ DCs would be crucially required for epicutaneous OVA-induced Tfh/GC response. To our surprise, when subjected to 30μm-LMP/OVA sensitization (**Fig 4A**), Lang^{DEP} mice did not exhibit a reduction in frequency and number of CXCR5$^+$ PD-1$^+$ Tfh cells, instead they tended to be higher compared to CT mice (**Fig 4B**). More strikingly, IL-4 expression by Tfh cells was higher in EDLN from LMP/OVA-treated Lang^{DEP}/4C13R$^{Tg/0}$ mice (**Fig 4C**). Accordingly, the GC B cell, IgG1$^+$ and IgE$^+$ B cell number were not reduced in LMP/OVA-treated Lang^{DEP} mice (**Fig 4D**), and serum OVA-specific IgE and OVA-specific IgG1 were

283 higher or tended to be higher (**Fig 4E**). Thus, in contrast to our expectation, Langerin^{+} DCs
284 are not required for the Tfh/GC response in LMP/OVA-induced AD model; instead, they
285 appear to play a counteracting role.

286 Because LCs are located on the suprabasal layer of the epidermis, we suspected that
287 Langerin^{+} cells would be only required in Tfh cell differentiation when allergens are
288 encountered superficially on the skin. To test this possibility, LMP was performed at the
289 depth of 11 μm, which disrupted only the cornified layer of the epidermis (**Fig 5A**). We
290 observed that the 11μm-LMP induced also the production of TSLP, even though its level
291 was lower compared to 30μm-LMP (**Fig 5B**). Treatment of wildtype control (CT) ears with
292 11μm-LMP/OVA induced significant increases (although milder than 30μm-LMP/OVA) in
293 Tfh cell frequency as well as GC B cell number, which were all abolished in *Tslp*$^{-/-}$ mice
294 (**Fig 5C**), indicating that, despite of a low induction of TSLP, the Tfh/GC response promoted
295 by 11μm-LMP/OVA is still crucially dependent on TSLP. However, when Lang^{DEP} mice
296 were subjected to 11μm-LMP/OVA treatment, they exhibited a significant increase in the
297 frequency of Tfh cells, in IL-4 expression by Tfh cells, as well as in GC B cell, IgG1^{+} and
298 IgE^{+} B cell numbers in EDLNs (**Fig 5D-F**), accompanied by augmented serum levels of
299 OVA-IgG1 and OVA-IgE (**Fig 5G**). Similar results were also obtained with huLang^{DEP} mice
300 (**Fig 5H-I**), indicating that LCs significantly counteract the Tfh/GC response induced upon
301 the 11μm-LMP/OVA sensitization.

302 Furthermore, we sought to compare antigen-specific Tfh cells between CT and
303 huLang^{DEP} mice using an activation-induced marker assay [36]. In this assay, the stimulation
304 of LN suspensions with specific antigen drives upregulation of CD154 (CD40L), CD25 and
305 OX40 on Tfh cells, providing a sensitive method for quantifying antigen-specific Tfh cells
306 in mice [36]. We showed that *in vitro* stimulation with OVA drove the upregulation of CD154,
307 OX40 and CD25 in EDLN-derived Tfh cells from LMP/OVA-sensitized CT mice; and such

upregulation was significantly higher in Tfh cells from LMP/OVA-sensitized huLang^{DEP} mice (**Fig 5J**), thus indicating a stronger OVA-specific Tfh cell differentiation in huLang^{DEP} mice upon OVA sensitization.

Together, these data indicate that LCs suppress the TSLP-dependent Tfh/GC response in epicutaneous OVA sensitization model.

Langerin$^+$ DCs or LCs limit epicutaneous OVA-induced Th2 skin inflammation and the subsequent asthma

Having observed the opposite role of Langerin$^+$ DCs or LCs in Tfh/GC response in the two mouse AD models, we further explored their involvement in the induction of Th2 cell response. Upon MC903 treatment, Lang^{DEP}/4C13R$^{Tg/0}$ mice exhibited a slight decrease in IL-4 and a tendency of decrease in IL-13 production by CXCR5$^-$CD4$^+$ cells in EDLN (**Fig E5A**), or by TCRβ$^+$ cells in dermis (**Fig E5B**), which suggests a role, even though minor, for Langerin$^+$ DCs in the development of Th2 cell response. In contrast, upon 30μm-LMP/OVA treatment, Lang^{DEP}/4C13R$^{Tg/0}$ mice exhibited a higher Th2 cell response in both skin (**Fig 6A**) and EDLN (**Fig E6**). This was in accordance with the observation that LMP/OVA-sensitized Lang^{DEP} mice exhibited a stronger skin inflammation (**Fig 6B**), accompanied with an increase in eosinophils and basophils (**Fig 6C**). Moreover, when subjected to 11μm-LMP/OVA sensitization, both Lang^{DEP} and huLang^{DEP} mice exhibited an enhanced AD-like skin inflammation compared to CT mice (**Fig E7**). Therefore, contrary to their minor role in promoting Th2 cell response in MC903-AD, LCs suppress the Th2 cell response in OVA-AD.

We further examined whether Langerin$^+$ DCs limit the atopic march. Upon *intranasal* (*i.n.*) OVA challenge following epicutaneous allergen sensitization (**Fig 6D**), the Lang^{DEP} mice developed a much stronger asthmatic inflammation compared with CT mice, exhibiting

an increase in the number of eosinophils in bronchoalveolar lavage fluid (BAL) (**Fig 6E**), and in RNA expression of Th2 cytokines IL-4, IL-5 and IL-13, as well as chemokine receptor CCR3 (eosinophils) and MCPT8 (basophils) by BAL cells (**Fig 6F**). In addition, H&E staining of lung sections of OVA-treated $Lang^{DEP}$ mice revealed an increased peribronchial and perivascular infiltration, and PAS staining showed an enhanced goblet cells hyperplasia (**Fig 6G**). Similar results were obtained with $huLang^{DEP}$ mice (**Fig E8 A-F**), indicating that LCs counteract the asthma development following epicutaneous allergen sensitization. To exclude the possibility that the enhanced asthmatic inflammation is due to any depletion of lung DCs during the intranasal challenge, we subjected $huLang^{DEP}$ mice to *i.p.* sensitization with OVA/alum and *i.n.* OVA challenge, and observed that these mice developed similar asthmatic inflammation as wildtype control mice (**Fig E8 G-H**). This suggests that the limitation of asthma inflammation by LCs is indeed due to their role in suppressing the epicutaneous allergen sensitization.

Taken together, these studies reveal opposite roles of LCs in two AD models: in MC903-AD, LCs play an important role in priming Tfh/GC response; they participate but to a lesser extend in promoting Th2 responses. In OVA-AD, LCs are neither required for Tfh/GC nor Th2 responses, instead, they suppress OVA-induced Tfh/GC and Th2 responses as well as the "atopic march".

Langerin$^+$ migratory DCs from MC903-AD but not from OVA-AD mice present profound transcriptomic changes

We next conducted transcriptomic studies to explore molecular insights underlying the opposite roles of Langerin$^+$ DCs in Tfh and Th2 cell differentiation in MC903-AD and OVA-AD, by taking use of $Lang^{GFP}$ mouse line in which GFP reports the expression of Langerin [30]. $Lang^{GFP}$ mice were treated with MC903 (at D0, D2 and D4) or LMP/OVA (at D0 and

D3), and at D5, Langerin^{+} (GFP^{pos}) and Langerin^{-} (GFP^{neg}) migratory DCs (migDCs) were sorted from EDLNs of non-treated (NT), MC903- or LMP/OVA-treated mice, and proceeded to mRNA sequencing (**Fig E9A**). The time point at D5 was selected to compare gene expression patterns of migDCs at the initiation stage of Tfh and Th2 cell differentiation.

Principle component analysis (PCA) for the RNAseq data revealed that the Pos_MC (GFP^{pos} migDCs from MC903-treated Lang^{GFP} mice) was clearly separated from the Pos_NT (GFP^{pos} migDCs from non-treated Lang^{GFP} mice); however, the Pos_OVA (GFP^{pos} migDCs from LMP/OVA-treated Lang^{GFP} mice) was inseparable from the Pos_NT (**Fig 7A**). Correspondingly, analyses of differentially expressed genes (DEGs) in Pos_MC vs Pos_NT identified 756 upregulated and 559 downregulated genes (with a fold change >1.5 and adjusted $p<0.05$; **Fig 7B**); in a sharp contrast, the comparison of Pos_OVA vs Pos_NT revealed only 39 upregulated and 9 downregulated genes (**Fig 7B**). Therefore, in MC903-AD, Langerin^{+} migDCs undergo profound transcriptomic changes, but in OVA-AD, they present almost no, or very little, transcriptomic changes.

As to Langerin^{-} migDCs, PCA showed that Neg_MC (GFP^{neg} migDCs from MC903-treated Lang^{GFP} mice), Neg_OVA (GFP^{neg} migDCs from LMP/OVA-treated Lang^{GFP} mice) and Neg_NT (GFP^{neg} migDCs from non-treated Lang^{GFP} mice) were all clustered away from each other (**Fig 7A**). Analyses of DEGs identified 710 upregulated and 698 downregulated genes for Neg_MC vs Neg_NT; and 431 upregulated and 427 downregulated genes for Neg_OVA vs Neg_NT (**Fig 7B**), suggesting that Langerin^{-} migDCs present major transcriptomic changes in both MC903-AD and OVA-AD, with considerable numbers of overlapped DEGs (249 upregulated and 215 downregulated).

Gene ontology analyses of DEGs in Langerin^{+} migDCs from MC903-treated mice

Next, using the upregulated or downregulated DEGs identified in Pos_MC (vs Pos_NT) as input, we performed cluster analyses of all the groups and generated heat map to visualize trends of expression for genes across the different groups. Results are presented in **Fig E9B** and **Fig E10A**. Further, we performed gene ontology (GO) analyses of the upregulated genes in Pos_MC (**Fig 7C**), and examined whether these genes were also significantly upregulated in Neg_MC (vs Neg_NT), and Neg_OVA (vs Neg_NT). We paid particular attention to the upregulated genes shared in all the three groups (Pos_MC, Neg_MC and Neg_OVA), standing here for "commonly upregulated" genes (highlighted in red in **Fig 7C**), as they could be implicated in TSLP-promoted Tfh and/or Th2, a common feature shared by MC903-AD and OVA-AD. Among them, we found genes related to: 1) "regulation of cell migration", many of which were reported to facilitate DC migration (*Mmp14* [37]; *Stat5* [38]; Nrp2 [39]*; Sema7a* [40]); 2) "T cell costimulation": *Cd80* and *Cd86* [41], *IL2ra* [42], *Pdcd1lg2* (PD-L2)[43], *Cd274* (PD-L1*), Gpr183* (EBI2)[44, 45]; 3) "cytokine signal": *Il2ra*, *Tnfrsf11b* and *Ccl22*; and 4) "transcription factors" such as *Ikzf4, Irf4, Stat4 and Stat5a*.

We examined TSLP signaling pathway among the upregulated genes in Pos_MC. Using the reported TSLP-regulated gene set [46], we identified *Cd84, Cd82, Ccl17, Ccl22 and Tnfrsf11b* (in the cluster with higher expression in Pos_MC than Neg_MC), as well as *Cish, Cd86, Cd80, Cd274, Il2ra, Il6, ccr2, Tgfb1* (in the cluster with higher expression in Neg_MC than Pos_MC) (**Fig 7D**). In addition, we identified *Irf4*, which has been recently shown to be downstream of TSLP signaling in human migratory LCs [47]. The upregulation of these TSLP-targeting genes by Langerin$^+$ migDCs suggests that these cells could be a direct responder to TSLP signaling, although it remains to be demonstrated that TSLP signals through its receptor on LCs drive their migration/activation. Besides these known TSLP downstream genes, more TSLP pathway genes identified from those "commonly upregulated" genes can be envisaged.

406 Interestingly, we did not find *Tnfsf4* (encoding OX40L) among the DEGs in Pos_MC,
407 despite that OX40L was reported to be TSLP-responsive gene and mediate TSLP-promoted
408 Th2 [48] and Tfh [49] cell differentiation. Actually, OX40L expression by GFP^{pos} cells was barely
409 detected in Pos_NT, Pos_MC or Pos_OVA (**Fig 7E**). On the other hand, OX40L was expressed
410 in Neg_NT, and its expression was further upregulated in Neg_MC and Neg_OVA. Therefore,
411 it is unlikely that OX40L would be responsible for the Tfh-promoting function of $Langerin^{+}$
412 DCs, while its precise function as a potential TSLP downstream factor in $Langerin^{-}$ DCs
413 remains to be defined (**Fig 7E**).
414 Among the above-mentioned TSLP-regulated gene, IL-6 has been shown to be a critical
415 cytokine for Tfh cell differentiation [50, 51]. We thus tested whether IL-6 neutralization decreases
416 Tfh / GC response in MC903-AD. Results showed that IL-6 was not required for the initiation
417 of Tfh cell differentiation and the overall GC reaction (**Fig E11)**, although it is possible that its
418 function in Tfh response is redundant with other signals as suggested by Eto et al [52]. Besides
419 IL-6, several other Tfh-promoting factors derived from DCs have been recently reported,
420 including IRF-4[53], IL-2Ra[42, 54] and EBI2 (*Gpr183*) [44, 45], whose expression was all "commonly
421 upregulated" in Pos_MC, Neg_MC and Neg_OVA (**Fig 7D**). The role of these potential
422 candidates in TSLP-promoting Tfh cell differentiation remains to be examined.
423 Finally, among the downregulated genes (**Fig E10B**), less knowledge was available, but
424 we could see *Il12b* (IL-23/IL-12p40), whose expression in DCs was previously reported to be
425 suppressed by TSLP [55]. Other commonly downregulated ones included genes related "T cell
426 costimulation" *Havcr2* (TIM3), *Lgals8* (Galectin 8); "Regulation of cell migration" *Adam15*
427 and *Ptk2* (negative regulators for cell migration) and "regulation of transcription" *Foxc2, Thrb,*
428 *Tcf7l2, Ehf* and *Lmo2.*
429

Discussion

In this study, we analyzed how Tfh cells were generated in two experimental AD mouse models, triggered by the overproduction of TSLP by topical application of MC903, or induced by epicutaneous OVA sensitization. We demonstrated a crucial role for TSLP in promoting Tfh cells and GC response in MC903-AD as well as OVA-AD. Intriguingly, we revealed a dual function of LCs in TSLP-promoted Tfh/Th2 cell differentiation: while they promoted Tfh cell differentiation in MC903-AD, they inhibited Tfh/GC response and suppressed Th2 skin inflammation and the atopic march in OVA-AD. This is schematically illustrated in **Fig 8**, and is discussed below.

1) TSLP: critical player for Th2 and Tfh cell response in AD

It has been recognized that TSLP is overproduced in AD lesional skin [56], however, its expression varies from high to low, which could be related with the cause (e.g. genetic mutation of *Spink5* which induces a high level of TSLP [57] vs skin barrier impairment which induces a low level of TSLP [35]), age (e.g. TSLP serum level in AD children is high at early stage and decreases with age [58]), or the nature of disease (e.g. intrinsic or extrinsic AD). Our study demonstrates that no matter in AD models associated with either high or low TSLP expression, TSLP is crucial for promoting Tfh/GC response in AD. Recently, the link between TSLP and Tfh cell differentiation was suggested by the study with human blood DC-T cell coculture system [49]. Thus, the Tfh-promoting function of TSLP appears to be conserved between mouse and human, which suggests that it is relevant and valuable to employ AD mouse models to elucidate mechanisms underlying the TSLP (skin)-Tfh (draining LN) axis, particularly the access of tissue and lymphoid organs is rather limited in human study.

Our data add new evidence that neutralization of TSLP or blocking TSLP downstream pathway will be helpful for reducing Th2 and Tfh cell responses in AD. Notably, TSLP is crucial for driving the downstream IL-4/IL-13 expression by Th2 cells, as well as IL-4 expression by Tfh cells. Indeed, blocking antibody against IL-4/-13R (Dupilumab), which may actually target both Th2 and Tfh cell responses, has been shown to achieve significant therapeutic effect on AD [59]. Intriguingly, neutralization TSLP antibody Tezepelumab has been demonstrated to significantly reduce annual asthma exacerbation rate in patients with uncontrolled asthma [60]. A recent study with Tezepelumab showed numeric improvements in patients with moderate to severe AD, despite that there were certain limitations in that study including patient selection, use of topical corticosteroids, duration of treatment and uncertain inhibition of TSLP with the dose used [61]. Given the preclinical evidence for the role of TSLP in AD, more clinical studies are required to evaluate TSLP as therapeutic target in AD.

It should be also noted that recent studies have recognized the importance of Tfh cells in AD [19-21], but the *in vivo* function of Tfh remains to be further delineated using AD mouse models. This is challenged by the lack of appropriate tools to deplete Tfh cells. We are under the way to generate mouse line in which DTR can be selectively expressed in Tfh cells, thus allowing the DT-induced depletion of Tfh cells.

2) LCs: function as migratory DCs to promote Tfh cell differentiation

LCs represent one of the most studied but controversial DC subtypes. Our study shows that LCs are importantly engaged in the initiation Tfh cell differentiation and GC response triggered by $TSLP^{over}$ in MC903-AD. This provides new evidence on the Tfh-promoting function of LCs in AD, in addition to several studies reporting the requirement of LCs for humoral responses in other contexts [62,63,64]. In MC903-AD, we observed that LCs play a dominant role in Tfh cell differentiation, although dermal $langerin^-$ DCs may also contribute. On the other hand, $langerin^-$

DCs (cDC2) appear to be the major player for the TSLP^{over}-induced Th2, while LCs have somewhat but minor contribution. Nevertheless, to provide direct evidence for the contribution of cDC2 in TSLP-driven Tfh and Th2 responses in AD, further studies could be performed using DC-specific KO of IRF4 or Dock8 mice, which have impaired development and migration of CD11b^{+} cDC2 [65], or CD301b-DTR mice in which CD301b^{+} cDC2 can be transiently depleted [66].

There have been long debates on the migration, antigen uptake, and T cell differentiation of LCs in different contexts; but transcriptomic study on migratory LCs in skin-draining LNs under inflammatory pathological contexts was lacking. Our transcriptomic data are therefore of value; however, one drawback is that migratory LCs and cDC1 were not separated in Langerin^{+} (GFP^{pos}) migDCs, thus the gene expression data still need to be cautiously interpreted concerning LCs. Nevertheless, we have shown that Langerin^{+} migDCs in EDLN of MC903-induced TSLP^{over} mice presented substantial transcriptional changes, suggesting that the activation and migration of Langerin^{+} DC to the draining LNs underlie its function to prime Tfh cell differentiation in MC903-AD. Indeed, when comparing numbers of GFP^{pos} and GFP^{neg} migratory DCs in EDLN of MC903-treated Lang^{GFP} mice at D5, we observed that both were increased (**Fig E12**), supporting that both Langerin^{+} DCs and Langerin^{-} DCs migrate to draining LNs in MC903-AD.

3) LCs: function as non-migratory cells in the skin to suppress Tfh/Th2 response?

Our study revealed a suppressive role of LCs for epicutaneous OVA-induced Tfh and Th2 cell differentiation. This is in contrast with two previous studies which reported a role of LCs in provoking AD inflammation by using a tape stripping (TS) OVA sensitization model [67, 68]. To examine whether the discrepancy is due to the different effects of LMP compared to TS, we performed TS/OVA sensitization on mouse ears. Results showed that, similar to LMP/OVA,

TS/OVA-sensitized Lang^{DEP} mouse EDLNs exhibited increased frequency and number of Tfh cells, increased IL-4 expression by Tfh cells, higher numbers of GC B cells, IgG1$^+$ and IgE$^+$ B cells, with elevated OVA-IgG1 and OVA-IgE in sera (**Fig E13 A-G**). Moreover, when *i.n.* challenged with OVA, Lang^{DEP} mice developed a stronger asthmatic inflammation (**Fig E13 H-I**). Therefore, the discrepancy with the previous reports [67, 68] is not explained by the difference of LMP vs TS technique in epicutaneous OVA sensitization; rather, it could be due to other factors remained yet to be determined, such as the allergen application method: topical OVA vs long exposure (2-day) of OVA placed on patch-test tape; the difference of mouse background: Balb/c vs C57Bl/6; or the site of allergen application: ear vs back.

Why are LCs not implicated in the promotion of Tfh/Th2 cell differentiation in EDLN in this context? Transcriptomic analyses showed that in sharp contrast to MC903-AD, Langerin$^+$ migDCs in OVA-AD presented almost the same transcriptomic program as in untreated mice, suggesting an absence of migration/activation of these cells. Indeed, Langerin$^+$ migDC numbers in EDLNs from LMP/OVA-treated or TS/OVA-treated mice at D5 were nearly unchanged, whereas Langerin$^-$ migDC number was increased (**Fig E12**). This is in agreement with previous studies showing that when skin was treated with fluorescence-conjugated OVA [66], HDM [69], or Dextran [70], antigen uptake and transport to draining LNs were mainly exerted by Langerin$^-$ DCs. Of note, it was recently shown that LCs can transfer antigen to cDC2 in the context of Langerin mAb-mediated targeting [71]. It will be interesting to see whether this occurs in AD models, and whether efficiency of LC antigen transfer could be altered in the two models, as another possible explication of different implication of LCs in Tfh cell differentiation.

Then how do LCs exert their anti-Tfh/Th2 role in OVA-AD? A recent study showed that LCs played an immunosuppressive role when OVA was applied on the intact skin, in accompany with the induction of IL-10 in LCs in skin-draining LNs [72]. However, this does not seem to be our case, because Langerin$^+$ migDCs in EDLN did not exhibit any transcriptional

change of Treg-inducing signals including IL-10 and TGFβ, or RALDH2. More likely, the anti-Tfh/Th2 effect of LCs is related to their immune suppression function *in situ* in the skin, in keeping with LC ontogeny not only as DCs but also as non-migratory macrophages [73, 74]. It should be further studied how LCs exert such functionality, for example, by limiting the antigen-uptake by cDC2 in the skin, or by promoting local Tregs in OVA-sensitized skin [75 76]. Transcriptomic analysis of LCs isolated from the OVA-treated skin site may provide further molecular insights.

4) What signals switch the function of LCs?

One intriguing question is what microenvironment cues and molecular signals switch the function of LC between anti-Tfh/Th2 to pro-Tfh/Th2 in AD contexts. Notably, MC903-AD and OVA-AD exhibit similar AD phenotype which is TSLP-dependent, but the quantity of TSLP and the nature of antigen are different in these two models. In MC903-AD, MC903 induced a high production of TSLP [7] (**Fig 8**) which was sufficient to induce Tfh and Th2 cell differentiation. As there was no administration of experimental allergen, the nature of antigen implicated in T cell differentiation in MC903 model may involve endogenous antigens or microbiota co-existing in the skin. On the other hand, in OVA-AD, the disruption of skin barrier with LMP induced TSLP expression however to a much lower extent (**Fig 8**). It is possible that LCs sense the quantity of TSLP. Indeed, as a danger signal, TSLP may convert the function of LCs when its level is above certain threshold. *In vitro* studies have shown that TSLP triggers DC migration [77], or promotes the survival, maturation and migration of human LCs, and allogenic naïve $CD4^+$ T cells cocultured with TSLP-conditioned LCs produced cytokines IL-4 and IL-13 [78], but quantitative study on TSLP signaling has never been performed. It will be interesting to explore whether and how quantitative TSLP signaling determines the role of LCs, by conducting *in vivo* or *ex vivo* dose-dependent experiments. In addition, the nature and

quantity of antigens can be also involved in the functional switch of LCs. To unravel such complexity, the emerging mathematic modeling [79, 80] may eventually help to integrate multiple parameters for a better understanding of functional switch of LCs.

It will be interesting to further explore in AD patients whether and how TSLP levels are correlated with the states and function of LCs. A better understanding of what molecular switch determines the function of LCs either as "pro-Tfh/Th2" or as "anti-Tfh/Th2", and of how LCs exert such functions, will allow us to shape LCs to act in suppressing the skin inflammation, limiting the allergen sensitization through AD skin, thus preventing the progression from AD to asthma. On the other hand, the potential of LCs to induce Tfh cell differentiation and GC response and the subsequent induction of antigen-specific antibodies has been of interest for transcutaneous vaccination [63, 81]. Therefore, the knowledge we obtain from this study should be also insightful for LC-based skin vaccination, including the use of TSLP at an appropriate level as an effective adjuvant for promoting Tfh cell differentiation and humoral response.

Acknowledgement

We thank the staff of animal facilities, mouse supporting services, flow cytometry, histopathology, microscopy and imaging, and cell culture of IGBMC and Institut Clinique de la Souris (ICS) for excellent technical assistance. We are grateful for B. Malissen for providing $Lang^{DTR}$ and $Lang^{GFP}$ mice, and W. Paul for providing $4C13R^{Tg/0}$ mice. Sequencing was performed by the GenomEast platform, a member of the 'France Génomique' consortium (ANR-10-INBS-0009), and we would like to thank M. Cerciat for library preparation and sequencing, and M. Jung for generating the data. We thank J. Heller and J. Demenez for helping with genotyping and histology analyses. We would like to acknowledge the funding supports from l'Agence Nationale de la Recherche (ANR-17-CE14-0025; ANR-19-CE17-0017; ANR-19-CE17-0021) to ML, from Fondation Recherche Medicale (Equipes-FRM 2018) to ML, and the first joint programme of the Freiburg Institute for Advanced Studies (FRIAS) and the University of Strasbourg Institute for Advanced Study (USIAS) to ML. The study was also supported by the grant ANR-10-LABX-0030-INRT, a French State fund managed by the Agence Nationale de la Recherche under the frame program Investissements d'Avenir ANR-10-IDEX-0002-02; the Centre National de la Recherche Scientifique (CNRS); the Institut National de la Santé et de la Recherche Médicale (INSERM), and the Université de Strasbourg (Unistra). PM was supported by PhD fellowship from Region Alsace, RW and YW by PhD fellowships from the Association pour la Recherche à l'IGBMC (ARI), JS by a PhD fellowship from Equipes-FRM 2018.

References

1. Weidinger S, Novak N. Atopic dermatitis. Lancet 2016; 387:1109-22.
2. Boguniewicz M, Leung DY. Atopic dermatitis: a disease of altered skin barrier and immune dysregulation. Immunol Rev 2011; 242:233-46.
3. Dharmage SC, Lowe AJ, Matheson MC, Burgess JA, Allen KJ, Abramson MJ. Atopic dermatitis and the atopic march revisited. Allergy 2014; 69:17-27.
4. Shaker M. New insights into the allergic march. Curr Opin Pediatr 2014; 26:516-20.
5. Yoo J, Omori M, Gyarmati D, Zhou B, Aye T, Brewer A, et al. Spontaneous atopic dermatitis in mice expressing an inducible thymic stromal lymphopoietin transgene specifically in the skin. J Exp Med 2005; 202:541-9.
6. Li M, Hener P, Zhang Z, Ganti KP, Metzger D, Chambon P. Induction of thymic stromal lymphopoietin expression in keratinocytes is necessary for generating an atopic dermatitis upon application of the active vitamin D3 analogue MC903 on mouse skin. J Invest Dermatol 2009; 129:498-502.
7. Li M, Hener P, Zhang Z, Kato S, Metzger D, Chambon P. Topical vitamin D3 and low-calcemic analogs induce thymic stromal lymphopoietin in mouse keratinocytes and trigger an atopic dermatitis. Proc Natl Acad Sci U S A 2006; 103:11736-41.
8. Li M, Messaddeq N, Teletin M, Pasquali JL, Metzger D, Chambon P. Retinoid X receptor ablation in adult mouse keratinocytes generates an atopic dermatitis triggered by thymic stromal lymphopoietin. Proc Natl Acad Sci U S A 2005; 102:14795-800.
9. Chapman MD, Rowntree S, Mitchell EB, Di Prisco de Fuenmajor MC, Platts-Mills TA. Quantitative assessments of IgG and IgE antibodies to inhalant allergens in patients with atopic dermatitis. J Allergy Clin Immunol 1983; 72:27-33.
10. Werfel T, Allam JP, Biedermann T, Eyerich K, Gilles S, Guttman-Yassky E, et al. Cellular and molecular immunologic mechanisms in patients with atopic dermatitis. J Allergy Clin Immunol 2016; 138:336-49.
11. Crotty S. T Follicular Helper Cell Biology: A Decade of Discovery and Diseases. Immunity 2019; 50:1132-48.
12. Hardtke S, Ohl L, Forster R. Balanced expression of CXCR5 and CCR7 on follicular T helper cells determines their transient positioning to lymph node follicles and is essential for efficient B-cell help. Blood 2005; 106:1924-31.
13. Haynes NM, Allen CD, Lesley R, Ansel KM, Killeen N, Cyster JG. Role of CXCR5 and CCR7 in follicular Th cell positioning and appearance of a programmed cell death gene-1high germinal center-associated subpopulation. J Immunol 2007; 179:5099-108.
14. Qi H. T follicular helper cells in space-time. Nat Rev Immunol 2016; 16:612-25.
15. Victora GD, Nussenzweig MC. Germinal centers. Annu Rev Immunol 2012; 30:429-57.
16. Sahoo A, Wali S, Nurieva R. T helper 2 and T follicular helper cells: Regulation and function of interleukin-4. Cytokine Growth Factor Rev 2016; 30:29-37.
17. Vijayanand P, Seumois G, Simpson LJ, Abdul-Wajid S, Baumjohann D, Panduro M, et al. Interleukin-4 production by follicular helper T cells requires the conserved Il4 enhancer hypersensitivity site V. Immunity 2012; 36:175-87.
18. Ueno H, Banchereau J, Vinuesa CG. Pathophysiology of T follicular helper cells in humans and mice. Nat Immunol 2015; 16:142-52.
19. Varricchi G, Harker J, Borriello F, Marone G, Durham SR, Shamji MH. T follicular helper (Tfh) cells in normal immune responses and in allergic disorders. Allergy 2016; 71:1086-94.

20. Kemeny DM. The role of the T follicular helper cells in allergic disease. Cell Mol Immunol 2012; 9:386-9.
21. Qin L, Waseem TC, Sahoo A, Bieerkehazhi S, Zhou H, Galkina EV, et al. Insights Into the Molecular Mechanisms of T Follicular Helper-Mediated Immunity and Pathology. Front Immunol 2018; 9:1884.
22. Szabo K, Gaspar K, Dajnoki Z, Papp G, Fabos B, Szegedi A, et al. Expansion of circulating follicular T helper cells associates with disease severity in childhood atopic dermatitis. Immunol Lett 2017; 189:101-8.
23. Kamekura R, Shigehara K, Miyajima S, Jitsukawa S, Kawata K, Yamashita K, et al. Alteration of circulating type 2 follicular helper T cells and regulatory B cells underlies the comorbid association of allergic rhinitis with bronchial asthma. Clin Immunol 2015; 158:204-11.
24. Yao Y, Chen CL, Wang N, Wang ZC, Ma J, Zhu RF, et al. Correlation of allergen-specific T follicular helper cell counts with specific IgE levels and efficacy of allergen immunotherapy. J Allergy Clin Immunol 2018; 142:321-4 e10.
25. Ballesteros-Tato A, Randall TD, Lund FE, Spolski R, Leonard WJ, León B. T Follicular Helper Cell Plasticity Shapes Pathogenic T Helper 2 Cell-Mediated Immunity to Inhaled House Dust Mite. Immunity 2016; 44:259-73.
26. Dolence JJ, Kobayashi T, Iijima K, Krempski J, Drake LY, Dent AL, et al. Airway exposure initiates peanut allergy by involving the IL-1 pathway and T follicular helper cells in mice. J Allergy Clin Immunol 2018; 142:1144-58 e8.
27. Leyva-Castillo JM, Hener P, Michea P, Karasuyama H, Chan S, Soumelis V, et al. Skin thymic stromal lymphopoietin initiates Th2 responses through an orchestrated immune cascade. Nat Commun 2013; 4:2847.
28. Roediger B, Kyle R, Yip KH, Sumaria N, Guy TV, Kim BS, et al. Cutaneous immunosurveillance and regulation of inflammation by group 2 innate lymphoid cells. Nat Immunol 2013; 14:564-73.
29. Liang HE, Reinhardt RL, Bando JK, Sullivan BM, Ho IC, Locksley RM. Divergent expression patterns of IL-4 and IL-13 define unique functions in allergic immunity. Nat Immunol 2011; 13:58-66.
30. Kissenpfennig A, Henri S, Dubois B, Laplace-Builhe C, Perrin P, Romani N, et al. Dynamics and function of Langerhans cells in vivo: dermal dendritic cells colonize lymph node areas distinct from slower migrating Langerhans cells. Immunity 2005; 22:643-54.
31. Henri S, Poulin LF, Tamoutounour S, Ardouin L, Guilliams M, de Bovis B, et al. CD207+ CD103+ dermal dendritic cells cross-present keratinocyte-derived antigens irrespective of the presence of Langerhans cells. J Exp Med 2010; 207:189-206.
32. Bobr A, Olvera-Gomez I, Igyarto BZ, Haley KM, Hogquist KA, Kaplan DH. Acute ablation of Langerhans cells enhances skin immune responses. J Immunol 2010; 185:4724-8.
33. Leyva-Castillo JM, Hener P, Jiang H, Li M. TSLP produced by keratinocytes promotes allergen sensitization through skin and thereby triggers atopic march in mice. J Invest Dermatol 2013; 133:154-63.
34. Scheiblhofer S, Thalhamer J, Weiss R. Laser microporation of the skin: prospects for painless application of protective and therapeutic vaccines. Expert Opin Drug Deliv 2013; 10:761-73.

35. Angelova-Fischer I, Fernandez IM, Donnadieu M-H, Bulfone-Paus S, Zillikens D, Fischer TW, et al. Injury to the Stratum Corneum Induces In Vivo Expression of Human Thymic Stromal Lymphopoietin in the Epidermis. J Invest Dermatol 2010; 130:2505-7.
36. Jiang W, Wragg KM, Tan HX, Kelly HG, Wheatley AK, Kent SJ, et al. Identification of murine antigen-specific T follicular helper cells using an activation-induced marker assay. J Immunol Methods 2019; 467:48-57.
37. Gawden-Bone C, Zhou Z, King E, Prescott A, Watts C, Lucocq J. Dendritic cell podosomes are protrusive and invade the extracellular matrix using metalloproteinase MMP-14. J Cell Sci 2010; 123:1427-37.
38. Bell BD, Kitajima M, Larson RP, Stoklasek TA, Dang K, Sakamoto K, et al. The transcription factor STAT5 is critical in dendritic cells for the development of TH2 but not TH1 responses. Nat Immunol 2013; 14:364-71.
39. Roy S, Bag AK, Singh RK, Talmadge JE, Batra SK, Datta K. Multifaceted Role of Neuropilins in the Immune System: Potential Targets for Immunotherapy. Front Immunol 2017; 8:1228.
40. van Rijn A, Paulis L, te Riet J, Vasaturo A, Reinieren-Beeren I, van der Schaaf A, et al. Semaphorin 7A Promotes Chemokine-Driven Dendritic Cell Migration. J Immunol 2016; 196:459-68.
41. Watanabe M, Fujihara C, Radtke AJ, Chiang YJ, Bhatia S, Germain RN, et al. Co-stimulatory function in primary germinal center responses: CD40 and B7 are required on distinct antigen-presenting cells. J Exp Med 2017; 214:2795-810.
42. Li J, Lu E, Yi T, Cyster JG. EBI2 augments Tfh cell fate by promoting interaction with IL-2-quenching dendritic cells. Nature 2016; 533:110-4.
43. Gao Y, Nish SA, Jiang R, Hou L, Licona-Limon P, Weinstein JS, et al. Control of T helper 2 responses by transcription factor IRF4-dependent dendritic cells. Immunity 2013; 39:722-32.
44. Lu E, Cyster JG. G-protein coupled receptors and ligands that organize humoral immune responses. Immunol Rev 2019; 289:158-72.
45. Barington L, Wanke F, Niss Arfelt K, Holst PJ, Kurschus FC, Rosenkilde MM. EBI2 in splenic and local immune responses and in autoimmunity. J Leukoc Biol 2018; 104:313-22.
46. Zhong J, Sharma J, Raju R, Palapetta SM, Prasad TS, Huang TC, et al. TSLP signaling pathway map: a platform for analysis of TSLP-mediated signaling. Database (Oxford) 2014; 2014:bau007.
47. Polak ME, Ung CY, Masapust J, Freeman TC, Ardern-Jones MR. Petri Net computational modelling of Langerhans cell Interferon Regulatory Factor Network predicts their role in T cell activation. Sci Rep 2017; 7:668.
48. Ito T, Wang YH, Duramad O, Hori T, Delespesse GJ, Watanabe N, et al. TSLP-activated dendritic cells induce an inflammatory T helper type 2 cell response through OX40 ligand. J Exp Med 2005; 202:1213-23.
49. Pattarini L, Trichot C, Bogiatzi S, Grandclaudon M, Meller S, Keuylian Z, et al. TSLP-activated dendritic cells induce human T follicular helper cell differentiation through OX40-ligand. J Exp Med 2017; 214:1529-46.
50. Eddahri F, Denanglaire S, Bureau F, Spolski R, Leonard WJ, Leo O, et al. Interleukin-6/STAT3 signaling regulates the ability of naive T cells to acquire B-cell help capacities. Blood 2009; 113:2426-33.

51. Chakarov S, Fazilleau N. Monocyte-derived dendritic cells promote T follicular helper cell differentiation. EMBO Mol Med 2014; 6:590-603.
52. Eto D, Lao C, DiToro D, Barnett B, Escobar TC, Kageyama R, et al. IL-21 and IL-6 are critical for different aspects of B cell immunity and redundantly induce optimal follicular helper CD4 T cell (Tfh) differentiation. PLoS ONE 2011; 6:e17739.
53. Calabro S, Gallman A, Gowthaman U, Liu D, Chen P, Liu J, et al. Bridging channel dendritic cells induce immunity to transfused red blood cells. J Exp Med 2016; 213:887-96.
54. Ballesteros-Tato A, Leon B, Graf BA, Moquin A, Adams PS, Lund FE, et al. Interleukin-2 inhibits germinal center formation by limiting T follicular helper cell differentiation. Immunity 2012; 36:847-56.
55. Taylor BC, Zaph C, Troy AE, Du Y, Guild KJ, Comeau MR, et al. TSLP regulates intestinal immunity and inflammation in mouse models of helminth infection and colitis. J Exp Med 2009; 206:655-67.
56. Soumelis V, Reche PA, Kanzler H, Yuan W, Edward G, Homey B, et al. Human epithelial cells trigger dendritic cell mediated allergic inflammation by producing TSLP. Nat Immunol 2002; 3:673-80.
57. Briot A, Deraison C, Lacroix M, Bonnart C, Robin A, Besson C, et al. Kallikrein 5 induces atopic dermatitis-like lesions through PAR2-mediated thymic stromal lymphopoietin expression in Netherton syndrome. J Exp Med 2009; 206:1135-47.
58. Yao W, Zhang Y, Jabeen R, Nguyen ET, Wilkes DS, Tepper RS, et al. Interleukin-9 Is Required for Allergic Airway Inflammation Mediated by the Cytokine TSLP. Immunity 2013; 38:360-72.
59. Simpson EL, Akinlade B, Ardeleanu M. Two Phase 3 Trials of Dupilumab versus Placebo in Atopic Dermatitis. N Engl J Med 2017; 376:1090-1.
60. Corren J, Parnes JR, Wang L, Mo M, Roseti SL, Griffiths JM, et al. Tezepelumab in Adults with Uncontrolled Asthma. N Engl J Med 2017; 377:936-46.
61. Simpson EL, Parnes JR, She D, Crouch S, Rees W, Mo M, et al. Tezepelumab, an anti-thymic stromal lymphopoietin monoclonal antibody, in the treatment of moderate to severe atopic dermatitis: A randomized phase 2a clinical trial. J Am Acad Dermatol 2019; 80:1013-21.
62. Zimara N, Florian C, Schmid M, Malissen B, Kissenpfennig A, Mannel DN, et al. Langerhans cells promote early germinal center formation in response to Leishmania-derived cutaneous antigens. Eur J Immunol 2014; 44:2955-67.
63. Yao C, Zurawski SM, Jarrett ES, Chicoine B, Crabtree J, Peterson EJ, et al. Skin dendritic cells induce follicular helper T cells and protective humoral immune responses. J Allergy Clin Immunol 2015; 136:1387-97 e1-7.
64. Levin C, Bonduelle O, Nuttens C, Primard C, Verrier B, Boissonnas A, et al. Critical Role for Skin-Derived Migratory DCs and Langerhans Cells in TFH and GC Responses after Intradermal Immunization. The Journal of investigative dermatology 2017; 137:1905-13.
65. Krishnaswamy JK, Alsen S, Yrlid U, Eisenbarth SC, Williams A. Determination of T Follicular Helper Cell Fate by Dendritic Cells. Front Immunol 2018; 9:2169.
66. Kumamoto Y, Linehan M, Weinstein JS, Laidlaw BJ, Craft JE, Iwasaki A. CD301b^{+} dermal dendritic cells drive T helper 2 cell-mediated immunity. Immunity 2013; 39:733-43.

67. Kim TG, Kim M, Lee JJ, Kim SH, Je JH, Lee Y, et al. CCCTC-binding factor controls the homeostatic maintenance and migration of Langerhans cells. J Allergy Clin Immunol 2015; 136:713-24.
68. Nakajima S, Igyarto BZ, Honda T, Egawa G, Otsuka A, Hara-Chikuma M, et al. Langerhans cells are critical in epicutaneous sensitization with protein antigen via thymic stromal lymphopoietin receptor signaling. J Allergy Clin Immunol 2012; 129:1048-55 e6.
69. Deckers J, Sichien D, Plantinga M, Van Moorleghem J, Vanheerswynghels M, Hoste E, et al. Epicutaneous sensitization to house dust mite allergen requires interferon regulatory factor 4-dependent dermal dendritic cells. J Allergy Clin Immunol 2017; 140:1364-77 e2.
70. Weiss R, Hessenberger M, Kitzmuller S, Bach D, Weinberger EE, Krautgartner WD, et al. Transcutaneous vaccination via laser microporation. J Control Release 2012; 162:391-9.
71. Yao C, Kaplan DH. Langerhans Cells Transfer Targeted Antigen to Dermal Dendritic Cells and Acquire Major Histocompatibility Complex II In Vivo. J Invest Dermatol 2018; 138:1665-8.
72. Luo Y, Wang S, Liu X, Wen H, Li W, Yao X. Langerhans cells mediate the skin-induced tolerance to ovalbumin via Langerin in a murine model. Allergy 2019; 74:1738-47.
73. Kashem SW, Haniffa M, Kaplan DH. Antigen-Presenting Cells in the Skin. Annu Rev Immunol 2017; 35:469-99.
74. West HC, Bennett CL. Redefining the Role of Langerhans Cells As Immune Regulators within the Skin. Front Immunol 2017; 8:1941.
75. Seneschal J, Clark RA, Gehad A, Baecher-Allan CM, Kupper TS. Human epidermal Langerhans cells maintain immune homeostasis in skin by activating skin resident regulatory T cells. Immunity 2012; 36:873-84.
76. Kitashima DY, Kobayashi T, Woodring T, Idouchi K, Doebel T, Voisin B, et al. Langerhans Cells Prevent Autoimmunity via Expansion of Keratinocyte Antigen-Specific Regulatory T Cells. EBioMedicine 2018; 27:293-303.
77. Fernandez M-I, Heuzé ML, Martinez-Cingolani C, Volpe E, Donnadieu M-H, Piel M, et al. The human cytokine TSLP triggers a cell autonomous dendritic cell migration in confined environments. Blood 2011; 118:3862-9.
78. Ebner S, Nguyen VA, Forstner M, Wang YH, Wolfram D, Liu YJ, et al. Thymic stromal lymphopoietin converts human epidermal Langerhans cells into antigen presenting cells that induce pro-allergic T cells. J Allergy Clin Immunol 2007.
79. Altan-Bonnet G, Mukherjee R. Cytokine-mediated communication: a quantitative appraisal of immune complexity. Nat Rev Immunol 2019; 19:205-17.
80. Bagnall J, Boddington C, England H, Brignall R, Downton P, Alsoufi Z, et al. Quantitative analysis of competitive cytokine signaling predicts tissue thresholds for the propagation of macrophage activation. Sci Signal 2018; 11:eaaf3998.
81. Romani N, Flacher V, Tripp CH, Sparber F, Ebner S, Stoitzner P. Targeting skin dendritic cells to improve intradermal vaccination. Curr Top Microbiol Immunol 2012; 351:113-38.

Figure Legends

FIG 1. Overproduction of TSLP in the skin triggers Tfh differentiation and GC reponse in MC903-induced AD mice. **A,** Experimental protocol. Mouse ears were topically treated with MC903 or ethanol (EtOH; as vehicle control) every other day from day (D) 0 to D10 and EDLNs were analyzed at D0, D7 and 11. **B**, Frequency and number of $CXCR5^+$ $PD\text{-}1^+$ Tfh cells in EDLN from MC903-treated Balb/c wildtype (WT) and *Tslp*$^{-/-}$ mice. **C**, Frequency of IL-4 $(AmCyan)^+$ in Tfh cells and cell number of $IL\text{-}4^+$ Tfh cells in EDLNs. **D-E**, Number of $CD95^+$ $GL\text{-}7^+$ GC B cells, $IgG1^+$ B cells and IgE^+ B cells in EDLNs. Values shown are means ± SEMs. **B-D**, one-way ANOVA with Tukey's multiple comparison post-hoc test; **E**, unpaired t-test with Welch's correction. Data are representative of 3 independent experiments with similar results.

FIG 2. Depletion of $Langerin^+$ cells diminishes the MC903-induced Tfh/GC response. **A**, Experimental protocol. $Lang^{DTR}$ mice and wildtype littermate controls (CT) were *i.p*. injected with DT at D-2 and D0 and then every 4 days. Mouse ears were topically treated with MC903 or EtOH every other day from D0 to D10 and EDLNs were analyzed at D11. **B**, Frequency and number of Tfh cells. **C**, IL-4 (AmCyan) expression by Tfh cells. **D**, Total number of GC B cells, $IgG1^+$ and IgE^+ B cells. Values shown are means ± SEMs; one-way ANOVA with Tukey's multiple comparison post-hoc test. Data are representative of 3 independent experiments with similar results.

FIG 3. OVA sensitization through laser-microporated (LMP) skin induces TSLP-dependent Tfh/GC response. **A**, H&E staining of untreated or 30μm-LMP ears of Balb/c WT mice. The red arrow points to a micropore with the disruption of the epidermis. Scale bar, 100 μm. **B**, TSLP protein levels in ears of WT mice at 48h after the indicated treatment. **C**, RNAscope in

situ hybridization for TSLP in untreated or 30μm-LMP-ears at 48h after the microporation. The black arrow points to one of the positive signals. Scale bar, 50 μm. **D**, Experimental protocol for OVA epicutaneous sensitization through LMP ears. OVA or PBS (vehicle) were topically applied on LMP ears at D0, D4, D7 and D11 and EDLNs were analyzed at D13. **E-F**, Frequency and cell number of Tfh cells (**E**) and IL-4 (AmCyan) producing Tfh cells (**F**) in EDLNs. **G**, GC B cell, $IgG1^+$ and IgE^+ B cell numbers in EDLNs. **H**, Serum levels of OVA-IgG1 and OVA-IgE. Values shown are mean ± SEM; one-way ANOVA with Tukey's multiple comparison post-hoc test. Data are representative of 3 independent experiments with similar results.

FIG 4. Depletion of $Langerin^+$ cells does not reduce but rather tends to augment 30μm-LMP/OVA-induced Tfh/GC response. **A**, Experimental protocol. $Lang^{DTR}$ mice and wildtype littermate controls (CT) were *i.p.* injected with DT at D-2, D0 and then every 4 days. Mouse ears were treated by 30μm-LMP/OVA or 30μm-LMP/PBS at D0, D4, D7 and D11 and EDLNs were analyzed at D13. **B**, Frequency and number of Tfh cells. **C**, IL-4 (AmCyan) expression by Tfh cells. **D**, Number of GC B cells, $IgG1^+$ and IgE^+ B cells. **E**, Serum levels of OVA-specific IgG1 and OVA-specific IgE in 30μm-LMP/OVA-sensitized $Lang^{DEP}$ or CT mice. Data are means ± SEM; **B-D**, one-way ANOVA with Tukey's multiple comparison post-hoc test. **E**, unpaired t-test with Welch's correction. Data are representative of 3 independent experiments with similar results.

FIG 5. Depletion of $Langerin^+$ cells or LCs enhances 11μm-LMP/OVA-induced TSLP-dependent Tfh/GC response. **A**, H&E staining of untreated or 11μm-LMP ears of Balb/c WT mice. The red arrow points to a micropore with the impairment of cornified layer. Scale bar, 100 μm. **B**, TSLP protein levels in ears of WT mice. **C**, Comparison of Tfh cells and GC B cells in EDLNs from WT or $Tslp^{-/-}$ mice. **D-F**, Comparison of Tfh cells (**D**), IL-4 (AmCyan)

expression by Tfh cells (**E**) and number of GC B cells, IgG1$^+$ B cells and IgE$^+$ B cells (**F**) in EDLNs from CT or Lang^{DEP} mice. **G**, Serum OVA-IgG1 and OVA-IgE levels. **H**, Experimental protocol. **I**, Comparison of Tfh cells, GC B cells, IgG1$^+$ and IgE$^+$ B cells in CT and huLang^{DEP} mice. **J**, Comparison of antigen-specific Tfh cells between LMP/OVA-sensitized CT and huLang^{DEP} mice. EDLNs were *in vitro* stimulated with OVA or PBS (vehicle control), and activation markers CD154, CD25 and OX40 expressed by EDLN-derived Tfh cells were examined. Values shown are mean ± SEM; one-way ANOVA with Tukey's multiple comparison post-hoc test. Data are representative of 2 independent experiments with similar results.

FIG 6. Langerin$^+$ cells counteract LMP/OVA sensitization-induced skin Th2 inflammation and the subsequent asthmatic phenotype. **A**, IL-4 (AmCyan) and IL-13 (DsRed) expression in TCRβ$^+$ dermal cells. **B**, H&E staining of mouse ears. **C**, IHC staining of mouse ears with anti-MBP (for eosinophils) or anti-MCPT8 (for basophils). Arrows point to positive signals. **D**, Experimental protocol for OVA epicutaneous sensitization and airway challenge. Mice were *i.p.* injected with DT at D-2, D0 and then every 4 days. Mice were either treated with OVA on LMP ears at D0, D4, D7 and D11 or non-treated (NT). All mice were subjected to *i.n.* instillation with OVA from D9 to D12, and analyzed at D13. **E**, Differential cell counting for eosinophils (Eos), neutrophils (Neutro), lymphocytes (Lympho) and macrophages (Macro) in BAL. **F**, RNA levels of indicated genes in BAL cells by RT-qPCR. **G**, Lung sections were stained with H&E for histology or PAS for goblet cell hyperplasia analyses. B: bronchiole, V: blood vessel. Scale bar, 100μm. Values shown are means ± SEM; one-way ANOVA with Tukey's multiple comparison post-hoc test. Data are representative of 2 independent experiments with similar results.

FIG 7. Transcriptomic analyses of migratory DCs in EDLNs of $Lang^{GFP}$ mice upon MC903 treatment or epicutaneous OVA sensitization. $Lang^{GFP}$ mice were treated with MC903 at D0, D2 and D4 or 30μm-LMP/OVA on D0 and D3; EDLNs were collected at D5 for cell sorting and RNAseq analyses. **A**, Left, percentage of variability explained by each Principal Component. Right, principal component analyses showing PC1, PC2 and PC3. **B,** Venn diagram showing the number of upregulated and downregulated genes (fold change > 1.5; $p < 0.05$; raw read > 200 in at least one sample of all groups), and the number of commonly upregulated or downregulated genes between the comparisons, as indicated. Pos_NT, Pos_MC, Pos_OVA: GFP^{Pos} migDCs from non-treated, MC903-treated or LMP/OVA-treated $Lang^{GFP}$ mice; Neg_NT, Neg_MC, Neg_OVA: GFP^{neg} migDCs from non-treated, MC903-treated or LMP/OVA-treated $Lang^{GFP}$ mice. **C**, Selected genes corresponding to gene ontology terms. *, $p<0.05$; NS, non significant. **D**, Heatmaps of the reported TSLP pathway genes, which are significantly upregulated in Pos_MC vs Pos_NT. **E**, Heatmap of Tnfsf4 (encoding OX40L) from RNAseq data, and RT-qPCR analyses.

FIG 8. A schematic representation of the dual functions of LCs in regulating TSLP-dependent Tfh cell and Th2 cell response, revealed by two experimental AD mouse models, triggered by the overproduction of TSLP through topical application of MC903, or induced by epicutaneous allergen ovalbumin (OVA) sensitization.

Supplementary Figure Legends

FIG E1. **(A)** CXCR5^{+} PD-1^{+} Tfh cells produce IL-4 (AmCyan) but not IL-13 (dsRed) in EDLNs of MC903-treated 4C13R$^{Tg/0}$ mice at D11. 4C13R$^{0/0}$ EDLNs were used as gating control. **(B)** Frequency and number of CXCR5^{-} CD4^{+} (non-Tfh) cells producing IL-4 (AmCyan) or IL-13 (dsRed), representing Th2 cells, in EDLNs from Balb/c wildype (WT) and *Tslp*$^{-/-}$ mice in the background of 4C13R$^{Tg/0}$, treated with MC903 or ethanol, and analyzed at D0, D7 and D11. **(C)** The majority of IgG1^{+} but not IgE^{+} B cells in EDLNs from MC903-treated wildtype Balb/c mice are GL-7^{+} CD95^{+}.

FIG E2. Germinal center staining. Wildtype (WT) and *Tslp*$^{-/-}$ mice were treated with MC903 **(A)** or subjected to OVA-sensitization **(B)** as shown in FIG 1A and 4D respectively. EDLN were collected and fixed overnight with 4% PFA at 4°C. After 2 times 30 minutes of wash in PBS at room temperature (RT), samples were included in 4% low melting point agarose in PBS. Vibratome sections of 100µm were blocked with 5% normal donkey serum (NDS), 0.1% Triton X-100 in PBS and then stained overnight at 4°C with anti CD4-AlexaFluor 647 (RM4-5, Biolegend, d=1/100; shown in blue), anti IgD-FITC (11-26c.2a, BD Biosciences, d=1/50; shown in green) and biotinylated PNA (Vectorlabs, d=1/250; shown in red) diluted in 5% NDS, 0.1% Triton X-100 in PBS. Sections were subsequently incubated 1h at RT with Neutravidin-Dylight550 (ref 84606, Thermofisher, d=1/200) diluted in PBS. After 2 washing of 30 minutes with PBS at RT, sections were kept at 4°C in PBS containing Hoechst 33342 (Sigma Aldrich) and images were acquired using Leica LSI confocal macroscope. Measurements were performed with ImageJ software. Data are means ± SEM; one-way ANOVA with Tukey's multiple comparison post-hoc test.

FIG E3. Selective depletion of LCs leads to a diminished Tfh cell differentiation in MC903 model. **(A)** Experimental protocol. $Lang^{DTR}$ mice and wildtype littermate controls were *intraperitoneally* (*i.p.*) injected with diphtheria toxin (DT) at D-2 and D0. Mouse were then topically treated with MC903 or EtOH every other day from D13 to D19 and ear draining lymph nodes (EDLN) were analyzed at D20. **(B)** Frequency and number of $CXCR5^+$ $PD\text{-}1^+$ Tfh cells in $Lang^{DEP}$ mice and CT at D20. **(C)** Experimental protocol. $huLang^{DTR}$ mice and wildtype littermate controls were intraperitoneally *i.p.* injected with DT at D-2 and D0. Mouse were then topically treated with MC903 or EtOH every other day from D0 to D10 and EDLN were analyzed at D11. **(D)** Frequency and number of $CXCR5^+$ $PD\text{-}1^+$ Tfh cells in $huLang^{DEP}$ mice and CT at D11. Values shown are means ± SEMs; one-way ANOVA with Tukey's multiple comparison post-hoc test. Data are representative of 2 independent experiments with similar results.

FIG E4. TSLP is crucially required for 30μm-LMP/OVA-induced skin Th2 inflammation. **(A)** Hematoxylin and eosin (HE) staining of mouse ears. **(B)** Immunohistochemistry staining of mouse ears with anti-MBP antibody (for eosinophils) or anti-MCPT8 antibody (for basophils). Arrow points to one of the positive cells. Scale bar, 100μm. **(C-D)** IL-4 (AmCyan) and IL-13 (dsRed) expression in $TCR\beta^+$ dermal cells **(C)** or $CXCR5^-$ $CD4^+$ (non-Tfh) cells **(D)**.

FIG E5. Depletion of $Langerin^+$ cells slightly diminishes the MC903- induced Th2 cell response. Comparison of IL-4 and IL-13 expression among $CXCR5^-CD4^+$ (non-Tfh) cell in the EDLN **(A)**, or among $TCR\beta^+$ cells in the dermis **(B)** of EtOH- or MC903-treated control (CT) or $Lang^{DEP}$ mice, all in the background of $4C13R^{Tg/0}$.

FIG E6. Depletion of Langerin^{+} cells increases the LMP/OVA-induced Th2 cell response in EDLNs. Comparison of IL-4 and IL-13 expression among CXCR5^{-}CD4^{+} (non-Tfh) cell in EDLNs from LMP/OVA-treated control (CT) or Lang^{DEP} in the background of 4C13R$^{Tg/0}$ mice.

FIG E7. 11μm-LMP/OVA-induced skin inflammation is enhanced in mice with the depletion of Langerin^{+} DCs or LCs. Hematoxylin and eosin staining of ears from Lang^{DEP} (**A**, top) and huLang^{DEP} (**B**, top) mice after 11μm-LMP/OVA sensitization. Immunohistochimstry for MBP (eosinophils) and MCPT8 (basophils) of ears from Lang^{DEP} (**A**, bottom) and huLang^{DEP} (**B**, bottom) mice after 11μm-LMP/OVA treatment. Scale bar, 100μm.

FIG E8. LCs counteract LMP/OVA sensitization-induced skin inflammation and the subsequent asthmatic response. **(A)** Experimental protocol for OVA epicutaneous sensitization and airway challenge. Mice were intraperitoneally injected with DT at D-2, D0. Mice were either treated with OVA on LMP ears at D0, D4, D7 and D11 or ears were non treated (NT). All mice were subjected to *intranasal* (*i.n.*) instillation with OVA from D9 to D12. Ears and lungs were analyzed at D13. **(B)** H&E staining of mouse ears. Scale bar, 100μm. **(C)** IHC staining of mouse 30μm-LMP/OVA ears with anti-MBP (for eosinophils) or anti-MCPT8 (for basophils). **(D)** Differential counting of eosinophils (Eos), neutrophils (Neutro), lymphocytes (Lympho) and macrophages (Macro) in BAL. **(E)** RNA levels of indicated genes in BAL cells by RT-qPCR. **(F)** Lung sections were stained with H&E for histological analyses or PAS for goblet cell hyperplasia analyses. B: bronchiole; V: blood vessel. Scale bar, 250μm. **(G)** Experimental protocol for OVA i.p. sensitization and airway challenge. Mice were *i.p.* injected with DT at D-2 and D0. Mice were *i.p.* sensitized with OVA/alum at D0 and D4, and subjected to *i.n.* instillation with OVA from D9 to D12. Lungs were analyzed at D13. **(H)** Differential cell counting in BAL. Data are means ± SEM; unpaired two-tailed t-test.

FIG E9. Transcriptomic analyses of migratory DCs in EDLNs of $Lang^{GFP}$ mice upon MC903 treatment or epicutaneous OVA sensitization. $Lang^{GFP}$ mice were treated with MC903 at D0, D2 and D4 or 30µm-LMP/OVA on D0 and D3; EDLNs were collected at D5 for cell sorting and RNAseq analyses. **(A)** Gating strategy used to sort resident (res) and migratory (mig) GFP^{pos} and GFP^{neg} DCs. **(B)** Heatmap generated with the input of upregulated genes identified in Pos_MC compared with Pos_NT (FC > 1.5; $p < 0.05$; raw read > 200 in at least one sample of the Pos groups), to visually assess the results of clustering on the data to observe trends of expression for genes across all groups. Z score of the expression level is used to generate heatmap. Pos_NT, Pos_MC, Pos_OVA: GFP^{pos} migDCs from non-treated, MC903-treated or LMP/OVA-treated $Lang^{GFP}$ mice; Neg_NT, Neg_MC, Neg_OVA: GFP^{neg} migDCs from non-treated, MC903-treated or LMP/OVA-treated $Lang^{GFP}$ mice.

Two clusters C1 and C2 were revealed. The cluster C1 genes exhibited the expression trends: 1) in non-treated groups, they had a lower expression in GFP^{pos} cells than in GFP^{neg} cells (Pos_NT < Neg_NT); 2) in MC903-treated groups, their expression in GFP^{pos} cells increased, reaching a similar or higher expression than non-treated GFP^{neg} cells (Pos_MC = or > Neg_NT), and their expression in GFP^{neg} cells was also increased (Neg_MC > Neg_NT), with a higher level than Pos_MC cells; 3) in OVA-treated groups, the expression of some genes was also increased in GFP^{neg} cells (Neg_OVA versus Neg_NT) (subcluters of C1: a, b and c) while others remained not changed. Together, expression features of the cluster C1 suggest that in the MC903-AD, $Langerin^{+}$ migDCs acquire many gene expression of $Langerin^{-}$ migDCs, and share the upregulation of these genes with $Langerin^{-}$ migDCs; and moreover, the upregulation of some (although less) of these genes also occurs in $Langerin^{-}$ migDCs (but not $Langerin^{+}$ migDCs) in OVA-AD.

Different from the cluster C1, the cluster C2 genes were highly upregulated in Pos_MC; some of them were also upregulated in Neg_MC (but reaching a lower level) and very few of them were upregulated in Neg_OVA, suggesting that this cluster represents the upregulated genes rather specific for Langerin^{+} migDCs under MC903 treatment.

FIG E10. (A) Heatmap generated with the input of downregulated genes identified in Pos_MC compared with Pos_NT (FC > 1.5; $p < 0.05$; raw read > 200 in at least one sample of the Pos groups), to visually assess the results of clustering on the data to observe trends of expression for genes across all groups. Z score of the expression level was used to generate heatmap. **(B)** Selected genes corresponding to gene ontology terms for Cytokine activity, Regulation of transcription, Regulation of cell migration, or T cell costimulation. *, adjusted $p<0.05$; NS, non significant.

FIG E11. IL-6 neutralization does not significantly diminish Tfh cell differentiation and GC B cell numbers. **(A)** experimental scheme. 4C13R$^{Tg/0}$ mice were i.p. injected with 200 mg anti-IL-6 neutralizing antibody (@IL-6; Clone MP5-20F3, BioXcell) every other day from D0 to D10, and mouse ears were topically treated with MC903 or EtOH every other day from D0 to D10. EDLNs were analyzed at D7 or D11. **(B)** Frequency and number of CXCR5^{+} PD-1^{+} Tfh cells. **(C)** IL-4 (AmCyan) expression by Tfh cells. **(D)** Frequency and number of CD95^{+} GL-7^{+} GC B cells at D11. Data are means ± SEM, one-way ANOVA with Tukey's multiple comparison post-hoc test.

FIG E12. MC903 treatment leads to increased numbers of both langerin-GFP^{pos} and langerin-GFP^{neg} migratory DCs in EDLNs at D5. Lang^{GFP} mice were treated with MC903 at D0, D2 and D4, or 30µm-LMP/OVA at D0 and D3, or tape-stripping (TS)/OVA at D0 and D3, and EDLNs

1039 were collected at D5 for flow cytometry analyses. Absolute numbers of GFP-positive (GFP^{pos})
1040 and -negative (GFP^{neg}) migratory DCs in EDLN, compared with non-treated (NT), are shown.
1041
1042 **FIG E13.** Depletion of $Langerin^{+}$ cells enhances the TS/OVA-induced Tfh/GC response and
1043 the subsequent asthmatic phenotype. **(A)** H&E staining of untreated or tape-stripped (TS)
1044 Balb/c wildtype mice. Arrow points to the absence of stratum corneum in TS-ear. Scale bar,
1045 100µm. **(B)** Dorsal side of ears of WT mice were tape-stripped 10 times and topical treated with
1046 200µg of OVA in 10µl PBS. TSLP protein levels in ears were measured by ELISA at 48h after
1047 treatment. **(C)** Experimental protocol. $Lang^{DTR}$ mice and wildtype littermate controls (CT), in
1048 the background of $4C13R^{Tg/0}$, were i.p. injected with DT at D-2, D0 and then every 4 days.
1049 OVA (200µg) were topically applied on TS-ears at D0, D4, D7 and D11. All mice were
1050 subjected to intranasal (i.n.) instillation with 50µg of OVA from D9 to D12 and analyzed at
1051 D13. **(D-F)** Frequency and number of Tfh cells **(D)**, IL-4 (AmCyan) expression by Tfh cells
1052 **(E)** and numbers of $CD95^{+}$ $GL\text{-}7^{+}$ GC B cells, $IgG1^{+}$ and IgE^{+} B cells in EDLNs **(F)**. **(G)** Serum
1053 levels of OVA-IgG1 and OVA-IgE. **(H)** Differential cell counting for eosinophils (Eos),
1054 neutrophils (Neutro), lymphocytes (Lympho) and macrophages (Macro) in BAL. **(I)** H&E
1055 staining of lung sections. B: bronchiole; V: blood vessel. Scale bar, 250µm. Data are means ±
1056 SEM; unpaired two-tailed t-test.
1057

1 **Title:**

2

3 # Dual function of Langerhans cells in skin TSLP-promoted Tfh cell

4 # differentiation in mouse atopic dermatitis

5

6 Pierre Marschall, PhD,[a] Ruicheng Wei, PhD,[a]* Justine Segaud, MS,[a]* Wenjin Yao, PhD,[a]

7 Pierre Hener, MS,[a] Beatriz Falcon German, MS,[a] Pierre Meyer, MS,[a] Cecile Hugel, MS,[a] Grace

8 Ada Da Silva, PhD,[a] Reinhard Braun, MS,[b], Daniel H. Kaplan, MD, PhD,[c,d] and Mei Li, PhD [a]

9

10 [a] Institut de Génétique et de Biologie Moléculaire et Cellulaire, CNRS UMR 7104 - Inserm U

11 1258 – Université de Strasboug, Illkirch, France

12 [b] PANTEC Biosolutions AG, Ruggell, Liechtenstein

13 [c] Department of Dermatology and [d] Department of Immunology, University of Pittsburgh

14 School of Medicine, Pittsburgh, Pennsylvania, USA.

15 *, equal contribution

16

17 **Disclosure of potential conflict of interest:** The authors declare that they have no relevant

18 conflicts of interest.

19

20 **Corresponding author**

21 Mei Li

22 Institut de Génétique et de Biologie Moléculaire et Cellulaire, CNRS UMR 7104 - Inserm U

23 1258 – Université de Strasboug,

24 1 Rue Laurent Fries, 67404, Illkirch, France

25 Telephone: +33 3 88 65 35 71

Fax: +33 3 88 65 32 01

Email: mei@igbmc.fr

Key words: Atopic dermatitis; TSLP; Dendritic cells; Langerhans cells; Tfh; Th2; allergen sensitization; mouse

Abbreviations used:

AD: atopic dermatitis

BAL: Bronchoalveolar lavage

CT: Wild-type Control

DC: Dendritic cell

DEG: Differentially expressed genes

DT: Diphtheria toxin

DTR: Diphtheria toxin receptor

EDLN: Ear-draining lymph node

GC: Germinal center

H&E: Hematoxylin and eosin

IHC: Immunohistochemistry

Ig: Immunoglobulin

i.n.: Intranasal

i.p.: Intraperitoneal

LC: Langerhans cell

LMP: laser-assisted skin microporation

LN: Lymph node

NT: Non-treated

PAS: Periodic Acid Schiff

PCA: Principle component analysis

Tfh: T follicular helper

Th2: T helper type 2

ELISA: Enzyme-linked immunosorbent assay

TS: Tape stripping

TSLP: Thymic stromal lymphopoietin

Key messages:

- TSLP is critically involved in mounting Tfh/GC response in mouse AD driven by MC903 or OVA-sensitization.
- LCs promote Tfh/GC response in MC903-induced AD.
- LCs suppress Tfh/GC response and Th2 skin inflammation in OVA sensitization-induced AD.

Abstract

Background: Atopic dermatitis (AD) is one of the most common chronic inflammatory skin diseases, usually occurring early in life, and often preceding other atopic diseases like asthma. Th2 cell has been believed to play a crucial role in cellular and humoral response in AD, but accumulating evidences have shown that T follicular helper (Tfh) cell, a critical player in humoral immunity, is associated with disease severity and plays an important role in AD pathogenesis.

Objectives: We aimed at investigating how Tfh cells are generated during the pathogenesis of AD, particularly what is the role of keratinocyte-derived cytokine TSLP and Langerhans cells (LCs).

Methods: We employed two experimental AD mouse models, triggered by the overproduction of TSLP through topical application of MC903, or induced by epicutaneous allergen ovalbumin (OVA) sensitization.

Results: We demonstrated that the development of Tfh cells and GC response were crucially dependent on TSLP in MC903 model and OVA sensitization model. Moreover, we found that LCs promoted Tfh cell differentiation and GC response in MC903 model, and the depletion of Langerin$^+$ DCs or selective depletion of LCs diminished the Tfh/GC response. By contrast, in the model with OVA sensitization, LCs inhibited Tfh/GC response and suppressed Th2 skin inflammation and the subsequent asthma. Transcriptomic analysis of Langerin$^+$ and Langerin$^-$ migratory DCs revealed that Langerin$^+$ DCs became activated in MC903 model, whereas these cells remained inactivated in OVA sensitization model.

Conclusion: Together, these studies revealed a dual functionality of LCs in TSLP-promoted Tfh and Th2 cell differentiation in AD pathogenesis.

Capsule Summary

This study demonstrates that keratinocyte-derived cytokine TSLP plays a critical role in promoting not only Th2 but also Tfh/GC response in the pathogenesis of atopic dermatitis, which implicates a dual function of epidermal Langerhans cells.

Introduction

Atopic dermatitis (AD) is one of the most common chronic inflammatory skin diseases which affects up to 20% of children and 3% of adults worldwide, with increasing prevalence in the industrialized countries during the last 30 years [1]. AD is characterized by chronic cutaneous inflammation, T helper type 2 (Th2) response and hyper immunoglobulin IgE. Patients suffering from AD often present genetic risk factors in the form of mutations affecting the skin barrier structure or the immune system [2]. Onset of AD usually occurs early in life and may lead to allergen sensitization, which can trigger the progression from AD to other atopic diseases such as asthma/allergic rhinitis, in a process called "atopic march" [3, 4].

It has been recognized that Th2 cell response is critically implicated in the pathogenesis of AD. Previous studies from us and others using mouse models have established a central role of the cytokine thymic stromal lymphopoietin (TSLP) expressed by epidermal keratinocytes in promoting Th2 cell response and driving the pathogenesis of AD [5-8]. In addition to Th2 cell response, humoral immune response is another key feature of AD, with increased serum IgE and IgG1 levels associated with AD, which contribute to AD pathology and the atopic march [9, 10]. For a long time, Th2 cell has been believed to play a crucial role both in cellular response and humoral response, e.g. helping B cells to produce Igs. However, such knowledge has been challenged with the identification of T follicular helper (Tfh) cell, which emerges to be a critical player in humoral immunity and T cell memory [11].

In lymphoid organs, Tfh cell differentiation process is believed to begin with an initial dendritic cell (DC) priming of naive $CD4^+$ T cells, which undergo a cell-fate decision with the acquisition of master transcription factor Bcl6 expression and chemokine receptor CXCR5 expressed on cell surface to become early Tfh cells, of which CXCR5 promotes their migration

126 from T cell zone to the B cell follicles [12, 13]. The full differentiation and maintenance of Tfh
127 cells implicate the Tfh cell-B cell interaction, leading to GC Tfh cells which are phenotypically
128 defined by their high expression of CXCR5 and PD-1 [14]. It has been shown that Tfh cells
129 coordinate generation of the GC, initiate help for antigen-specific B cells, and promote selection
130 of high-affinity B cells and differentiation into either memory B cells or long-lived plasma cells
131 [15]. Recent studies have identified Tfh cells as an important source of IL-4, a master regulator in
132 type 2 immunity which was previously thought to be produced by Th2 cells, for providing
133 critical B-cell help by its anti-apoptotic and IgE and IgG1 class switch effects [16]. In addition, it
134 was reported that Tfh cells produce IL-4 in a GATA3-independent manner [17], suggesting
135 distinct mechanisms employed by Tfh and Th2 cells in the regulation of IL-4.

136 Since their initial identification, the biological functions of Tfh cells and their mechanisms
137 of action in the onset and development of diseases have been studied in autoimmuity, infectious
138 diseases, immunodeficiencies and vaccination [18]. Less is known on Tfh cells in the context of
139 AD and other atopic diseases, but more and more evidences have suggested that Tfh cells are
140 associated with disease severity and Tfh cells play an important role in the pathogenesis [19-21].
141 In human, alteration of circulating Tfh cells is correlated with severity of the disease in children
142 with AD [22], or with the comorbid association of allergic rhinitis with asthma [23], and allergen-
143 specific T follicular helper cell counts are correlated with specific IgE levels and efficacy of
144 allergen immunotherapy [24]. In mice, it has been reported that Tfh cells are important for house
145 dust mite-induced asthma [25] or peanut allergy [26].

146 Despite of these accumulating evidences showing the importance of Tfh cells in atopic
147 diseases, how Tfh cells and humoral responses are generated and regulated in AD remained to
148 be investigated. In this study, by employing two experimental AD mouse models, one triggered
149 by the overexpression of TSLP in mouse skin through topical application of MC903 [6, 7, 27], and
150 the other one induced by epicutaneous allergen ovalbumin (OVA) sensitization, we

151 demonstrated that skin TSLP plays a crucial role in driving/promoting Tfh cell differentiation
152 and GC response, in addition to its recognized role in promoting Th2 cell response. Moreover,
153 we investigated the role of skin DCs in mediating the Tfh cell differentiation. We uncovered a
154 dual functionality of epidermal langerhans cells (LCs) in TSLP-promoted Tfh/Th2 cell
155 differentiation in AD pathogenesis, and further explored the molecular insights by
156 transcriptomic analyses, thus shedding new light onto the long-standing controversy of LCs in
157 skin immunity.
158

Methods

Details on the methods used in this study are described in the Methods section in this article's Online Repository, including Experimental mice; MC903 topical application; Epicutaneous OVA sensitization and airway challenge; Depletion of Langerin$^+$ DCs or LCs in mice; Cell preparation for flow cytometry analyses; Surface staining for flow cytometry analyses; LN cell culture and antigen stimulation; RNA sequencing; BAL cell analyses; ELISA; Histopathology; IHC staining; RNA in situ hybridization and Statistics.

Results

Topical MC903 treatment induces TSLP-dependent Tfh cell differentiation and GC response

We have previously reported that topical treatment with MC903, a low calcemic analog of vitamin D3, induces the overproduction of TSLP (TSLP^{over}) and the pathogenesis of AD [6, 7]. To examine the Tfh cell differentiation and GC response in MC903-induced AD model, Balb/c wildtype (WT) mouse ears were topically treated every other day from day (D) 0 to D10 with MC903 and ear-draining lymph nodes (EDLN) were analyzed at D0, D7 and D11 (**Fig 1A**). Results showed that the frequency and number of CXCR5$^+$ PD-1$^+$ Tfh cells were both increased in MC903-treated WT mice at D7 and further augmented at D11 (**Fig 1B**). We next examined the expression of IL-4, a key signal provided by Tfh cells to sustain B cell maturation, by taking use of *Il4*/*Il13* dual reporter 4C13R$^{Tg/0}$ mice, in which AmCyan and dsRed are expressed under the control of IL-4 and IL-13 regulatory elements, respectively [28]. In agreement with a previous report [29], CXCR5$^+$ PD-1$^+$ Tfh cells in EDLNs express IL-4 (AmCyan) but not IL-13 (dsRed) (**Fig E1A**), and the IL-4 expression by Tfh cells was augmented in MC903-treated 4C13R$^{Tg/0}$ mice at both D7 and D11 (**Fig 1C**).

Together, MC903 treatment induces not only Tfh cell differentiation but also the production of IL-4 by Tfh cells.

To examine whether the induction of Tfh cells in MC903 model is triggered by TSLP, mice lacking TSLP (*Tslp*$^{-/-}$) [6] were subjected to MC903 treatment. Results showed that these mice exhibited highly diminished Tfh cell frequency and number at D7 and D11, compared to WT mice (**Fig 1B**). By breeding *Tslp*$^{-/-}$ with 4C13R$^{Tg/0}$ to generate *Tslp*$^{-/-}$/4C13R$^{Tg/0}$ mice, we showed that MC903-induced IL-4 expression in Tfh cells was abrogated in the absence of TSLP (**Fig 1C**). In agreement with the recognized role of TSLP in Th2 cell differentiation, we showed that the MC903-induced IL-4- or IL-13-expressing CXCR5^{-} CD4^{+} non-Tfh cells (representing Th2 cells) were also abrogated in *Tslp*$^{-/-}$ mice (**Fig E1B**). These results indicate that the overproduction of TSLP triggers not only Th2 cell differentiation, but also Tfh cell differentiation and IL-4 expression by these cells.

Next, we examined the GC response in MC903-treated Balb/c WT mice. The number of GC B cells, identified as GL-7^{+} CD95^{+} B cells, exhibited an increase in MC903-treated WT mice at D11, but not at D7 (**Fig 1D**). Such increase was abrogated in MC903-treated *Tslp*$^{-/-}$ mice (**Fig 1D**). This was confirmed by immunofluorescence (IF) staining for GCs (**Fig E2A**). In addition, both IgG1^{+} and IgE^{+} B cells exhibited an increase in their numbers in MC903-treated WT mice at D11, which was also abrogated in MC903-treated *Tslp*$^{-/-}$ mice (**Fig 1E**). Of note, we observed that most of the IgG1^{+} B cells were GL-7^{+} CD95^{+} (**Fig E1C**), suggesting that these cells harbor a GC phenotype; however, this was not the case for IgE^{+} B cells (**Fig E1C**).

Taken together, these data indicate that the overproduction of TSLP triggers Tfh cell differentiation and GC response.

Depletion of Langerin$^+$ DCs or LCs diminishes the TSLP^{over}-triggered Tfh/GC response

LCs reside in the epidermis as a dense network of immune system sentinels, in close proximity to keratinocytes. We then asked whether LCs mediate the TSLP^{over}-triggered Tfh/GC response. To this aim, we first employed Langerin-DTR knock-in mice (Lang^{DTR}) in which Langerin$^+$ cells, including LCs and Langerin$^+$ dermal DCs, express the human diphtheria toxin receptor (DTR) and can thus be depleted upon injection of diphtheria toxin (DT) [30]. Lang^{DTR} mice and their wildtype control littermates were intraperitoneally (*i.p.*) injected with DT at D-2, D0 and every 4 days to maintain the depletion of Langerin$^+$ cells (named Lang^{DEP} and CT respectively), and were subjected to topical MC903 treatment (**Fig 2A**). Results showed that the TSLP^{over}-triggered Tfh cell differentiation was largely diminished in Lang^{DEP} mice (**Fig 2B**). The expression of IL-4 (AmCyan) by Tfh cells was also reduced in Lang^{DEP}/4C13R$^{Tg/0}$ mice (**Fig 2C**). Accordingly, GC B cell number was lower and IgG1$^+$ (however not in IgE$^+$) B cell number was significantly decreased (**Fig 2D**). Therefore, these results indicate that Langerin$^+$ DCs play an important role in mediating the TSLP^{over}-induced Tfh/GC response.

As LCs and Langerin$^+$ cDC1s were both depleted in Lang^{DEP} mice, we next examined whether LCs mediate Tfh cell differentiation by depleting selectively LCs using two strategies: one took use of the differential recovery time between LCs and Langerin$^+$ cDC1s after DT-induced depletion as previously reported [31] (**Fig E3A-B**), and the other one employed human Langerin-DTR (huLang^{DTR}) mice in which DT injection efficiently depletes LCs but not Langerin$^+$ cDC1s [32] (**Fig E3C-D**). In both cases, we showed that the selective depletion of LCs led to a decrease in frequency and number of Tfh cells, suggesting an important role for LCs in TSLP^{over}-triggered Tfh cell differentiation.

Epicutaneous OVA sensitization induces a TSLP-dependent Tfh cell differentiation and GC response

We have previously reported that TSLP plays a crucial role for promoting skin sensitization to allergens, using an experimental mouse protocol in which OVA sensitization through tape-stripped (TS) skin leads to an allergic AD inflammation, accompanied by Th2 cell response, and an increased production of OVA-specific IgG1 and IgE in sera [33]. Here, we developed a novel experimental protocol, in which Precise Laser Epidermal System (P.L.E.A.S.E.®) [34] was used to disrupt skin barrier and to generate patterned micropores in mouse skin. This protocol allowed us to deliver allergens to micropores at precise depths of the epidermis, thereby achieving a higher efficiency and reproducibility of allergen sensitization through the skin compared with experiments based on TS. We showed that micropores at a depth of 30μm (30μm-LMP) on Balb/c WT mouse ears reached basal layer of ear epidermis (**Fig 3A**). ELISA analyses indicated that the protein level of TSLP increased at 48 hours after treatment (**Fig 3B**), in agreement with the previous studies showing that barrier disruption induces TSLP production in mouse [33] and human skin [35]. Notably, such level of TSLP was comparable to our previously reported TSLP level in TS skin [33], although it was much lower compared to that of MC903-treated skin (**Fig 3B; see also Fig E13B**). The administration of OVA did not further induce the TSLP level (**Fig 3B**). *In situ* hybridization showed that TSLP RNA expression was restricted to epidermal keratinocytes in LMP skin (**Fig 3C**).

As expected, OVA treatment on LMP ears (named "LMP/OVA"; **Fig 3D**) induced a Th2-type skin inflammation in TSLP-dependent manner, showing that OVA sensitization-induced infiltration of eosinophils and basophils (**Fig E4A-B**), Th2 cytokines (IL-4 and IL-13) expression by T cells in the skin (**Fig E4C**) and by $CXCR5^{-}CD4^{+}$ cells in EDLNs (**Fig E4D**), were all abolished in mice lacking TSLP. Examination of EDLNs revealed that both

frequency and number of Tfh cells were increased in LMP/OVA- compared to LMP/PBS-treated WT mice, and such increase was largely diminished in *Tslp*$^{-/-}$ mice (**Fig 3E**). Note that LMP/PBS was not sufficient to induce Tfh cell differentiation (despite of the induction of TSLP), but LMP plus OVA together promoted Tfh/GC response which was TSLP-dependent (**Fig 3E**). Moreover, IL-4 production by Tfh cells was augmented in LMP/OVA-treated *Tslp*$^{+/+}$/4C13R$^{Tg/0}$ mice but not *Tslp*$^{-/-}$/4C13R$^{Tg/0}$ mice (**Fig 3F**). GC B cell number analyzed by flow cytometry (**Fig 3G**) and GC size analyzed by immunofluorescence (**Fig E2B**) both showed an increase in LMP/OVA-treated WT mice, and this increase was abrogated in the absence of TSLP. IgG1$^+$ and IgE$^+$ B cell numbers were also increased in LMP/OVA-treated WT mice, and they were much lower in LMP/OVA-treated *Tslp*$^{-/-}$ mice (**Fig 3G**). Accordingly, serum levels of OVA-IgG1 and OVA-IgE were decreased in *Tslp*$^{-/-}$ mice compared to WT mice upon LMP/OVA treatment (**Fig 3H**). Together, these results demonstrate that TSLP is crucially required for epicutaneous OVA sensitization-induced Th2 and Tfh/GC responses.

Depletion of Langerin$^+$ DCs or LCs augments the Tfh/GC response induced by epicutaneous OVA sensitization

Based on the above data from MC903-induced AD, we had expected that Langerin$^+$ DCs would be crucially required for epicutaneous OVA-induced Tfh/GC response. To our surprise, when subjected to 30μm-LMP/OVA sensitization (**Fig 4A**), Lang^{DEP} mice did not exhibit a reduction in frequency and number of CXCR5$^+$ PD-1$^+$ Tfh cells, instead they tended to be higher compared to CT mice (**Fig 4B**). More strikingly, IL-4 expression by Tfh cells was higher in EDLN from LMP/OVA-treated Lang^{DEP}/4C13R$^{Tg/0}$ mice (**Fig 4C**). Accordingly, the GC B cell, IgG1$^+$ and IgE$^+$ B cell number were not reduced in LMP/OVA-treated Lang^{DEP} mice (**Fig 4D**), and serum OVA-specific IgE and OVA-specific IgG1 were

283 higher or tended to be higher (**Fig 4E**). Thus, in contrast to our expectation, Langerin^{+} DCs
284 are not required for the Tfh/GC response in LMP/OVA-induced AD model; instead, they
285 appear to play a counteracting role.

286 Because LCs are located on the suprabasal layer of the epidermis, we suspected that
287 Langerin^{+} cells would be only required in Tfh cell differentiation when allergens are
288 encountered superficially on the skin. To test this possibility, LMP was performed at the
289 depth of 11 μm, which disrupted only the cornified layer of the epidermis (**Fig 5A**). We
290 observed that the 11μm-LMP induced also the production of TSLP, even though its level
291 was lower compared to 30μm-LMP (**Fig 5B**). Treatment of wildtype control (CT) ears with
292 11μm-LMP/OVA induced significant increases (although milder than 30μm-LMP/OVA) in
293 Tfh cell frequency as well as GC B cell number, which were all abolished in *Tslp*$^{-/-}$ mice
294 (**Fig 5C**), indicating that, despite of a low induction of TSLP, the Tfh/GC response promoted
295 by 11μm-LMP/OVA is still crucially dependent on TSLP. However, when Lang^{DEP} mice
296 were subjected to 11μm-LMP/OVA treatment, they exhibited a significant increase in the
297 frequency of Tfh cells, in IL-4 expression by Tfh cells, as well as in GC B cell, IgG1^{+} and
298 IgE^{+} B cell numbers in EDLNs (**Fig 5D-F**), accompanied by augmented serum levels of
299 OVA-IgG1 and OVA-IgE (**Fig 5G**). Similar results were also obtained with huLang^{DEP} mice
300 (**Fig 5H-I**), indicating that LCs significantly counteract the Tfh/GC response induced upon
301 the 11μm-LMP/OVA sensitization.

302 Furthermore, we sought to compare antigen-specific Tfh cells between CT and
303 huLang^{DEP} mice using an activation-induced marker assay [36]. In this assay, the stimulation
304 of LN suspensions with specific antigen drives upregulation of CD154 (CD40L), CD25 and
305 OX40 on Tfh cells, providing a sensitive method for quantifying antigen-specific Tfh cells
306 in mice [36]. We showed that *in vitro* stimulation with OVA drove the upregulation of CD154,
307 OX40 and CD25 in EDLN-derived Tfh cells from LMP/OVA-sensitized CT mice; and such

upregulation was significantly higher in Tfh cells from LMP/OVA-sensitized huLang^{DEP} mice (**Fig 5J**), thus indicating a stronger OVA-specific Tfh cell differentiation in huLang^{DEP} mice upon OVA sensitization.

Together, these data indicate that LCs suppress the TSLP-dependent Tfh/GC response in epicutaneous OVA sensitization model.

Langerin$^+$ DCs or LCs limit epicutaneous OVA-induced Th2 skin inflammation and the subsequent asthma

Having observed the opposite role of Langerin$^+$ DCs or LCs in Tfh/GC response in the two mouse AD models, we further explored their involvement in the induction of Th2 cell response. Upon MC903 treatment, Lang^{DEP}/4C13R$^{Tg/0}$ mice exhibited a slight decrease in IL-4 and a tendency of decrease in IL-13 production by CXCR5$^-$CD4$^+$ cells in EDLN (**Fig E5A**), or by TCRβ$^+$ cells in dermis (**Fig E5B**), which suggests a role, even though minor, for Langerin$^+$ DCs in the development of Th2 cell response. In contrast, upon 30μm-LMP/OVA treatment, Lang^{DEP}/4C13R$^{Tg/0}$ mice exhibited a higher Th2 cell response in both skin (**Fig 6A**) and EDLN (**Fig E6**). This was in accordance with the observation that LMP/OVA-sensitized Lang^{DEP} mice exhibited a stronger skin inflammation (**Fig 6B**), accompanied with an increase in eosinophils and basophils (**Fig 6C**). Moreover, when subjected to 11μm-LMP/OVA sensitization, both Lang^{DEP} and huLang^{DEP} mice exhibited an enhanced AD-like skin inflammation compared to CT mice (**Fig E7**). Therefore, contrary to their minor role in promoting Th2 cell response in MC903-AD, LCs suppress the Th2 cell response in OVA-AD.

We further examined whether Langerin$^+$ DCs limit the atopic march. Upon *intranasal* (*i.n.*) OVA challenge following epicutaneous allergen sensitization (**Fig 6D**), the Lang^{DEP} mice developed a much stronger asthmatic inflammation compared with CT mice, exhibiting

an increase in the number of eosinophils in bronchoalveolar lavage fluid (BAL) (**Fig 6E**), and in RNA expression of Th2 cytokines IL-4, IL-5 and IL-13, as well as chemokine receptor CCR3 (eosinophils) and MCPT8 (basophils) by BAL cells (**Fig 6F**). In addition, H&E staining of lung sections of OVA-treated $Lang^{DEP}$ mice revealed an increased peribronchial and perivascular infiltration, and PAS staining showed an enhanced goblet cells hyperplasia (**Fig 6G**). Similar results were obtained with $huLang^{DEP}$ mice (**Fig E8 A-F**), indicating that LCs counteract the asthma development following epicutaneous allergen sensitization. To exclude the possibility that the enhanced asthmatic inflammation is due to any depletion of lung DCs during the intranasal challenge, we subjected $huLang^{DEP}$ mice to *i.p.* sensitization with OVA/alum and *i.n.* OVA challenge, and observed that these mice developed similar asthmatic inflammation as wildtype control mice (**Fig E8 G-H**). This suggests that the limitation of asthma inflammation by LCs is indeed due to their role in suppressing the epicutaneous allergen sensitization.

Taken together, these studies reveal opposite roles of LCs in two AD models: in MC903-AD, LCs play an important role in priming Tfh/GC response; they participate but to a lesser extend in promoting Th2 responses. In OVA-AD, LCs are neither required for Tfh/GC nor Th2 responses, instead, they suppress OVA-induced Tfh/GC and Th2 responses as well as the "atopic march".

Langerin$^+$ migratory DCs from MC903-AD but not from OVA-AD mice present profound transcriptomic changes

We next conducted transcriptomic studies to explore molecular insights underlying the opposite roles of Langerin$^+$ DCs in Tfh and Th2 cell differentiation in MC903-AD and OVA-AD, by taking use of $Lang^{GFP}$ mouse line in which GFP reports the expression of Langerin [30]. $Lang^{GFP}$ mice were treated with MC903 (at D0, D2 and D4) or LMP/OVA (at D0 and

D3), and at D5, Langerin^{+} (GFP^{pos}) and Langerin^{-} (GFP^{neg}) migratory DCs (migDCs) were sorted from EDLNs of non-treated (NT), MC903- or LMP/OVA-treated mice, and proceeded to mRNA sequencing (**Fig E9A**). The time point at D5 was selected to compare gene expression patterns of migDCs at the initiation stage of Tfh and Th2 cell differentiation.

Principle component analysis (PCA) for the RNAseq data revealed that the Pos_MC (GFP^{pos} migDCs from MC903-treated Lang^{GFP} mice) was clearly separated from the Pos_NT (GFP^{pos} migDCs from non-treated Lang^{GFP} mice); however, the Pos_OVA (GFP^{pos} migDCs from LMP/OVA-treated Lang^{GFP} mice) was inseparable from the Pos_NT (**Fig 7A**). Correspondingly, analyses of differentially expressed genes (DEGs) in Pos_MC vs Pos_NT identified 756 upregulated and 559 downregulated genes (with a fold change >1.5 and adjusted $p<0.05$; **Fig 7B**); in a sharp contrast, the comparison of Pos_OVA vs Pos_NT revealed only 39 upregulated and 9 downregulated genes (**Fig 7B**). Therefore, in MC903-AD, Langerin^{+} migDCs undergo profound transcriptomic changes, but in OVA-AD, they present almost no, or very little, transcriptomic changes.

As to Langerin^{-} migDCs, PCA showed that Neg_MC (GFP^{neg} migDCs from MC903-treated Lang^{GFP} mice), Neg_OVA (GFP^{neg} migDCs from LMP/OVA-treated Lang^{GFP} mice) and Neg_NT (GFP^{neg} migDCs from non-treated Lang^{GFP} mice) were all clustered away from each other (**Fig 7A**). Analyses of DEGs identified 710 upregulated and 698 downregulated genes for Neg_MC vs Neg_NT; and 431 upregulated and 427 downregulated genes for Neg_OVA vs Neg_NT (**Fig 7B**), suggesting that Langerin^{-} migDCs present major transcriptomic changes in both MC903-AD and OVA-AD, with considerable numbers of overlapped DEGs (249 upregulated and 215 downregulated).

Gene ontology analyses of DEGs in Langerin^{+} migDCs from MC903-treated mice

Next, using the upregulated or downregulated DEGs identified in Pos_MC (vs Pos_NT) as input, we performed cluster analyses of all the groups and generated heat map to visualize trends of expression for genes across the different groups. Results are presented in **Fig E9B** and **Fig E10A**. Further, we performed gene ontology (GO) analyses of the upregulated genes in Pos_MC (**Fig 7C**), and examined whether these genes were also significantly upregulated in Neg_MC (vs Neg_NT), and Neg_OVA (vs Neg_NT). We paid particular attention to the upregulated genes shared in all the three groups (Pos_MC, Neg_MC and Neg_OVA), standing here for "commonly upregulated" genes (highlighted in red in **Fig 7C**), as they could be implicated in TSLP-promoted Tfh and/or Th2, a common feature shared by MC903-AD and OVA-AD. Among them, we found genes related to: 1) "regulation of cell migration", many of which were reported to facilitate DC migration (*Mmp14* [37]; *Stat5* [38]; Nrp2 [39]*; Sema7a* [40]); 2) "T cell costimulation": *Cd80* and *Cd86* [41], *IL2ra* [42], *Pdcd1lg2* (PD-L2)[43], *Cd274* (PD-L1*), Gpr183* (EBI2)[44, 45]; 3) "cytokine signal": *Il2ra*, *Tnfrsf11b* and *Ccl22*; and 4) "transcription factors" such as *Ikzf4, Irf4, Stat4 and Stat5a*.

We examined TSLP signaling pathway among the upregulated genes in Pos_MC. Using the reported TSLP-regulated gene set [46], we identified *Cd84, Cd82, Ccl17, Ccl22 and Tnfrsf11b* (in the cluster with higher expression in Pos_MC than Neg_MC), as well as *Cish, Cd86, Cd80, Cd274, Il2ra, Il6, ccr2, Tgfb1* (in the cluster with higher expression in Neg_MC than Pos_MC) (**Fig 7D**). In addition, we identified *Irf4*, which has been recently shown to be downstream of TSLP signaling in human migratory LCs [47]. The upregulation of these TSLP-targeting genes by Langerin$^+$ migDCs suggests that these cells could be a direct responder to TSLP signaling, although it remains to be demonstrated that TSLP signals through its receptor on LCs drive their migration/activation. Besides these known TSLP downstream genes, more TSLP pathway genes identified from those "commonly upregulated" genes can be envisaged.

406 Interestingly, we did not find *Tnfsf4* (encoding OX40L) among the DEGs in Pos_MC,
407 despite that OX40L was reported to be TSLP-responsive gene and mediate TSLP-promoted
408 Th2 [48] and Tfh [49] cell differentiation. Actually, OX40L expression by GFP^{pos} cells was barely
409 detected in Pos_NT, Pos_MC or Pos_OVA (**Fig 7E**). On the other hand, OX40L was expressed
410 in Neg_NT, and its expression was further upregulated in Neg_MC and Neg_OVA. Therefore,
411 it is unlikely that OX40L would be responsible for the Tfh-promoting function of $Langerin^{+}$
412 DCs, while its precise function as a potential TSLP downstream factor in $Langerin^{-}$ DCs
413 remains to be defined (**Fig 7E**).
414 Among the above-mentioned TSLP-regulated gene, IL-6 has been shown to be a critical
415 cytokine for Tfh cell differentiation [50, 51]. We thus tested whether IL-6 neutralization decreases
416 Tfh / GC response in MC903-AD. Results showed that IL-6 was not required for the initiation
417 of Tfh cell differentiation and the overall GC reaction (**Fig E11)**, although it is possible that its
418 function in Tfh response is redundant with other signals as suggested by Eto et al [52]. Besides
419 IL-6, several other Tfh-promoting factors derived from DCs have been recently reported,
420 including IRF-4[53], IL-2Ra[42, 54] and EBI2 (*Gpr183*) [44, 45], whose expression was all "commonly
421 upregulated" in Pos_MC, Neg_MC and Neg_OVA (**Fig 7D**). The role of these potential
422 candidates in TSLP-promoting Tfh cell differentiation remains to be examined.
423 Finally, among the downregulated genes (**Fig E10B**), less knowledge was available, but
424 we could see *Il12b* (IL-23/IL-12p40), whose expression in DCs was previously reported to be
425 suppressed by TSLP [55]. Other commonly downregulated ones included genes related "T cell
426 costimulation" *Havcr2* (TIM3), *Lgals8* (Galectin 8); "Regulation of cell migration" *Adam15*
427 and *Ptk2* (negative regulators for cell migration) and "regulation of transcription" *Foxc2, Thrb,*
428 *Tcf7l2, Ehf* and *Lmo2.*
429

Discussion

In this study, we analyzed how Tfh cells were generated in two experimental AD mouse models, triggered by the overproduction of TSLP by topical application of MC903, or induced by epicutaneous OVA sensitization. We demonstrated a crucial role for TSLP in promoting Tfh cells and GC response in MC903-AD as well as OVA-AD. Intriguingly, we revealed a dual function of LCs in TSLP-promoted Tfh/Th2 cell differentiation: while they promoted Tfh cell differentiation in MC903-AD, they inhibited Tfh/GC response and suppressed Th2 skin inflammation and the atopic march in OVA-AD. This is schematically illustrated in **Fig 8**, and is discussed below.

1) TSLP: critical player for Th2 and Tfh cell response in AD

It has been recognized that TSLP is overproduced in AD lesional skin [56], however, its expression varies from high to low, which could be related with the cause (e.g. genetic mutation of *Spink5* which induces a high level of TSLP [57] vs skin barrier impairment which induces a low level of TSLP [35]), age (e.g. TSLP serum level in AD children is high at early stage and decreases with age [58]), or the nature of disease (e.g. intrinsic or extrinsic AD). Our study demonstrates that no matter in AD models associated with either high or low TSLP expression, TSLP is crucial for promoting Tfh/GC response in AD. Recently, the link between TSLP and Tfh cell differentiation was suggested by the study with human blood DC-T cell coculture system [49]. Thus, the Tfh-promoting function of TSLP appears to be conserved between mouse and human, which suggests that it is relevant and valuable to employ AD mouse models to elucidate mechanisms underlying the TSLP (skin)-Tfh (draining LN) axis, particularly the access of tissue and lymphoid organs is rather limited in human study.

Our data add new evidence that neutralization of TSLP or blocking TSLP downstream pathway will be helpful for reducing Th2 and Tfh cell responses in AD. Notably, TSLP is crucial for driving the downstream IL-4/IL-13 expression by Th2 cells, as well as IL-4 expression by Tfh cells. Indeed, blocking antibody against IL-4/-13R (Dupilumab), which may actually target both Th2 and Tfh cell responses, has been shown to achieve significant therapeutic effect on AD [59]. Intriguingly, neutralization TSLP antibody Tezepelumab has been demonstrated to significantly reduce annual asthma exacerbation rate in patients with uncontrolled asthma [60]. A recent study with Tezepelumab showed numeric improvements in patients with moderate to severe AD, despite that there were certain limitations in that study including patient selection, use of topical corticosteroids, duration of treatment and uncertain inhibition of TSLP with the dose used [61]. Given the preclinical evidence for the role of TSLP in AD, more clinical studies are required to evaluate TSLP as therapeutic target in AD.

It should be also noted that recent studies have recognized the importance of Tfh cells in AD [19-21], but the *in vivo* function of Tfh remains to be further delineated using AD mouse models. This is challenged by the lack of appropriate tools to deplete Tfh cells. We are under the way to generate mouse line in which DTR can be selectively expressed in Tfh cells, thus allowing the DT-induced depletion of Tfh cells.

2) LCs: function as migratory DCs to promote Tfh cell differentiation

LCs represent one of the most studied but controversial DC subtypes. Our study shows that LCs are importantly engaged in the initiation Tfh cell differentiation and GC response triggered by $TSLP^{over}$ in MC903-AD. This provides new evidence on the Tfh-promoting function of LCs in AD, in addition to several studies reporting the requirement of LCs for humoral responses in other contexts [62,63,64]. In MC903-AD, we observed that LCs play a dominant role in Tfh cell differentiation, although dermal $langerin^-$ DCs may also contribute. On the other hand, $langerin^-$

DCs (cDC2) appear to be the major player for the TSLP^{over}-induced Th2, while LCs have somewhat but minor contribution. Nevertheless, to provide direct evidence for the contribution of cDC2 in TSLP-driven Tfh and Th2 responses in AD, further studies could be performed using DC-specific KO of IRF4 or Dock8 mice, which have impaired development and migration of CD11b^{+} cDC2 [65], or CD301b-DTR mice in which CD301b^{+} cDC2 can be transiently depleted [66].

There have been long debates on the migration, antigen uptake, and T cell differentiation of LCs in different contexts; but transcriptomic study on migratory LCs in skin-draining LNs under inflammatory pathological contexts was lacking. Our transcriptomic data are therefore of value; however, one drawback is that migratory LCs and cDC1 were not separated in Langerin^{+} (GFP^{pos}) migDCs, thus the gene expression data still need to be cautiously interpreted concerning LCs. Nevertheless, we have shown that Langerin^{+} migDCs in EDLN of MC903-induced TSLP^{over} mice presented substantial transcriptional changes, suggesting that the activation and migration of Langerin^{+} DC to the draining LNs underlie its function to prime Tfh cell differentiation in MC903-AD. Indeed, when comparing numbers of GFP^{pos} and GFP^{neg} migratory DCs in EDLN of MC903-treated Lang^{GFP} mice at D5, we observed that both were increased (**Fig E12**), supporting that both Langerin^{+} DCs and Langerin^{-} DCs migrate to draining LNs in MC903-AD.

3) LCs: function as non-migratory cells in the skin to suppress Tfh/Th2 response?

Our study revealed a suppressive role of LCs for epicutaneous OVA-induced Tfh and Th2 cell differentiation. This is in contrast with two previous studies which reported a role of LCs in provoking AD inflammation by using a tape stripping (TS) OVA sensitization model [67, 68]. To examine whether the discrepancy is due to the different effects of LMP compared to TS, we performed TS/OVA sensitization on mouse ears. Results showed that, similar to LMP/OVA,

TS/OVA-sensitized Lang^{DEP} mouse EDLNs exhibited increased frequency and number of Tfh cells, increased IL-4 expression by Tfh cells, higher numbers of GC B cells, IgG1$^+$ and IgE$^+$ B cells, with elevated OVA-IgG1 and OVA-IgE in sera (**Fig E13 A-G**). Moreover, when *i.n.* challenged with OVA, Lang^{DEP} mice developed a stronger asthmatic inflammation (**Fig E13 H-I**). Therefore, the discrepancy with the previous reports [67, 68] is not explained by the difference of LMP vs TS technique in epicutaneous OVA sensitization; rather, it could be due to other factors remained yet to be determined, such as the allergen application method: topical OVA vs long exposure (2-day) of OVA placed on patch-test tape; the difference of mouse background: Balb/c vs C57Bl/6; or the site of allergen application: ear vs back.

Why are LCs not implicated in the promotion of Tfh/Th2 cell differentiation in EDLN in this context? Transcriptomic analyses showed that in sharp contrast to MC903-AD, Langerin$^+$ migDCs in OVA-AD presented almost the same transcriptomic program as in untreated mice, suggesting an absence of migration/activation of these cells. Indeed, Langerin$^+$ migDC numbers in EDLNs from LMP/OVA-treated or TS/OVA-treated mice at D5 were nearly unchanged, whereas Langerin$^-$ migDC number was increased (**Fig E12**). This is in agreement with previous studies showing that when skin was treated with fluorescence-conjugated OVA [66], HDM [69], or Dextran [70], antigen uptake and transport to draining LNs were mainly exerted by Langerin$^-$ DCs. Of note, it was recently shown that LCs can transfer antigen to cDC2 in the context of Langerin mAb-mediated targeting [71]. It will be interesting to see whether this occurs in AD models, and whether efficiency of LC antigen transfer could be altered in the two models, as another possible explication of different implication of LCs in Tfh cell differentiation.

Then how do LCs exert their anti-Tfh/Th2 role in OVA-AD? A recent study showed that LCs played an immunosuppressive role when OVA was applied on the intact skin, in accompany with the induction of IL-10 in LCs in skin-draining LNs [72]. However, this does not seem to be our case, because Langerin$^+$ migDCs in EDLN did not exhibit any transcriptional

change of Treg-inducing signals including IL-10 and TGFβ, or RALDH2. More likely, the anti-Tfh/Th2 effect of LCs is related to their immune suppression function *in situ* in the skin, in keeping with LC ontogeny not only as DCs but also as non-migratory macrophages [73, 74]. It should be further studied how LCs exert such functionality, for example, by limiting the antigen-uptake by cDC2 in the skin, or by promoting local Tregs in OVA-sensitized skin [75 76]. Transcriptomic analysis of LCs isolated from the OVA-treated skin site may provide further molecular insights.

4) What signals switch the function of LCs?

One intriguing question is what microenvironment cues and molecular signals switch the function of LC between anti-Tfh/Th2 to pro-Tfh/Th2 in AD contexts. Notably, MC903-AD and OVA-AD exhibit similar AD phenotype which is TSLP-dependent, but the quantity of TSLP and the nature of antigen are different in these two models. In MC903-AD, MC903 induced a high production of TSLP [7] (**Fig 8**) which was sufficient to induce Tfh and Th2 cell differentiation. As there was no administration of experimental allergen, the nature of antigen implicated in T cell differentiation in MC903 model may involve endogenous antigens or microbiota co-existing in the skin. On the other hand, in OVA-AD, the disruption of skin barrier with LMP induced TSLP expression however to a much lower extent (**Fig 8**). It is possible that LCs sense the quantity of TSLP. Indeed, as a danger signal, TSLP may convert the function of LCs when its level is above certain threshold. *In vitro* studies have shown that TSLP triggers DC migration [77], or promotes the survival, maturation and migration of human LCs, and allogenic naïve $CD4^+$ T cells cocultured with TSLP-conditioned LCs produced cytokines IL-4 and IL-13 [78], but quantitative study on TSLP signaling has never been performed. It will be interesting to explore whether and how quantitative TSLP signaling determines the role of LCs, by conducting *in vivo* or *ex vivo* dose-dependent experiments. In addition, the nature and

554 quantity of antigens can be also involved in the functional switch of LCs. To unravel such
555 complexity, the emerging mathematic modeling [79, 80] may eventually help to integrate multiple
556 parameters for a better understanding of functional switch of LCs.

557 It will be interesting to further explore in AD patients whether and how TSLP levels are
558 correlated with the states and function of LCs. A better understanding of what molecular switch
559 determines the function of LCs either as "pro-Tfh/Th2" or as "anti-Tfh/Th2", and of how LCs
560 exert such functions, will allow us to shape LCs to act in suppressing the skin inflammation,
561 limiting the allergen sensitization through AD skin, thus preventing the progression from AD
562 to asthma. On the other hand, the potential of LCs to induce Tfh cell differentiation and GC
563 response and the subsequent induction of antigen-specific antibodies has been of interest for
564 transcutaneous vaccination [63, 81]. Therefore, the knowledge we obtain from this study should be
565 also insightful for LC-based skin vaccination, including the use of TSLP at an appropriate level
566 as an effective adjuvant for promoting Tfh cell differentiation and humoral response.
567

Acknowledgement

We thank the staff of animal facilities, mouse supporting services, flow cytometry, histopathology, microscopy and imaging, and cell culture of IGBMC and Institut Clinique de la Souris (ICS) for excellent technical assistance. We are grateful for B. Malissen for providing $Lang^{DTR}$ and $Lang^{GFP}$ mice, and W. Paul for providing $4C13R^{Tg/0}$ mice. Sequencing was performed by the GenomEast platform, a member of the 'France Génomique' consortium (ANR-10-INBS-0009), and we would like to thank M. Cerciat for library preparation and sequencing, and M. Jung for generating the data. We thank J. Heller and J. Demenez for helping with genotyping and histology analyses. We would like to acknowledge the funding supports from l'Agence Nationale de la Recherche (ANR-17-CE14-0025; ANR-19-CE17-0017; ANR-19-CE17-0021) to ML, from Fondation Recherche Medicale (Equipes-FRM 2018) to ML, and the first joint programme of the Freiburg Institute for Advanced Studies (FRIAS) and the University of Strasbourg Institute for Advanced Study (USIAS) to ML. The study was also supported by the grant ANR-10-LABX-0030-INRT, a French State fund managed by the Agence Nationale de la Recherche under the frame program Investissements d'Avenir ANR-10-IDEX-0002-02; the Centre National de la Recherche Scientifique (CNRS); the Institut National de la Santé et de la Recherche Médicale (INSERM), and the Université de Strasbourg (Unistra). PM was supported by PhD fellowship from Region Alsace, RW and YW by PhD fellowships from the Association pour la Recherche à l'IGBMC (ARI), JS by a PhD fellowship from Equipes-FRM 2018.

References

1. Weidinger S, Novak N. Atopic dermatitis. Lancet 2016; 387:1109-22.
2. Boguniewicz M, Leung DY. Atopic dermatitis: a disease of altered skin barrier and immune dysregulation. Immunol Rev 2011; 242:233-46.
3. Dharmage SC, Lowe AJ, Matheson MC, Burgess JA, Allen KJ, Abramson MJ. Atopic dermatitis and the atopic march revisited. Allergy 2014; 69:17-27.
4. Shaker M. New insights into the allergic march. Curr Opin Pediatr 2014; 26:516-20.
5. Yoo J, Omori M, Gyarmati D, Zhou B, Aye T, Brewer A, et al. Spontaneous atopic dermatitis in mice expressing an inducible thymic stromal lymphopoietin transgene specifically in the skin. J Exp Med 2005; 202:541-9.
6. Li M, Hener P, Zhang Z, Ganti KP, Metzger D, Chambon P. Induction of thymic stromal lymphopoietin expression in keratinocytes is necessary for generating an atopic dermatitis upon application of the active vitamin D3 analogue MC903 on mouse skin. J Invest Dermatol 2009; 129:498-502.
7. Li M, Hener P, Zhang Z, Kato S, Metzger D, Chambon P. Topical vitamin D3 and low-calcemic analogs induce thymic stromal lymphopoietin in mouse keratinocytes and trigger an atopic dermatitis. Proc Natl Acad Sci U S A 2006; 103:11736-41.
8. Li M, Messaddeq N, Teletin M, Pasquali JL, Metzger D, Chambon P. Retinoid X receptor ablation in adult mouse keratinocytes generates an atopic dermatitis triggered by thymic stromal lymphopoietin. Proc Natl Acad Sci U S A 2005; 102:14795-800.
9. Chapman MD, Rowntree S, Mitchell EB, Di Prisco de Fuenmajor MC, Platts-Mills TA. Quantitative assessments of IgG and IgE antibodies to inhalant allergens in patients with atopic dermatitis. J Allergy Clin Immunol 1983; 72:27-33.
10. Werfel T, Allam JP, Biedermann T, Eyerich K, Gilles S, Guttman-Yassky E, et al. Cellular and molecular immunologic mechanisms in patients with atopic dermatitis. J Allergy Clin Immunol 2016; 138:336-49.
11. Crotty S. T Follicular Helper Cell Biology: A Decade of Discovery and Diseases. Immunity 2019; 50:1132-48.
12. Hardtke S, Ohl L, Forster R. Balanced expression of CXCR5 and CCR7 on follicular T helper cells determines their transient positioning to lymph node follicles and is essential for efficient B-cell help. Blood 2005; 106:1924-31.
13. Haynes NM, Allen CD, Lesley R, Ansel KM, Killeen N, Cyster JG. Role of CXCR5 and CCR7 in follicular Th cell positioning and appearance of a programmed cell death gene-1high germinal center-associated subpopulation. J Immunol 2007; 179:5099-108.
14. Qi H. T follicular helper cells in space-time. Nat Rev Immunol 2016; 16:612-25.
15. Victora GD, Nussenzweig MC. Germinal centers. Annu Rev Immunol 2012; 30:429-57.
16. Sahoo A, Wali S, Nurieva R. T helper 2 and T follicular helper cells: Regulation and function of interleukin-4. Cytokine Growth Factor Rev 2016; 30:29-37.
17. Vijayanand P, Seumois G, Simpson LJ, Abdul-Wajid S, Baumjohann D, Panduro M, et al. Interleukin-4 production by follicular helper T cells requires the conserved Il4 enhancer hypersensitivity site V. Immunity 2012; 36:175-87.
18. Ueno H, Banchereau J, Vinuesa CG. Pathophysiology of T follicular helper cells in humans and mice. Nat Immunol 2015; 16:142-52.
19. Varricchi G, Harker J, Borriello F, Marone G, Durham SR, Shamji MH. T follicular helper (Tfh) cells in normal immune responses and in allergic disorders. Allergy 2016; 71:1086-94.

20. Kemeny DM. The role of the T follicular helper cells in allergic disease. Cell Mol Immunol 2012; 9:386-9.
21. Qin L, Waseem TC, Sahoo A, Bieerkehazhi S, Zhou H, Galkina EV, et al. Insights Into the Molecular Mechanisms of T Follicular Helper-Mediated Immunity and Pathology. Front Immunol 2018; 9:1884.
22. Szabo K, Gaspar K, Dajnoki Z, Papp G, Fabos B, Szegedi A, et al. Expansion of circulating follicular T helper cells associates with disease severity in childhood atopic dermatitis. Immunol Lett 2017; 189:101-8.
23. Kamekura R, Shigehara K, Miyajima S, Jitsukawa S, Kawata K, Yamashita K, et al. Alteration of circulating type 2 follicular helper T cells and regulatory B cells underlies the comorbid association of allergic rhinitis with bronchial asthma. Clin Immunol 2015; 158:204-11.
24. Yao Y, Chen CL, Wang N, Wang ZC, Ma J, Zhu RF, et al. Correlation of allergen-specific T follicular helper cell counts with specific IgE levels and efficacy of allergen immunotherapy. J Allergy Clin Immunol 2018; 142:321-4 e10.
25. Ballesteros-Tato A, Randall TD, Lund FE, Spolski R, Leonard WJ, León B. T Follicular Helper Cell Plasticity Shapes Pathogenic T Helper 2 Cell-Mediated Immunity to Inhaled House Dust Mite. Immunity 2016; 44:259-73.
26. Dolence JJ, Kobayashi T, Iijima K, Krempski J, Drake LY, Dent AL, et al. Airway exposure initiates peanut allergy by involving the IL-1 pathway and T follicular helper cells in mice. J Allergy Clin Immunol 2018; 142:1144-58 e8.
27. Leyva-Castillo JM, Hener P, Michea P, Karasuyama H, Chan S, Soumelis V, et al. Skin thymic stromal lymphopoietin initiates Th2 responses through an orchestrated immune cascade. Nat Commun 2013; 4:2847.
28. Roediger B, Kyle R, Yip KH, Sumaria N, Guy TV, Kim BS, et al. Cutaneous immunosurveillance and regulation of inflammation by group 2 innate lymphoid cells. Nat Immunol 2013; 14:564-73.
29. Liang HE, Reinhardt RL, Bando JK, Sullivan BM, Ho IC, Locksley RM. Divergent expression patterns of IL-4 and IL-13 define unique functions in allergic immunity. Nat Immunol 2011; 13:58-66.
30. Kissenpfennig A, Henri S, Dubois B, Laplace-Builhe C, Perrin P, Romani N, et al. Dynamics and function of Langerhans cells in vivo: dermal dendritic cells colonize lymph node areas distinct from slower migrating Langerhans cells. Immunity 2005; 22:643-54.
31. Henri S, Poulin LF, Tamoutounour S, Ardouin L, Guilliams M, de Bovis B, et al. CD207+ CD103+ dermal dendritic cells cross-present keratinocyte-derived antigens irrespective of the presence of Langerhans cells. J Exp Med 2010; 207:189-206.
32. Bobr A, Olvera-Gomez I, Igyarto BZ, Haley KM, Hogquist KA, Kaplan DH. Acute ablation of Langerhans cells enhances skin immune responses. J Immunol 2010; 185:4724-8.
33. Leyva-Castillo JM, Hener P, Jiang H, Li M. TSLP produced by keratinocytes promotes allergen sensitization through skin and thereby triggers atopic march in mice. J Invest Dermatol 2013; 133:154-63.
34. Scheiblhofer S, Thalhamer J, Weiss R. Laser microporation of the skin: prospects for painless application of protective and therapeutic vaccines. Expert Opin Drug Deliv 2013; 10:761-73.

35. Angelova-Fischer I, Fernandez IM, Donnadieu M-H, Bulfone-Paus S, Zillikens D, Fischer TW, et al. Injury to the Stratum Corneum Induces In Vivo Expression of Human Thymic Stromal Lymphopoietin in the Epidermis. J Invest Dermatol 2010; 130:2505-7.
36. Jiang W, Wragg KM, Tan HX, Kelly HG, Wheatley AK, Kent SJ, et al. Identification of murine antigen-specific T follicular helper cells using an activation-induced marker assay. J Immunol Methods 2019; 467:48-57.
37. Gawden-Bone C, Zhou Z, King E, Prescott A, Watts C, Lucocq J. Dendritic cell podosomes are protrusive and invade the extracellular matrix using metalloproteinase MMP-14. J Cell Sci 2010; 123:1427-37.
38. Bell BD, Kitajima M, Larson RP, Stoklasek TA, Dang K, Sakamoto K, et al. The transcription factor STAT5 is critical in dendritic cells for the development of TH2 but not TH1 responses. Nat Immunol 2013; 14:364-71.
39. Roy S, Bag AK, Singh RK, Talmadge JE, Batra SK, Datta K. Multifaceted Role of Neuropilins in the Immune System: Potential Targets for Immunotherapy. Front Immunol 2017; 8:1228.
40. van Rijn A, Paulis L, te Riet J, Vasaturo A, Reinieren-Beeren I, van der Schaaf A, et al. Semaphorin 7A Promotes Chemokine-Driven Dendritic Cell Migration. J Immunol 2016; 196:459-68.
41. Watanabe M, Fujihara C, Radtke AJ, Chiang YJ, Bhatia S, Germain RN, et al. Co-stimulatory function in primary germinal center responses: CD40 and B7 are required on distinct antigen-presenting cells. J Exp Med 2017; 214:2795-810.
42. Li J, Lu E, Yi T, Cyster JG. EBI2 augments Tfh cell fate by promoting interaction with IL-2-quenching dendritic cells. Nature 2016; 533:110-4.
43. Gao Y, Nish SA, Jiang R, Hou L, Licona-Limon P, Weinstein JS, et al. Control of T helper 2 responses by transcription factor IRF4-dependent dendritic cells. Immunity 2013; 39:722-32.
44. Lu E, Cyster JG. G-protein coupled receptors and ligands that organize humoral immune responses. Immunol Rev 2019; 289:158-72.
45. Barington L, Wanke F, Niss Arfelt K, Holst PJ, Kurschus FC, Rosenkilde MM. EBI2 in splenic and local immune responses and in autoimmunity. J Leukoc Biol 2018; 104:313-22.
46. Zhong J, Sharma J, Raju R, Palapetta SM, Prasad TS, Huang TC, et al. TSLP signaling pathway map: a platform for analysis of TSLP-mediated signaling. Database (Oxford) 2014; 2014:bau007.
47. Polak ME, Ung CY, Masapust J, Freeman TC, Ardern-Jones MR. Petri Net computational modelling of Langerhans cell Interferon Regulatory Factor Network predicts their role in T cell activation. Sci Rep 2017; 7:668.
48. Ito T, Wang YH, Duramad O, Hori T, Delespesse GJ, Watanabe N, et al. TSLP-activated dendritic cells induce an inflammatory T helper type 2 cell response through OX40 ligand. J Exp Med 2005; 202:1213-23.
49. Pattarini L, Trichot C, Bogiatzi S, Grandclaudon M, Meller S, Keuylian Z, et al. TSLP-activated dendritic cells induce human T follicular helper cell differentiation through OX40-ligand. J Exp Med 2017; 214:1529-46.
50. Eddahri F, Denanglaire S, Bureau F, Spolski R, Leonard WJ, Leo O, et al. Interleukin-6/STAT3 signaling regulates the ability of naive T cells to acquire B-cell help capacities. Blood 2009; 113:2426-33.

730 51. Chakarov S, Fazilleau N. Monocyte-derived dendritic cells promote T follicular helper
731 cell differentiation. EMBO Mol Med 2014; 6:590-603.
732 52. Eto D, Lao C, DiToro D, Barnett B, Escobar TC, Kageyama R, et al. IL-21 and IL-6 are
733 critical for different aspects of B cell immunity and redundantly induce optimal
734 follicular helper CD4 T cell (Tfh) differentiation. PLoS ONE 2011; 6:e17739.
735 53. Calabro S, Gallman A, Gowthaman U, Liu D, Chen P, Liu J, et al. Bridging channel
736 dendritic cells induce immunity to transfused red blood cells. J Exp Med 2016; 213:887-
737 96.
738 54. Ballesteros-Tato A, Leon B, Graf BA, Moquin A, Adams PS, Lund FE, et al. Interleukin-2
739 inhibits germinal center formation by limiting T follicular helper cell differentiation.
740 Immunity 2012; 36:847-56.
741 55. Taylor BC, Zaph C, Troy AE, Du Y, Guild KJ, Comeau MR, et al. TSLP regulates intestinal
742 immunity and inflammation in mouse models of helminth infection and colitis. J Exp
743 Med 2009; 206:655-67.
744 56. Soumelis V, Reche PA, Kanzler H, Yuan W, Edward G, Homey B, et al. Human epithelial
745 cells trigger dendritic cell mediated allergic inflammation by producing TSLP. Nat
746 Immunol 2002; 3:673-80.
747 57. Briot A, Deraison C, Lacroix M, Bonnart C, Robin A, Besson C, et al. Kallikrein 5 induces
748 atopic dermatitis-like lesions through PAR2-mediated thymic stromal lymphopoietin
749 expression in Netherton syndrome. J Exp Med 2009; 206:1135-47.
750 58. Yao W, Zhang Y, Jabeen R, Nguyen ET, Wilkes DS, Tepper RS, et al. Interleukin-9 Is
751 Required for Allergic Airway Inflammation Mediated by the Cytokine TSLP. Immunity
752 2013; 38:360-72.
753 59. Simpson EL, Akinlade B, Ardeleanu M. Two Phase 3 Trials of Dupilumab versus Placebo
754 in Atopic Dermatitis. N Engl J Med 2017; 376:1090-1.
755 60. Corren J, Parnes JR, Wang L, Mo M, Roseti SL, Griffiths JM, et al. Tezepelumab in Adults
756 with Uncontrolled Asthma. N Engl J Med 2017; 377:936-46.
757 61. Simpson EL, Parnes JR, She D, Crouch S, Rees W, Mo M, et al. Tezepelumab, an anti-
758 thymic stromal lymphopoietin monoclonal antibody, in the treatment of moderate to
759 severe atopic dermatitis: A randomized phase 2a clinical trial. J Am Acad Dermatol
760 2019; 80:1013-21.
761 62. Zimara N, Florian C, Schmid M, Malissen B, Kissenpfennig A, Mannel DN, et al.
762 Langerhans cells promote early germinal center formation in response to Leishmania-
763 derived cutaneous antigens. Eur J Immunol 2014; 44:2955-67.
764 63. Yao C, Zurawski SM, Jarrett ES, Chicoine B, Crabtree J, Peterson EJ, et al. Skin dendritic
765 cells induce follicular helper T cells and protective humoral immune responses. J
766 Allergy Clin Immunol 2015; 136:1387-97 e1-7.
767 64. Levin C, Bonduelle O, Nuttens C, Primard C, Verrier B, Boissonnas A, et al. Critical Role
768 for Skin-Derived Migratory DCs and Langerhans Cells in TFH and GC Responses after
769 Intradermal Immunization. The Journal of investigative dermatology 2017; 137:1905-
770 13.
771 65. Krishnaswamy JK, Alsen S, Yrlid U, Eisenbarth SC, Williams A. Determination of T
772 Follicular Helper Cell Fate by Dendritic Cells. Front Immunol 2018; 9:2169.
773 66. Kumamoto Y, Linehan M, Weinstein JS, Laidlaw BJ, Craft JE, Iwasaki A. CD301b^{+} dermal
774 dendritic cells drive T helper 2 cell-mediated immunity. Immunity 2013; 39:733-43.

67. Kim TG, Kim M, Lee JJ, Kim SH, Je JH, Lee Y, et al. CCCTC-binding factor controls the homeostatic maintenance and migration of Langerhans cells. J Allergy Clin Immunol 2015; 136:713-24.
68. Nakajima S, Igyarto BZ, Honda T, Egawa G, Otsuka A, Hara-Chikuma M, et al. Langerhans cells are critical in epicutaneous sensitization with protein antigen via thymic stromal lymphopoietin receptor signaling. J Allergy Clin Immunol 2012; 129:1048-55 e6.
69. Deckers J, Sichien D, Plantinga M, Van Moorleghem J, Vanheerswynghels M, Hoste E, et al. Epicutaneous sensitization to house dust mite allergen requires interferon regulatory factor 4-dependent dermal dendritic cells. J Allergy Clin Immunol 2017; 140:1364-77 e2.
70. Weiss R, Hessenberger M, Kitzmuller S, Bach D, Weinberger EE, Krautgartner WD, et al. Transcutaneous vaccination via laser microporation. J Control Release 2012; 162:391-9.
71. Yao C, Kaplan DH. Langerhans Cells Transfer Targeted Antigen to Dermal Dendritic Cells and Acquire Major Histocompatibility Complex II In Vivo. J Invest Dermatol 2018; 138:1665-8.
72. Luo Y, Wang S, Liu X, Wen H, Li W, Yao X. Langerhans cells mediate the skin-induced tolerance to ovalbumin via Langerin in a murine model. Allergy 2019; 74:1738-47.
73. Kashem SW, Haniffa M, Kaplan DH. Antigen-Presenting Cells in the Skin. Annu Rev Immunol 2017; 35:469-99.
74. West HC, Bennett CL. Redefining the Role of Langerhans Cells As Immune Regulators within the Skin. Front Immunol 2017; 8:1941.
75. Seneschal J, Clark RA, Gehad A, Baecher-Allan CM, Kupper TS. Human epidermal Langerhans cells maintain immune homeostasis in skin by activating skin resident regulatory T cells. Immunity 2012; 36:873-84.
76. Kitashima DY, Kobayashi T, Woodring T, Idouchi K, Doebel T, Voisin B, et al. Langerhans Cells Prevent Autoimmunity via Expansion of Keratinocyte Antigen-Specific Regulatory T Cells. EBioMedicine 2018; 27:293-303.
77. Fernandez M-I, Heuzé ML, Martinez-Cingolani C, Volpe E, Donnadieu M-H, Piel M, et al. The human cytokine TSLP triggers a cell autonomous dendritic cell migration in confined environments. Blood 2011; 118:3862-9.
78. Ebner S, Nguyen VA, Forstner M, Wang YH, Wolfram D, Liu YJ, et al. Thymic stromal lymphopoietin converts human epidermal Langerhans cells into antigen presenting cells that induce pro-allergic T cells. J Allergy Clin Immunol 2007.
79. Altan-Bonnet G, Mukherjee R. Cytokine-mediated communication: a quantitative appraisal of immune complexity. Nat Rev Immunol 2019; 19:205-17.
80. Bagnall J, Boddington C, England H, Brignall R, Downton P, Alsoufi Z, et al. Quantitative analysis of competitive cytokine signaling predicts tissue thresholds for the propagation of macrophage activation. Sci Signal 2018; 11:eaaf3998.
81. Romani N, Flacher V, Tripp CH, Sparber F, Ebner S, Stoitzner P. Targeting skin dendritic cells to improve intradermal vaccination. Curr Top Microbiol Immunol 2012; 351:113-38.

Figure Legends

FIG 1. Overproduction of TSLP in the skin triggers Tfh differentiation and GC reponse in MC903-induced AD mice. **A,** Experimental protocol. Mouse ears were topically treated with MC903 or ethanol (EtOH; as vehicle control) every other day from day (D) 0 to D10 and EDLNs were analyzed at D0, D7 and 11. **B**, Frequency and number of $CXCR5^+$ $PD\text{-}1^+$ Tfh cells in EDLN from MC903-treated Balb/c wildtype (WT) and *Tslp*$^{-/-}$ mice. **C**, Frequency of IL-4 $(AmCyan)^+$ in Tfh cells and cell number of $IL\text{-}4^+$ Tfh cells in EDLNs. **D-E**, Number of $CD95^+$ $GL\text{-}7^+$ GC B cells, $IgG1^+$ B cells and IgE^+ B cells in EDLNs. Values shown are means ± SEMs. **B-D**, one-way ANOVA with Tukey's multiple comparison post-hoc test; **E**, unpaired t-test with Welch's correction. Data are representative of 3 independent experiments with similar results.

FIG 2. Depletion of $Langerin^+$ cells diminishes the MC903-induced Tfh/GC response. **A**, Experimental protocol. $Lang^{DTR}$ mice and wildtype littermate controls (CT) were *i.p*. injected with DT at D-2 and D0 and then every 4 days. Mouse ears were topically treated with MC903 or EtOH every other day from D0 to D10 and EDLNs were analyzed at D11. **B**, Frequency and number of Tfh cells. **C**, IL-4 (AmCyan) expression by Tfh cells. **D**, Total number of GC B cells, $IgG1^+$ and IgE^+ B cells. Values shown are means ± SEMs; one-way ANOVA with Tukey's multiple comparison post-hoc test. Data are representative of 3 independent experiments with similar results.

FIG 3. OVA sensitization through laser-microporated (LMP) skin induces TSLP-dependent Tfh/GC response. **A**, H&E staining of untreated or 30μm-LMP ears of Balb/c WT mice. The red arrow points to a micropore with the disruption of the epidermis. Scale bar, 100 μm. **B**, TSLP protein levels in ears of WT mice at 48h after the indicated treatment. **C**, RNAscope in

situ hybridization for TSLP in untreated or 30μm-LMP-ears at 48h after the microporation. The black arrow points to one of the positive signals. Scale bar, 50 μm. **D**, Experimental protocol for OVA epicutaneous sensitization through LMP ears. OVA or PBS (vehicle) were topically applied on LMP ears at D0, D4, D7 and D11 and EDLNs were analyzed at D13. **E-F**, Frequency and cell number of Tfh cells (**E**) and IL-4 (AmCyan) producing Tfh cells (**F**) in EDLNs. **G**, GC B cell, $IgG1^+$ and IgE^+ B cell numbers in EDLNs. **H**, Serum levels of OVA-IgG1 and OVA-IgE. Values shown are mean ± SEM; one-way ANOVA with Tukey's multiple comparison post-hoc test. Data are representative of 3 independent experiments with similar results.

FIG 4. Depletion of $Langerin^+$ cells does not reduce but rather tends to augment 30μm-LMP/OVA-induced Tfh/GC response. **A**, Experimental protocol. $Lang^{DTR}$ mice and wildtype littermate controls (CT) were *i.p.* injected with DT at D-2, D0 and then every 4 days. Mouse ears were treated by 30μm-LMP/OVA or 30μm-LMP/PBS at D0, D4, D7 and D11 and EDLNs were analyzed at D13. **B**, Frequency and number of Tfh cells. **C**, IL-4 (AmCyan) expression by Tfh cells. **D**, Number of GC B cells, $IgG1^+$ and IgE^+ B cells. **E**, Serum levels of OVA-specific IgG1 and OVA-specific IgE in 30μm-LMP/OVA-sensitized $Lang^{DEP}$ or CT mice. Data are means ± SEM; **B-D**, one-way ANOVA with Tukey's multiple comparison post-hoc test. **E**, unpaired t-test with Welch's correction. Data are representative of 3 independent experiments with similar results.

FIG 5. Depletion of $Langerin^+$ cells or LCs enhances 11μm-LMP/OVA-induced TSLP-dependent Tfh/GC response. **A**, H&E staining of untreated or 11μm-LMP ears of Balb/c WT mice. The red arrow points to a micropore with the impairment of cornified layer. Scale bar, 100 μm. **B**, TSLP protein levels in ears of WT mice. **C**, Comparison of Tfh cells and GC B cells in EDLNs from WT or $Tslp^{-/-}$ mice. **D-F**, Comparison of Tfh cells (**D**), IL-4 (AmCyan)

expression by Tfh cells (**E**) and number of GC B cells, $IgG1^+$ B cells and IgE^+ B cells (**F**) in EDLNs from CT or $Lang^{DEP}$ mice. **G**, Serum OVA-IgG1 and OVA-IgE levels. **H**, Experimental protocol. **I**, Comparison of Tfh cells, GC B cells, $IgG1^+$ and IgE^+ B cells in CT and $huLang^{DEP}$ mice. **J**, Comparison of antigen-specific Tfh cells between LMP/OVA-sensitized CT and $huLang^{DEP}$ mice. EDLNs were *in vitro* stimulated with OVA or PBS (vehicle control), and activation markers CD154, CD25 and OX40 expressed by EDLN-derived Tfh cells were examined. Values shown are mean ± SEM; one-way ANOVA with Tukey's multiple comparison post-hoc test. Data are representative of 2 independent experiments with similar results.

FIG 6. $Langerin^+$ cells counteract LMP/OVA sensitization-induced skin Th2 inflammation and the subsequent asthmatic phenotype. **A**, IL-4 (AmCyan) and IL-13 (DsRed) expression in $TCR\beta^+$ dermal cells. **B**, H&E staining of mouse ears. **C**, IHC staining of mouse ears with anti-MBP (for eosinophils) or anti-MCPT8 (for basophils). Arrows point to positive signals. **D**, Experimental protocol for OVA epicutaneous sensitization and airway challenge. Mice were *i.p.* injected with DT at D-2, D0 and then every 4 days. Mice were either treated with OVA on LMP ears at D0, D4, D7 and D11 or non-treated (NT). All mice were subjected to *i.n.* instillation with OVA from D9 to D12, and analyzed at D13. **E**, Differential cell counting for eosinophils (Eos), neutrophils (Neutro), lymphocytes (Lympho) and macrophages (Macro) in BAL. **F**, RNA levels of indicated genes in BAL cells by RT-qPCR. **G**, Lung sections were stained with H&E for histology or PAS for goblet cell hyperplasia analyses. B: bronchiole, V: blood vessel. Scale bar, 100μm. Values shown are means ± SEM; one-way ANOVA with Tukey's multiple comparison post-hoc test. Data are representative of 2 independent experiments with similar results.

FIG 7. Transcriptomic analyses of migratory DCs in EDLNs of Lang^{GFP} mice upon MC903 treatment or epicutaneous OVA sensitization. Lang^{GFP} mice were treated with MC903 at D0, D2 and D4 or 30μm-LMP/OVA on D0 and D3; EDLNs were collected at D5 for cell sorting and RNAseq analyses. **A**, Left, percentage of variability explained by each Principal Component. Right, principal component analyses showing PC1, PC2 and PC3. **B,** Venn diagram showing the number of upregulated and downregulated genes (fold change > 1.5; $p < 0.05$; raw read > 200 in at least one sample of all groups), and the number of commonly upregulated or downregulated genes between the comparisons, as indicated. Pos_NT, Pos_MC, Pos_OVA: GFP^{Pos} migDCs from non-treated, MC903-treated or LMP/OVA-treated Lang^{GFP} mice; Neg_NT, Neg_MC, Neg_OVA: GFP^{neg} migDCs from non-treated, MC903-treated or LMP/OVA-treated Lang^{GFP} mice. **C**, Selected genes corresponding to gene ontology terms. *, $p<0.05$; NS, non significant. **D**, Heatmaps of the reported TSLP pathway genes, which are significantly upregulated in Pos_MC vs Pos_NT. **E**, Heatmap of Tnfsf4 (encoding OX40L) from RNAseq data, and RT-qPCR analyses.

FIG 8. A schematic representation of the dual functions of LCs in regulating TSLP-dependent Tfh cell and Th2 cell response, revealed by two experimental AD mouse models, triggered by the overproduction of TSLP through topical application of MC903, or induced by epicutaneous allergen ovalbumin (OVA) sensitization.

Supplementary Figure Legends

FIG E1. **(A)** CXCR5^{+} PD-1^{+} Tfh cells produce IL-4 (AmCyan) but not IL-13 (dsRed) in EDLNs of MC903-treated 4C13R$^{Tg/0}$ mice at D11. 4C13R$^{0/0}$ EDLNs were used as gating control. **(B)** Frequency and number of CXCR5^{-} CD4^{+} (non-Tfh) cells producing IL-4 (AmCyan) or IL-13 (dsRed), representing Th2 cells, in EDLNs from Balb/c wildype (WT) and *Tslp*$^{-/-}$ mice in the background of 4C13R$^{Tg/0}$, treated with MC903 or ethanol, and analyzed at D0, D7 and D11. **(C)** The majority of IgG1^{+} but not IgE^{+} B cells in EDLNs from MC903-treated wildtype Balb/c mice are GL-7^{+} CD95^{+}.

FIG E2. Germinal center staining. Wildtype (WT) and *Tslp*$^{-/-}$ mice were treated with MC903 **(A)** or subjected to OVA-sensitization **(B)** as shown in FIG 1A and 4D respectively. EDLN were collected and fixed overnight with 4% PFA at 4°C. After 2 times 30 minutes of wash in PBS at room temperature (RT), samples were included in 4% low melting point agarose in PBS. Vibratome sections of 100µm were blocked with 5% normal donkey serum (NDS), 0.1% Triton X-100 in PBS and then stained overnight at 4°C with anti CD4-AlexaFluor 647 (RM4-5, Biolegend, d=1/100; shown in blue), anti IgD-FITC (11-26c.2a, BD Biosciences, d=1/50; shown in green) and biotinylated PNA (Vectorlabs, d=1/250; shown in red) diluted in 5% NDS, 0.1% Triton X-100 in PBS. Sections were subsequently incubated 1h at RT with Neutravidin-Dylight550 (ref 84606, Thermofisher, d=1/200) diluted in PBS. After 2 washing of 30 minutes with PBS at RT, sections were kept at 4°C in PBS containing Hoechst 33342 (Sigma Aldrich) and images were acquired using Leica LSI confocal macroscope. Measurements were performed with ImageJ software. Data are means ± SEM; one-way ANOVA with Tukey's multiple comparison post-hoc test.

FIG E3. Selective depletion of LCs leads to a diminished Tfh cell differentiation in MC903 model. **(A)** Experimental protocol. $Lang^{DTR}$ mice and wildtype littermate controls were *intraperitoneally* (*i.p.*) injected with diphtheria toxin (DT) at D-2 and D0. Mouse were then topically treated with MC903 or EtOH every other day from D13 to D19 and ear draining lymph nodes (EDLN) were analyzed at D20. **(B)** Frequency and number of $CXCR5^+$ $PD\text{-}1^+$ Tfh cells in $Lang^{DEP}$ mice and CT at D20. **(C)** Experimental protocol. $huLang^{DTR}$ mice and wildtype littermate controls were intraperitoneally *i.p.* injected with DT at D-2 and D0. Mouse were then topically treated with MC903 or EtOH every other day from D0 to D10 and EDLN were analyzed at D11. **(D)** Frequency and number of $CXCR5^+$ $PD\text{-}1^+$ Tfh cells in $huLang^{DEP}$ mice and CT at D11. Values shown are means ± SEMs; one-way ANOVA with Tukey's multiple comparison post-hoc test. Data are representative of 2 independent experiments with similar results.

FIG E4. TSLP is crucially required for 30μm-LMP/OVA-induced skin Th2 inflammation. **(A)** Hematoxylin and eosin (HE) staining of mouse ears. **(B)** Immunohistochemistry staining of mouse ears with anti-MBP antibody (for eosinophils) or anti-MCPT8 antibody (for basophils). Arrow points to one of the positive cells. Scale bar, 100μm. **(C-D)** IL-4 (AmCyan) and IL-13 (dsRed) expression in $TCR\beta^+$ dermal cells **(C)** or $CXCR5^-$ $CD4^+$ (non-Tfh) cells **(D)**.

FIG E5. Depletion of $Langerin^+$ cells slightly diminishes the MC903- induced Th2 cell response. Comparison of IL-4 and IL-13 expression among $CXCR5^-CD4^+$ (non-Tfh) cell in the EDLN **(A)**, or among $TCR\beta^+$ cells in the dermis **(B)** of EtOH- or MC903-treated control (CT) or $Lang^{DEP}$ mice, all in the background of $4C13R^{Tg/0}$.

FIG E6. Depletion of Langerin^{+} cells increases the LMP/OVA-induced Th2 cell response in EDLNs. Comparison of IL-4 and IL-13 expression among CXCR5^{-}CD4^{+} (non-Tfh) cell in EDLNs from LMP/OVA-treated control (CT) or Lang^{DEP} in the background of 4C13R$^{Tg/0}$ mice.

FIG E7. 11μm-LMP/OVA-induced skin inflammation is enhanced in mice with the depletion of Langerin^{+} DCs or LCs. Hematoxylin and eosin staining of ears from Lang^{DEP} (**A**, top) and huLang^{DEP} (**B**, top) mice after 11μm-LMP/OVA sensitization. Immunohistochimstry for MBP (eosinophils) and MCPT8 (basophils) of ears from Lang^{DEP} (**A**, bottom) and huLang^{DEP} (**B**, bottom) mice after 11μm-LMP/OVA treatment. Scale bar, 100μm.

FIG E8. LCs counteract LMP/OVA sensitization-induced skin inflammation and the subsequent asthmatic response. **(A)** Experimental protocol for OVA epicutaneous sensitization and airway challenge. Mice were intraperitoneally injected with DT at D-2, D0. Mice were either treated with OVA on LMP ears at D0, D4, D7 and D11 or ears were non treated (NT). All mice were subjected to *intranasal* (*i.n.*) instillation with OVA from D9 to D12. Ears and lungs were analyzed at D13. **(B)** H&E staining of mouse ears. Scale bar, 100μm. **(C)** IHC staining of mouse 30μm-LMP/OVA ears with anti-MBP (for eosinophils) or anti-MCPT8 (for basophils). **(D)** Differential counting of eosinophils (Eos), neutrophils (Neutro), lymphocytes (Lympho) and macrophages (Macro) in BAL. **(E)** RNA levels of indicated genes in BAL cells by RT-qPCR. **(F)** Lung sections were stained with H&E for histological analyses or PAS for goblet cell hyperplasia analyses. B: bronchiole; V: blood vessel. Scale bar, 250μm. **(G)** Experimental protocol for OVA i.p. sensitization and airway challenge. Mice were *i.p.* injected with DT at D-2 and D0. Mice were *i.p.* sensitized with OVA/alum at D0 and D4, and subjected to *i.n.* instillation with OVA from D9 to D12. Lungs were analyzed at D13. **(H)** Differential cell counting in BAL. Data are means ± SEM; unpaired two-tailed t-test.

FIG E9. Transcriptomic analyses of migratory DCs in EDLNs of $Lang^{GFP}$ mice upon MC903 treatment or epicutaneous OVA sensitization. $Lang^{GFP}$ mice were treated with MC903 at D0, D2 and D4 or 30µm-LMP/OVA on D0 and D3; EDLNs were collected at D5 for cell sorting and RNAseq analyses. **(A)** Gating strategy used to sort resident (res) and migratory (mig) GFP^{pos} and GFP^{neg} DCs. **(B)** Heatmap generated with the input of upregulated genes identified in Pos_MC compared with Pos_NT (FC > 1.5; $p < 0.05$; raw read > 200 in at least one sample of the Pos groups), to visually assess the results of clustering on the data to observe trends of expression for genes across all groups. Z score of the expression level is used to generate heatmap. Pos_NT, Pos_MC, Pos_OVA: GFP^{pos} migDCs from non-treated, MC903-treated or LMP/OVA-treated $Lang^{GFP}$ mice; Neg_NT, Neg_MC, Neg_OVA: GFP^{neg} migDCs from non-treated, MC903-treated or LMP/OVA-treated $Lang^{GFP}$ mice.

Two clusters C1 and C2 were revealed. The cluster C1 genes exhibited the expression trends: 1) in non-treated groups, they had a lower expression in GFP^{pos} cells than in GFP^{neg} cells (Pos_NT < Neg_NT); 2) in MC903-treated groups, their expression in GFP^{pos} cells increased, reaching a similar or higher expression than non-treated GFP^{neg} cells (Pos_MC = or > Neg_NT), and their expression in GFP^{neg} cells was also increased (Neg_MC > Neg_NT), with a higher level than Pos_MC cells; 3) in OVA-treated groups, the expression of some genes was also increased in GFP^{neg} cells (Neg_OVA versus Neg_NT) (subcluters of C1: a, b and c) while others remained not changed. Together, expression features of the cluster C1 suggest that in the MC903-AD, $Langerin^{+}$ migDCs acquire many gene expression of $Langerin^{-}$ migDCs, and share the upregulation of these genes with $Langerin^{-}$ migDCs; and moreover, the upregulation of some (although less) of these genes also occurs in $Langerin^{-}$ migDCs (but not $Langerin^{+}$ migDCs) in OVA-AD.

Different from the cluster C1, the cluster C2 genes were highly upregulated in Pos_MC; some of them were also upregulated in Neg_MC (but reaching a lower level) and very few of them were upregulated in Neg_OVA, suggesting that this cluster represents the upregulated genes rather specific for Langerin^{+} migDCs under MC903 treatment.

FIG E10. (A) Heatmap generated with the input of downregulated genes identified in Pos_MC compared with Pos_NT (FC > 1.5; $p < 0.05$; raw read > 200 in at least one sample of the Pos groups), to visually assess the results of clustering on the data to observe trends of expression for genes across all groups. Z score of the expression level was used to generate heatmap. **(B)** Selected genes corresponding to gene ontology terms for Cytokine activity, Regulation of transcription, Regulation of cell migration, or T cell costimulation. *, adjusted $p<0.05$; NS, non significant.

FIG E11. IL-6 neutralization does not significantly diminish Tfh cell differentiation and GC B cell numbers. **(A)** experimental scheme. 4C13R$^{Tg/0}$ mice were i.p. injected with 200 mg anti-IL-6 neutralizing antibody (@IL-6; Clone MP5-20F3, BioXcell) every other day from D0 to D10, and mouse ears were topically treated with MC903 or EtOH every other day from D0 to D10. EDLNs were analyzed at D7 or D11. **(B)** Frequency and number of CXCR5^{+} PD-1^{+} Tfh cells. **(C)** IL-4 (AmCyan) expression by Tfh cells. **(D)** Frequency and number of CD95^{+} GL-7^{+} GC B cells at D11. Data are means ± SEM, one-way ANOVA with Tukey's multiple comparison post-hoc test.

FIG E12. MC903 treatment leads to increased numbers of both langerin-GFP^{pos} and langerin-GFP^{neg} migratory DCs in EDLNs at D5. Lang^{GFP} mice were treated with MC903 at D0, D2 and D4, or 30µm-LMP/OVA at D0 and D3, or tape-stripping (TS)/OVA at D0 and D3, and EDLNs

were collected at D5 for flow cytometry analyses. Absolute numbers of GFP-positive (GFP^{pos}) and -negative (GFP^{neg}) migratory DCs in EDLN, compared with non-treated (NT), are shown.

FIG E13. Depletion of $Langerin^{+}$ cells enhances the TS/OVA-induced Tfh/GC response and the subsequent asthmatic phenotype. **(A)** H&E staining of untreated or tape-stripped (TS) Balb/c wildtype mice. Arrow points to the absence of stratum corneum in TS-ear. Scale bar, 100µm. **(B)** Dorsal side of ears of WT mice were tape-stripped 10 times and topical treated with 200µg of OVA in 10µl PBS. TSLP protein levels in ears were measured by ELISA at 48h after treatment. **(C)** Experimental protocol. $Lang^{DTR}$ mice and wildtype littermate controls (CT), in the background of $4C13R^{Tg/0}$, were i.p. injected with DT at D-2, D0 and then every 4 days. OVA (200µg) were topically applied on TS-ears at D0, D4, D7 and D11. All mice were subjected to intranasal (i.n.) instillation with 50µg of OVA from D9 to D12 and analyzed at D13. **(D-F)** Frequency and number of Tfh cells **(D)**, IL-4 (AmCyan) expression by Tfh cells **(E)** and numbers of $CD95^{+}$ $GL\text{-}7^{+}$ GC B cells, $IgG1^{+}$ and IgE^{+} B cells in EDLNs **(F)**. **(G)** Serum levels of OVA-IgG1 and OVA-IgE. **(H)** Differential cell counting for eosinophils (Eos), neutrophils (Neutro), lymphocytes (Lympho) and macrophages (Macro) in BAL. **(I)** H&E staining of lung sections. B: bronchiole; V: blood vessel. Scale bar, 250µm. Data are means ± SEM; unpaired two-tailed t-test.

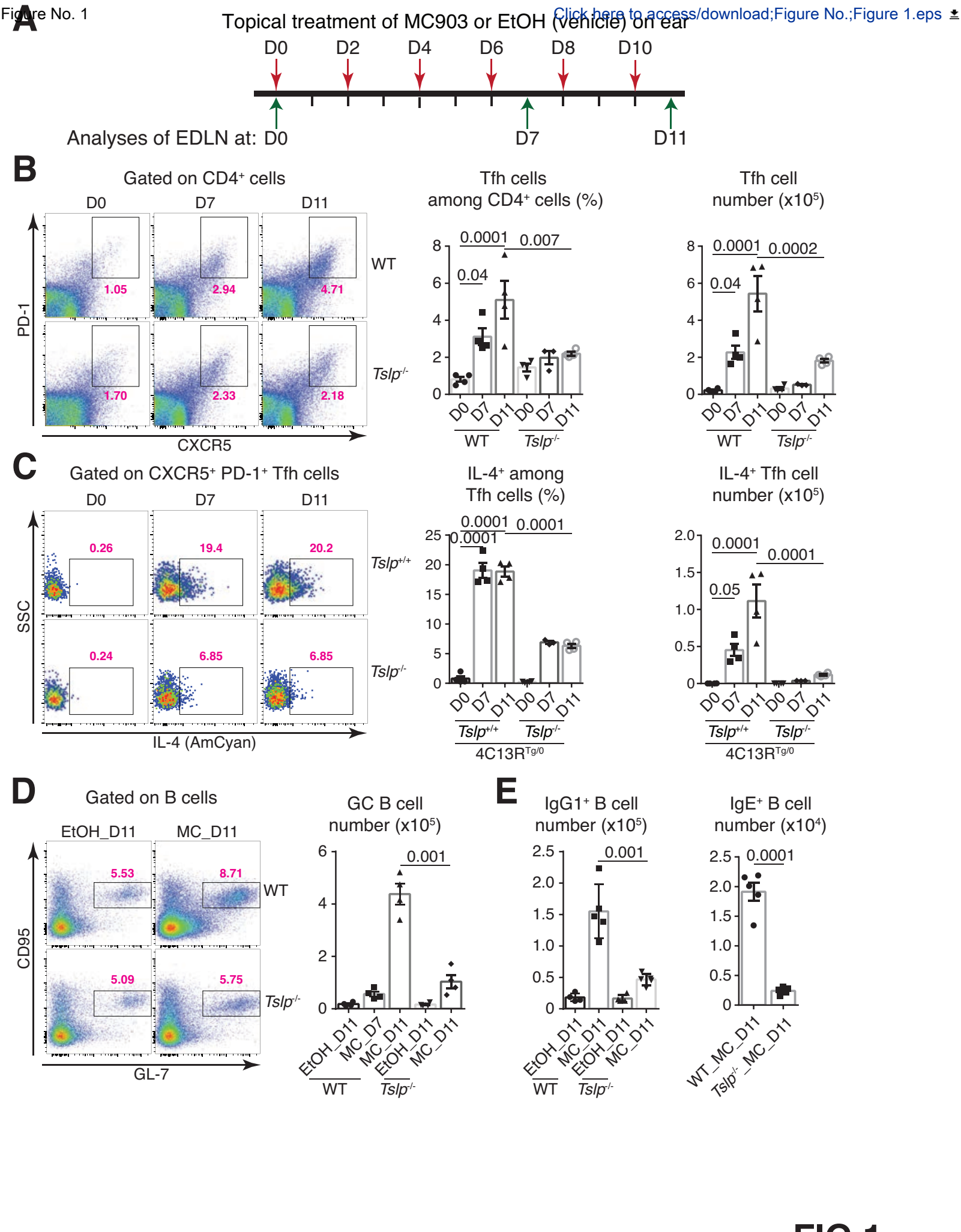

FIG 1

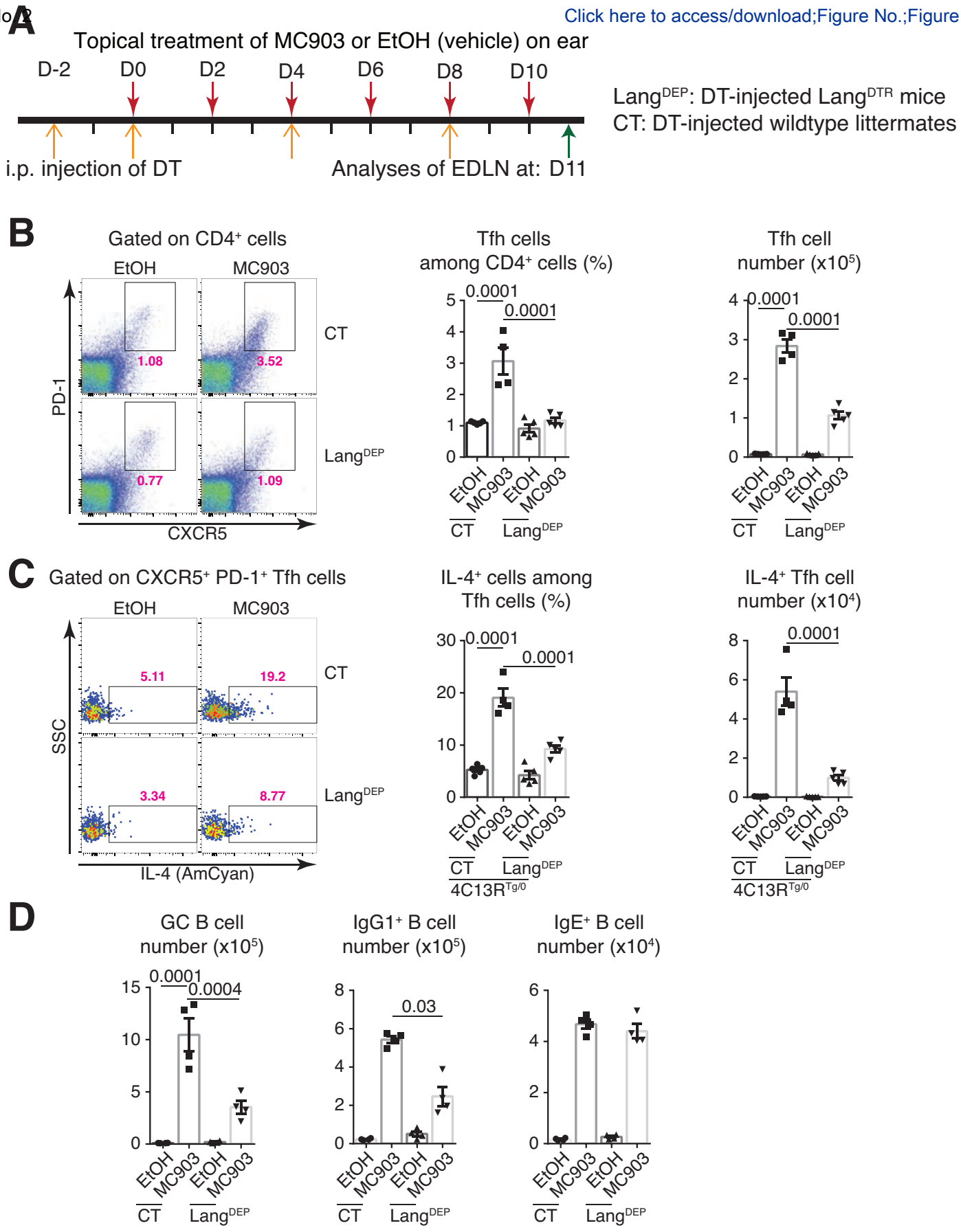

FIG 2

Figure No. 3

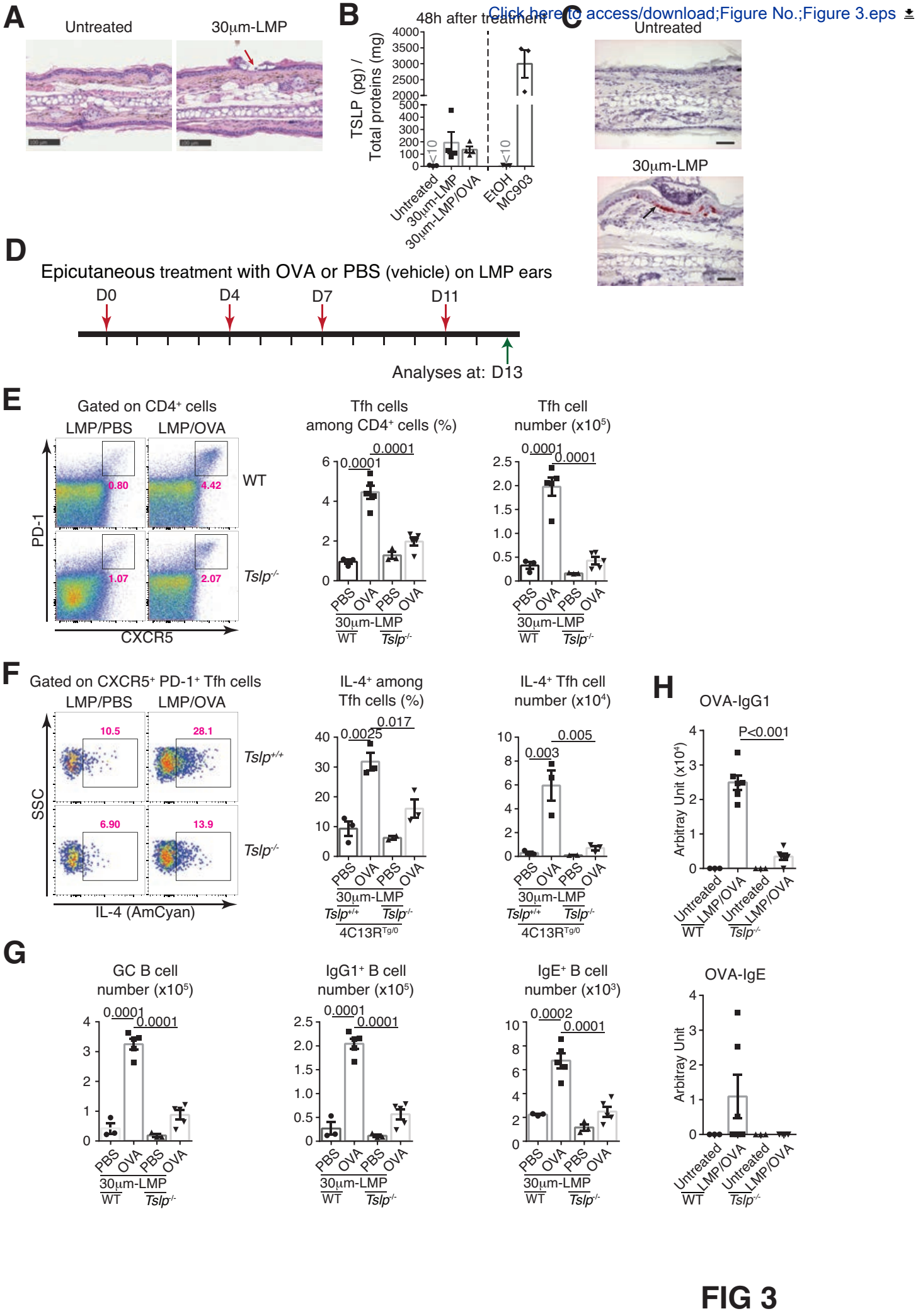

FIG 3

Figure No. 4

Click here to access/download;Figure No.;Figure 4.eps

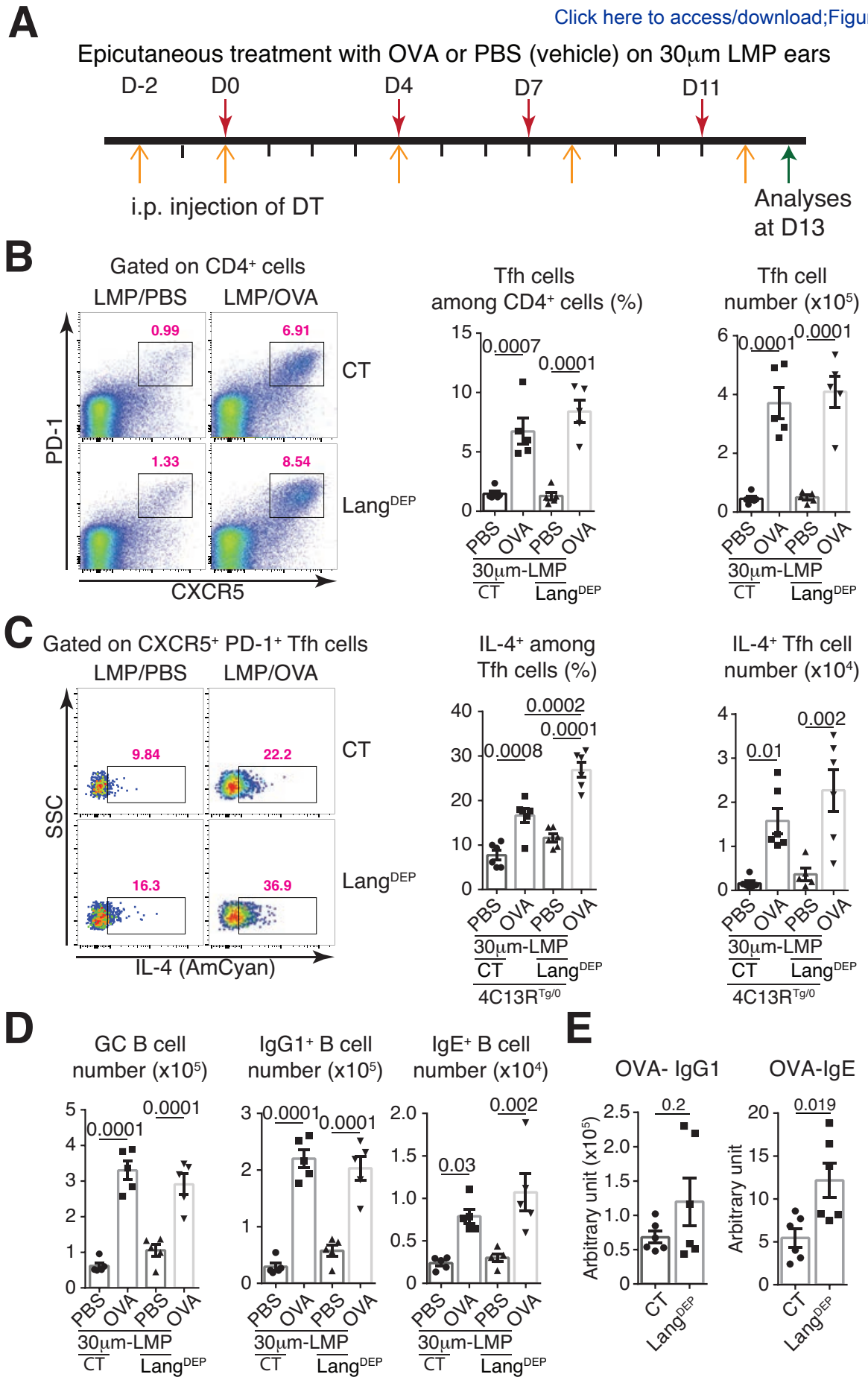

FIG 4

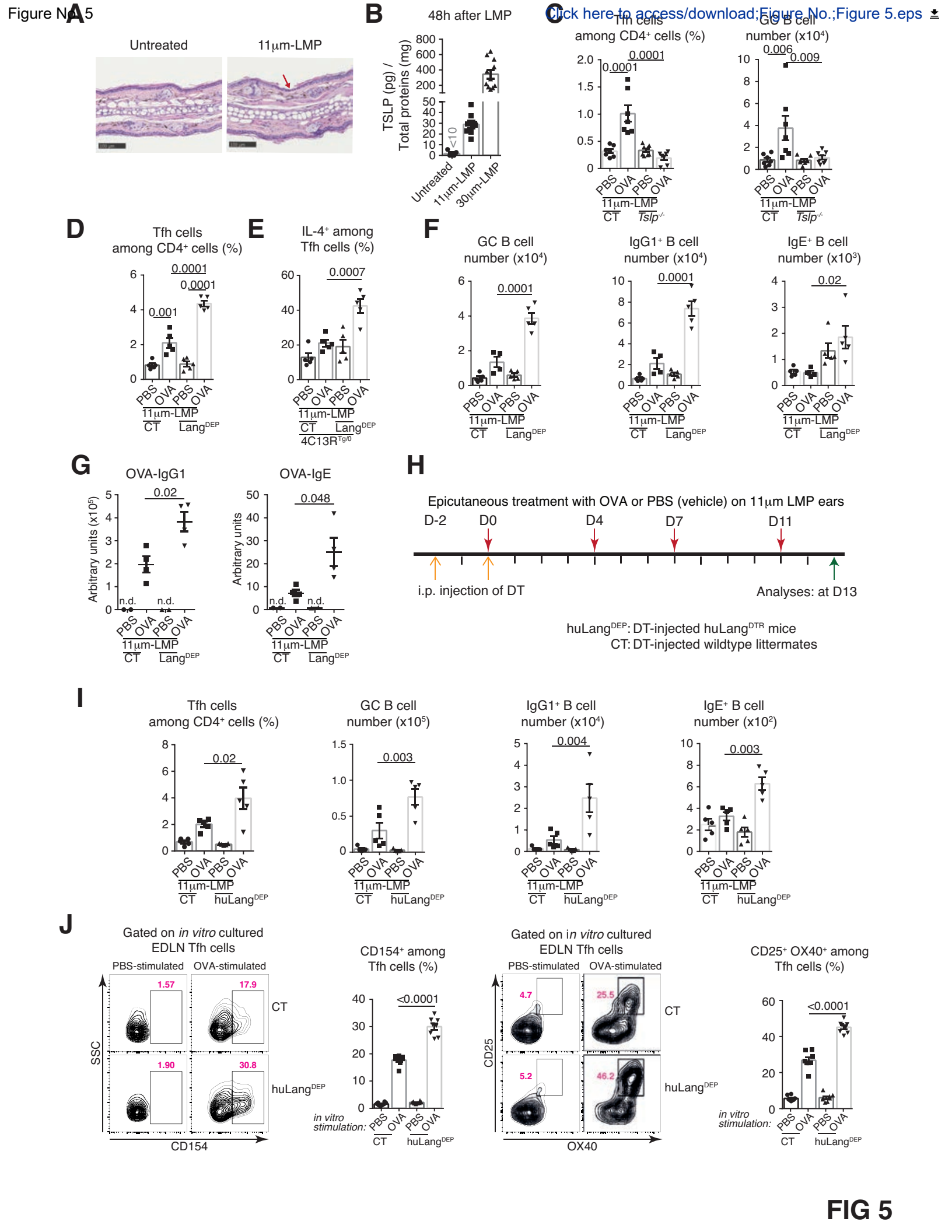

FIG 5

Figure No. 6

Click here to access/download;Figure No.;Figure 6.eps

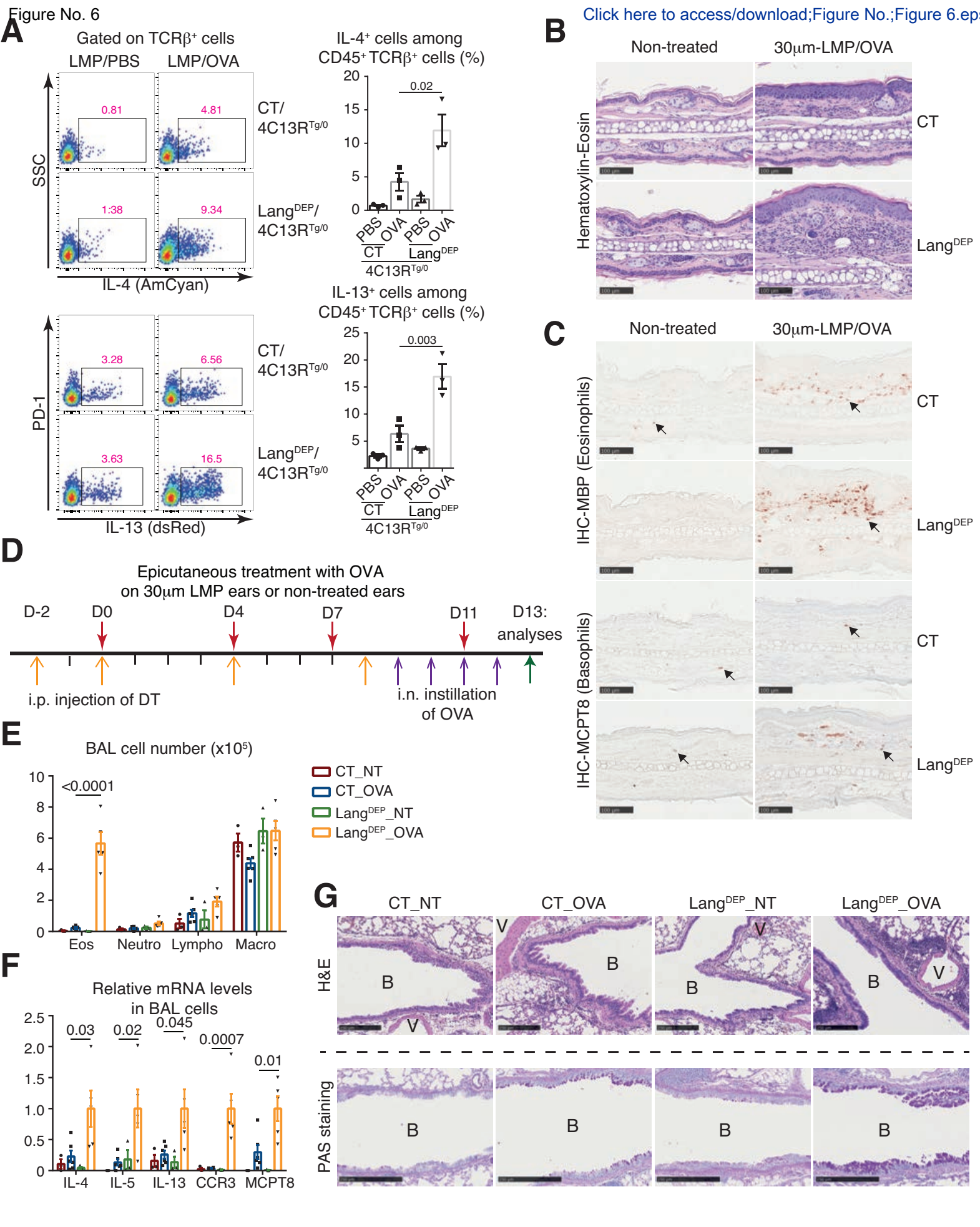

FIG 6

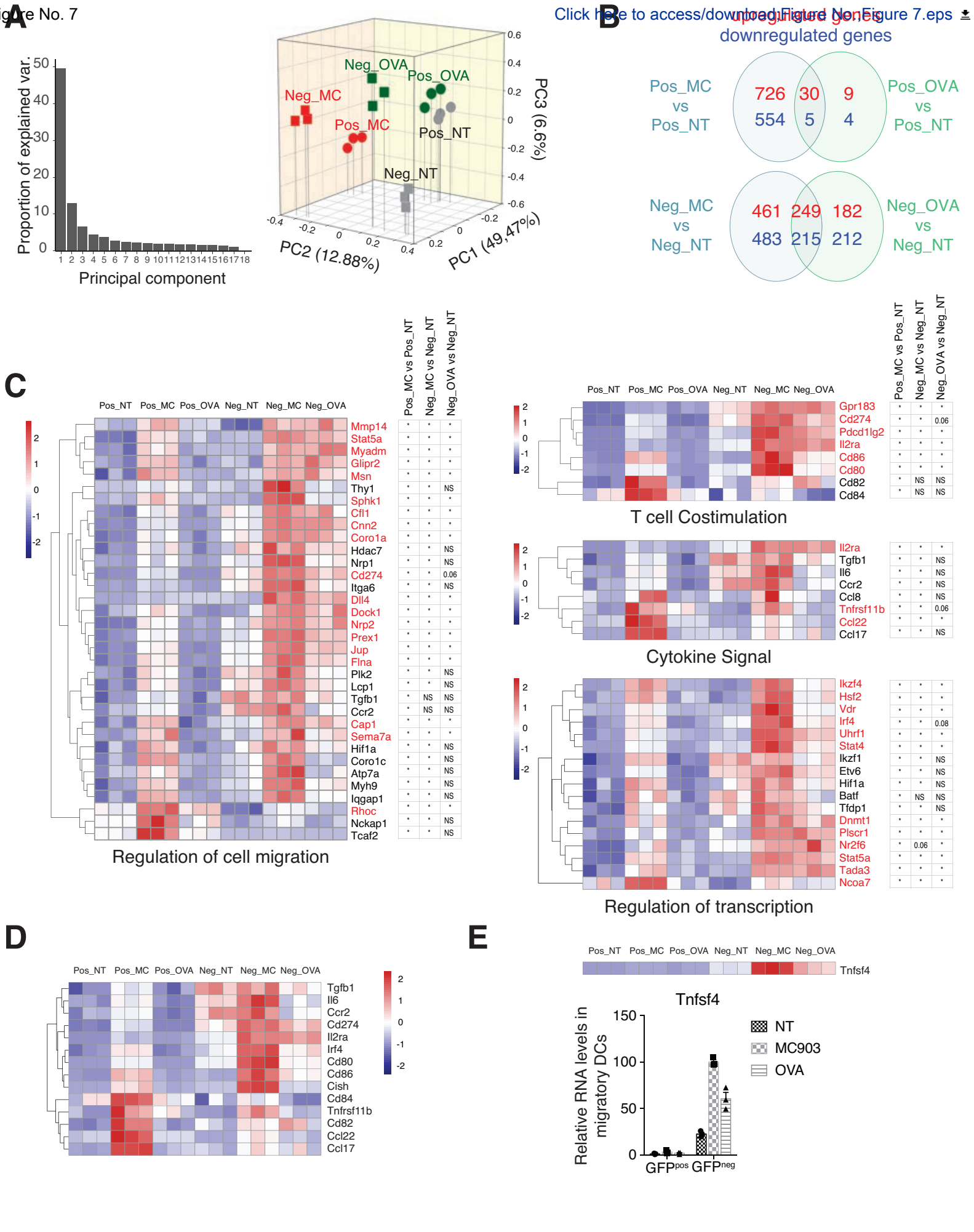

FIG 7

Figure No. 8

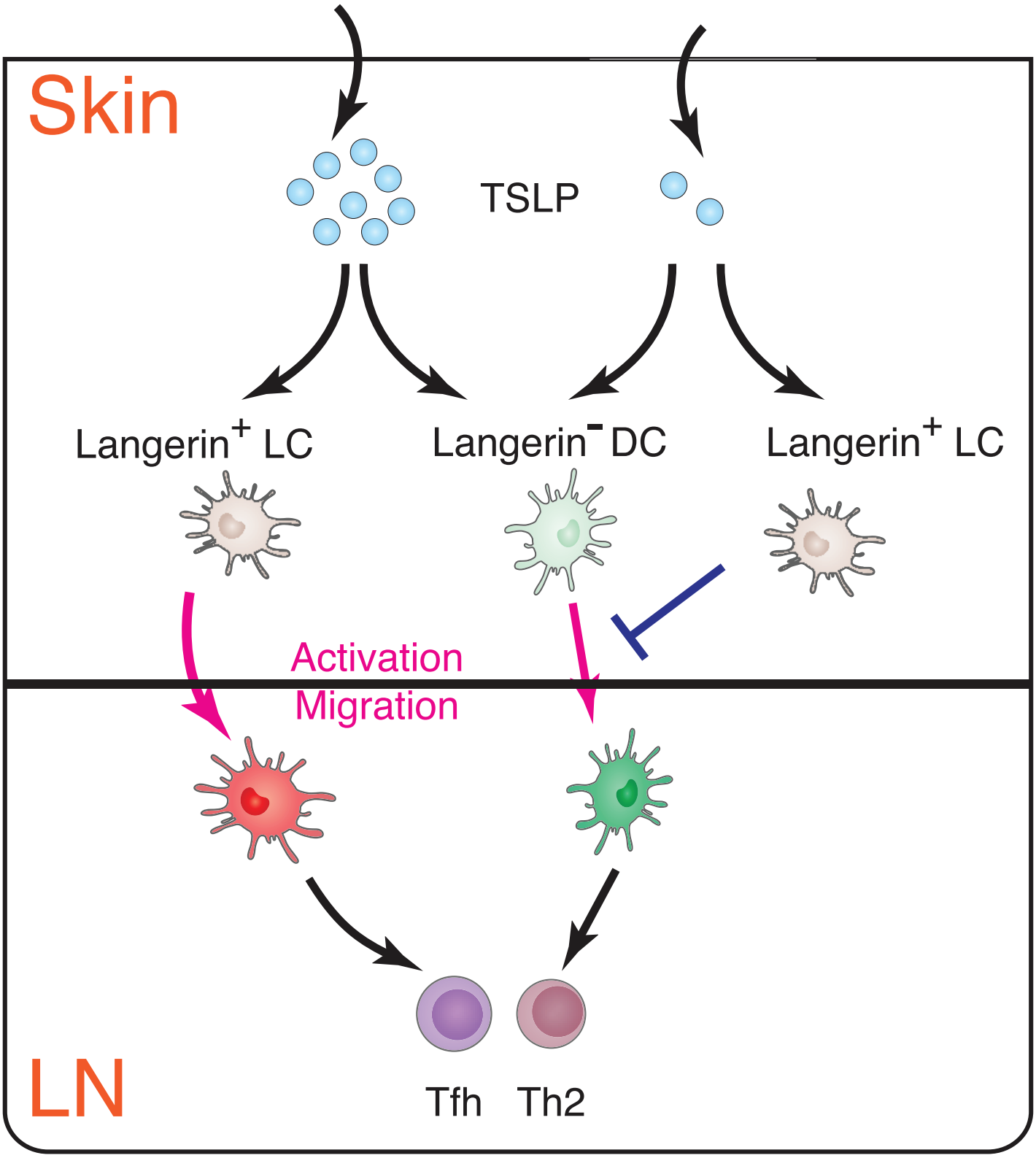

FIG 8

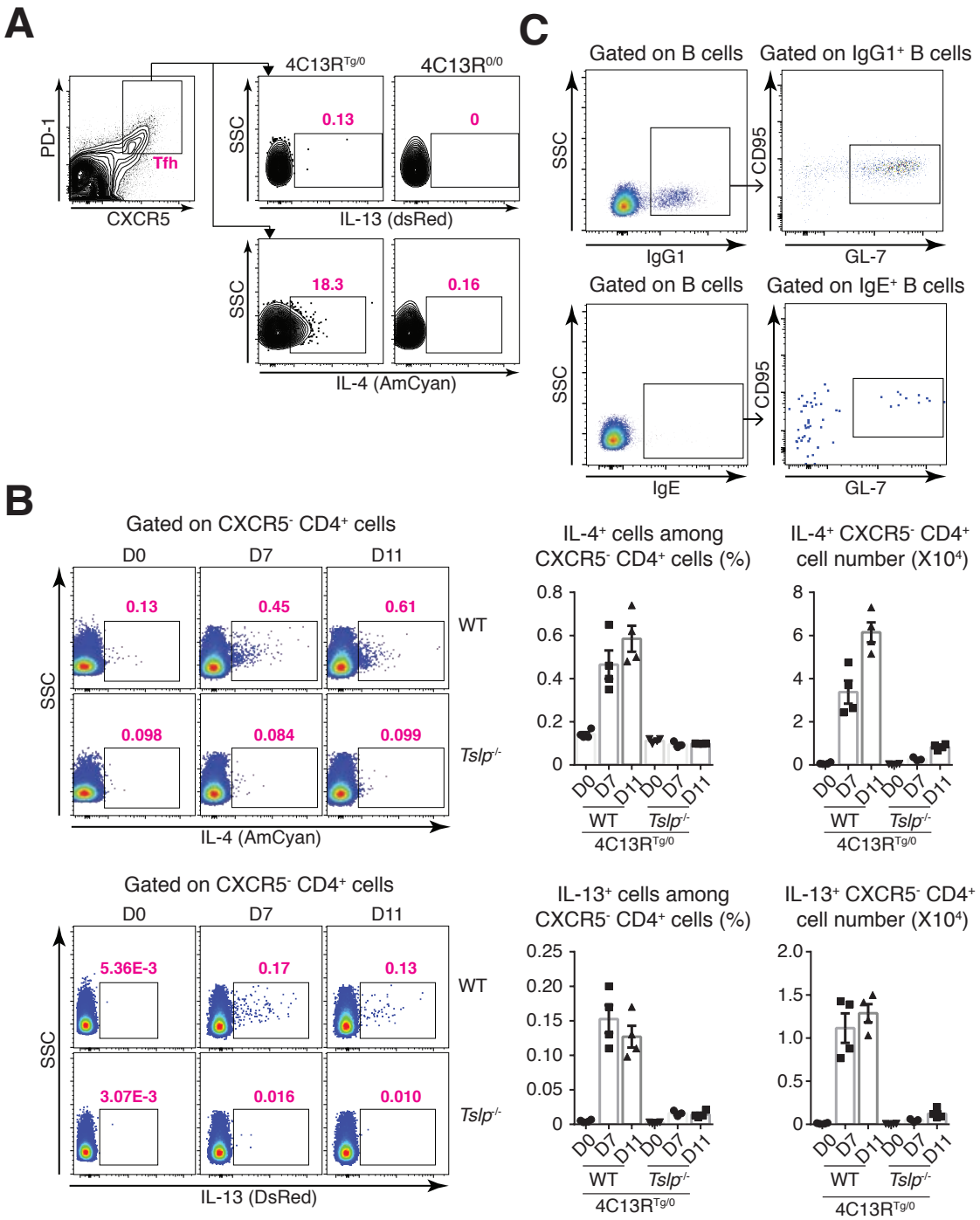

FIG E1.

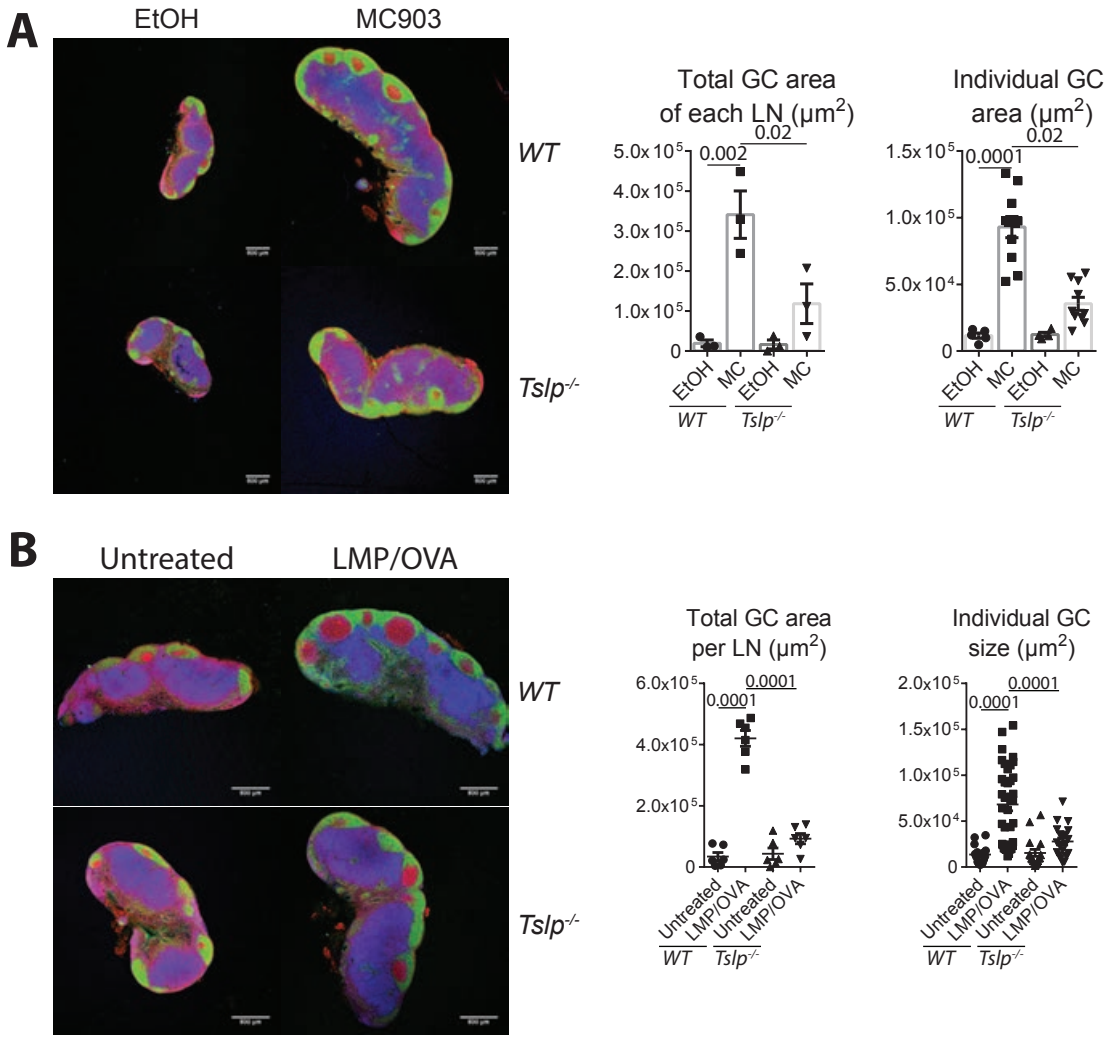
A
EtOH
MC903
WT
Tslp-/-
Total GC area of each LN (μm2)
Individual GC area (μm2)
0.02
0.002
0.0001
EtOH
MC
WT
Tslp-/-
B
Untreated
LMP/OVA
Total GC area per LN (μm2)
Individual GC size (μm2)
0.0001

FIG E2.

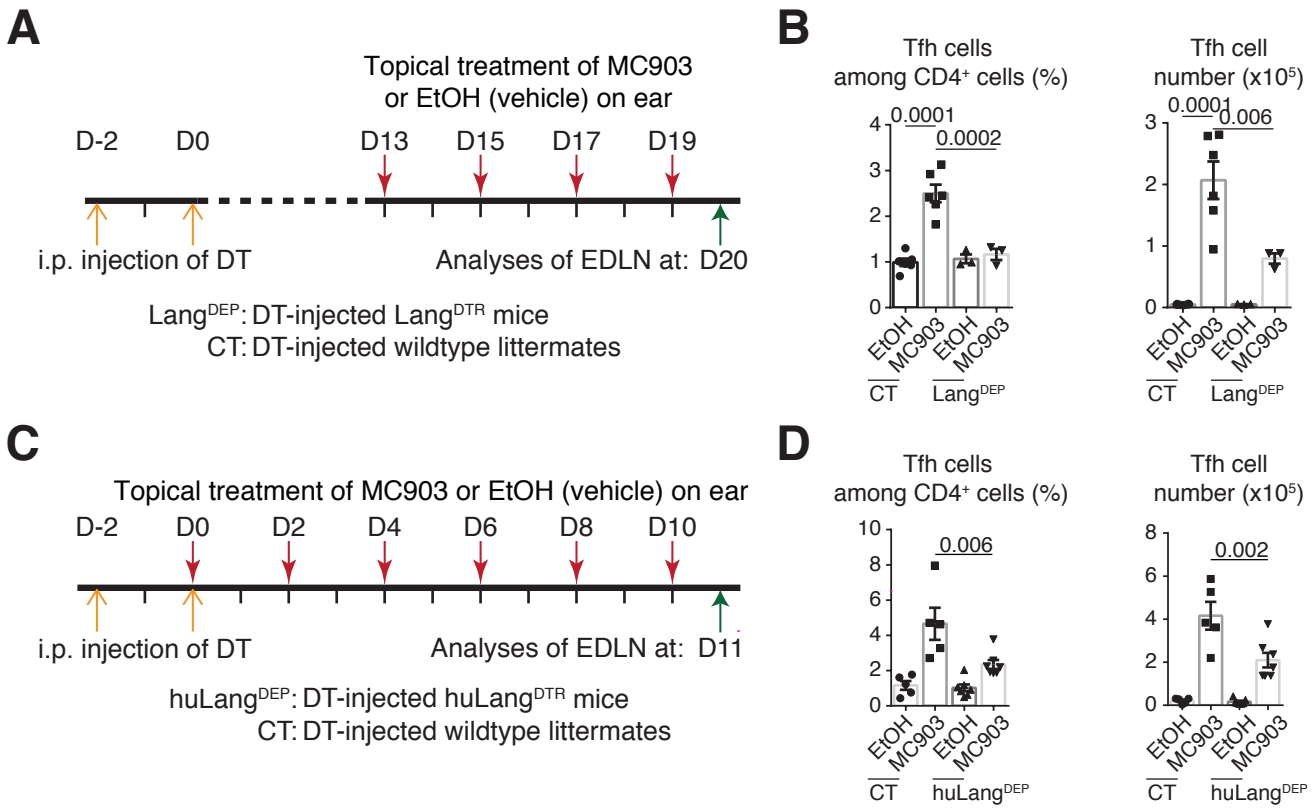
A
Topical treatment of MC903
or EtOH (vehicle) on ear
D-2
D0
D13
D15
D17
D19
i.p. injection of DT
Analyses of EDLN at: D20
Lang^DEP: DT-injected Lang^DTR mice
CT: DT-injected wildtype littermates
B
Tfh cells
among CD4+ cells (%)
0.0001
0.0002
EtOH
MC903
EtOH
MC903
CT
Lang^DEP
Tfh cell
number (x10^5)
0.0001
0.006
EtOH
MC903
EtOH
MC903
CT
Lang^DEP
C
Topical treatment of MC903 or EtOH (vehicle) on ear
D-2
D0
D2
D4
D6
D8
D10
i.p. injection of DT
Analyses of EDLN at: D11
huLang^DEP: DT-injected huLang^DTR mice
CT: DT-injected wildtype littermates
D
Tfh cells
among CD4+ cells (%)
0.006
EtOH
MC903
EtOH
MC903
CT
huLang^DEP
Tfh cell
number (x10^5)
0.002
EtOH
MC903
EtOH
MC903
CT
huLang^DEP

FIG E3.

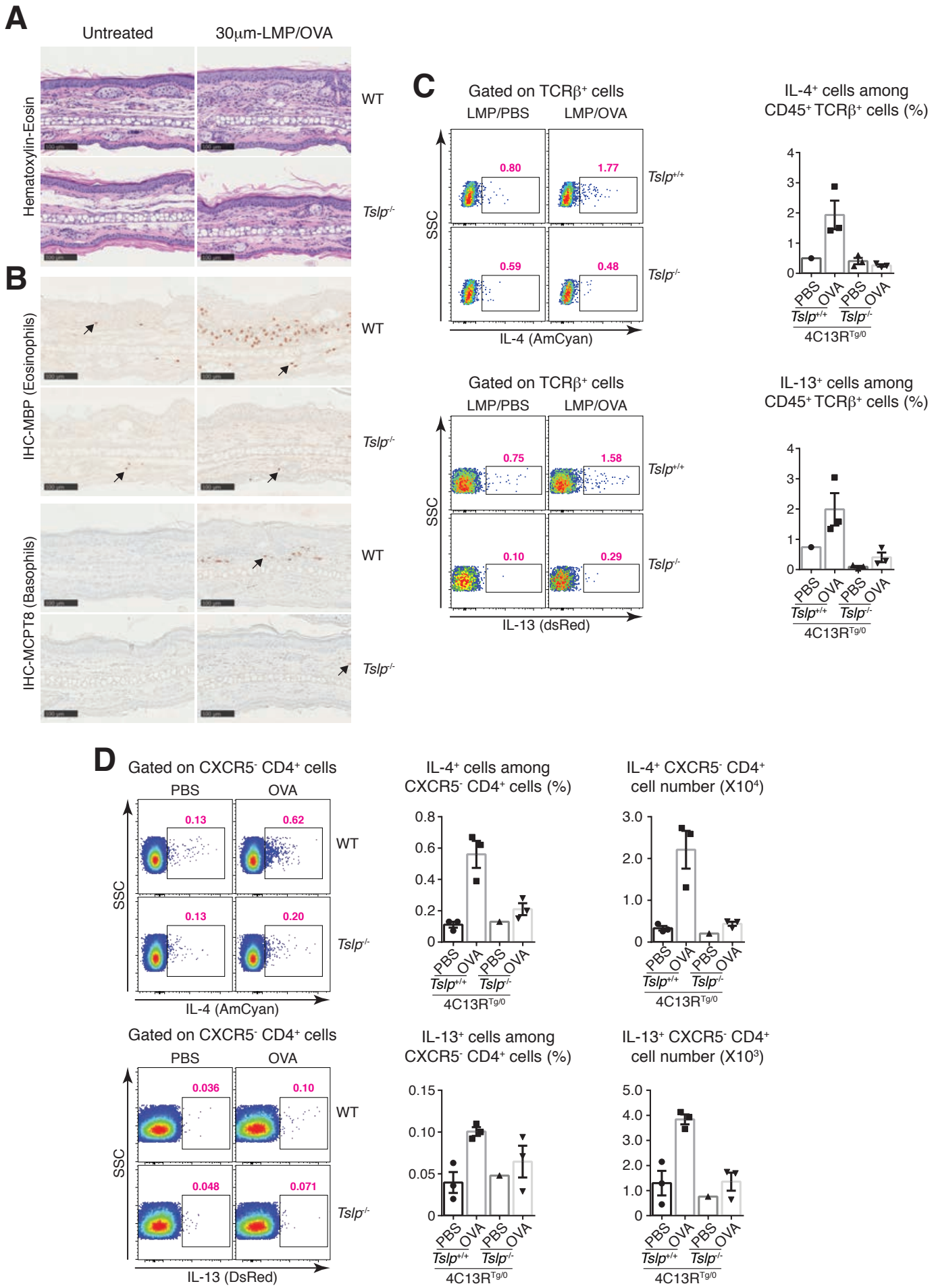
A
Untreated
30μm-LMP/OVA
Hematoxylin-Eosin
WT
Tslp-/-
B
IHC-MBP (Eosinophils)
IHC-MCPT8 (Basophils)
C
Gated on TCRβ+ cells
LMP/PBS
LMP/OVA
0.80
1.77
0.59
0.48
SSC
IL-4 (AmCyan)
IL-4+ cells among CD45+ TCRβ+ cells (%)
PBS
OVA
Tslp+/+
Tslp-/-
4C13RTg/0
0.75
1.58
0.10
0.29
IL-13 (dsRed)
IL-13+ cells among CD45+ TCRβ+ cells (%)
D
Gated on CXCR5- CD4+ cells
0.13
0.62
0.13
0.20
IL-4+ cells among CXCR5- CD4+ cells (%)
IL-4+ CXCR5- CD4+ cell number (X10⁴)
0.036
0.10
0.048
0.071
IL-13+ cells among CXCR5- CD4+ cells (%)
IL-13+ CXCR5- CD4+ cell number (X10³)

FIG E4.

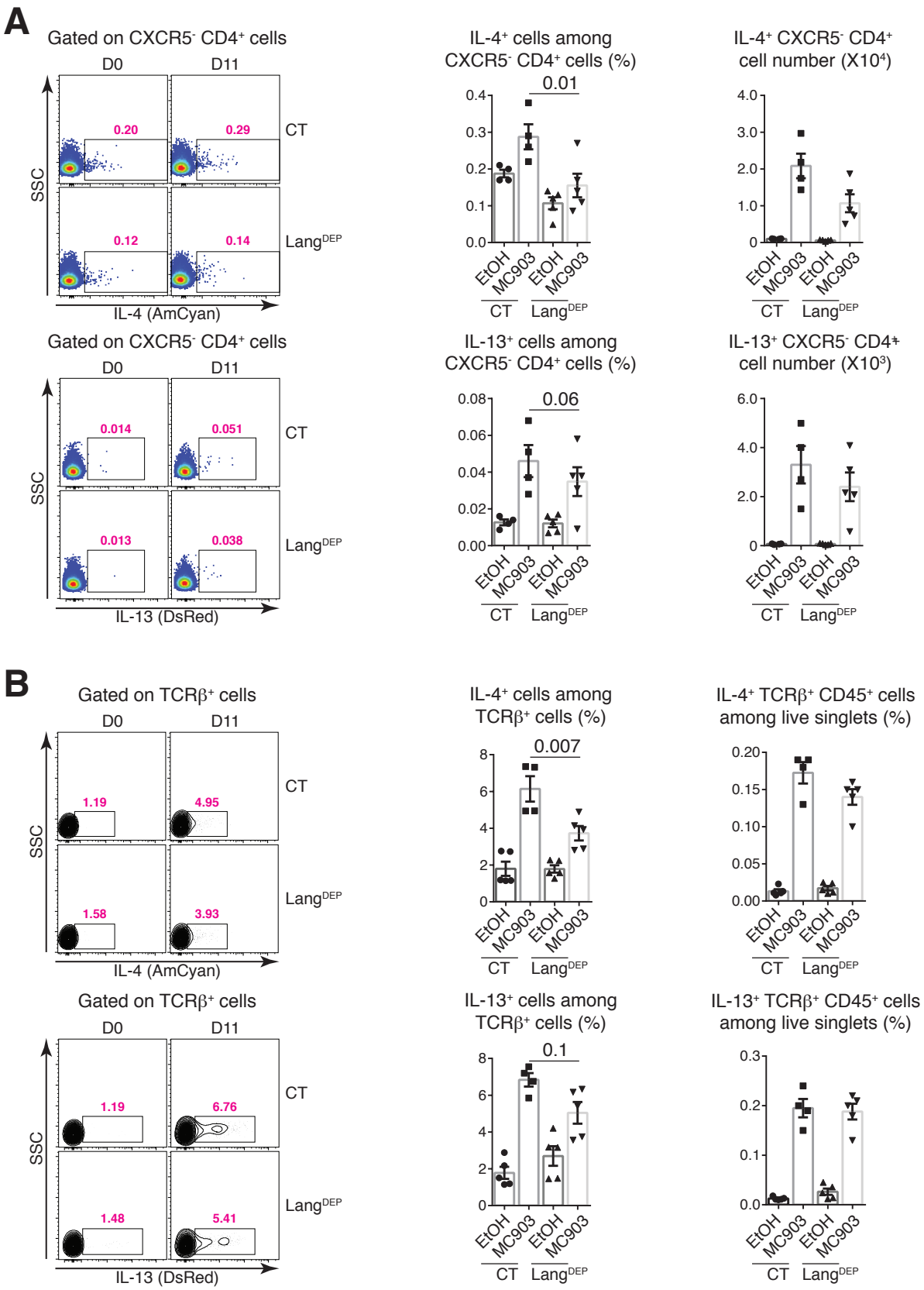
A
Gated on CXCR5- CD4+ cells
D0
D11
0.20
0.29
0.12
0.14
CT
LangDEP
SSC
IL-4 (AmCyan)
IL-4+ cells among CXCR5- CD4+ cells (%)
0.01
IL-4+ CXCR5- CD4+ cell number (X10⁴)
Gated on CXCR5- CD4+ cells
0.014
0.051
0.013
0.038
IL-13 (DsRed)
IL-13+ cells among CXCR5- CD4+ cells (%)
0.06
IL-13+ CXCR5- CD4+ cell number (X10³)
EtOH
MC903
B
Gated on TCRβ+ cells
1.19
4.95
1.58
3.93
IL-4+ cells among TCRβ+ cells (%)
0.007
IL-4+ TCRβ+ CD45+ cells among live singlets (%)
6.76
1.48
5.41
IL-13+ cells among TCRβ+ cells (%)
0.1
IL-13+ TCRβ+ CD45+ cells among live singlets (%)

FIG E5.

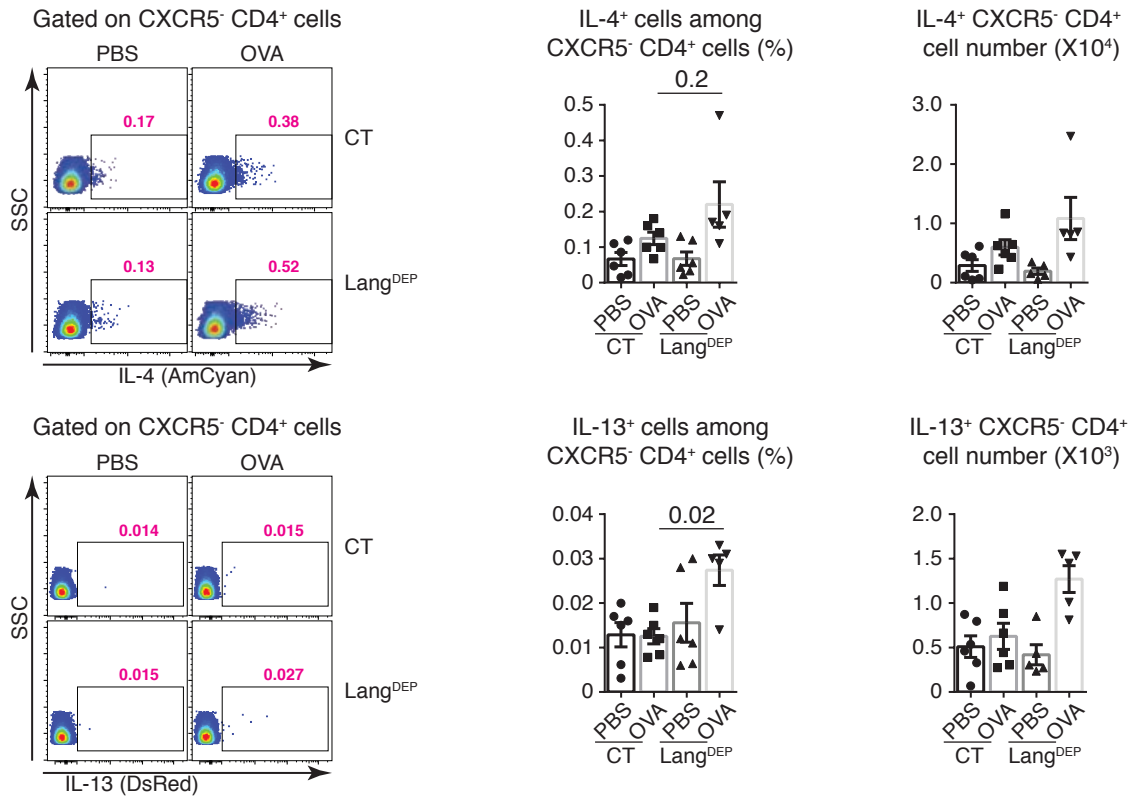
Gated on CXCR5- CD4+ cells
PBS
OVA
0.17
0.38
0.13
0.52
CT
LangDEP
SSC
IL-4 (AmCyan)
IL-4+ cells among CXCR5- CD4+ cells (%)
0.2
IL-4+ CXCR5- CD4+ cell number (X10⁴)
Gated on CXCR5- CD4+ cells
0.014
0.015
0.015
0.027
IL-13 (DsRed)
IL-13+ cells among CXCR5- CD4+ cells (%)
0.02
IL-13+ CXCR5- CD4+ cell number (X10³)

FIG E6.

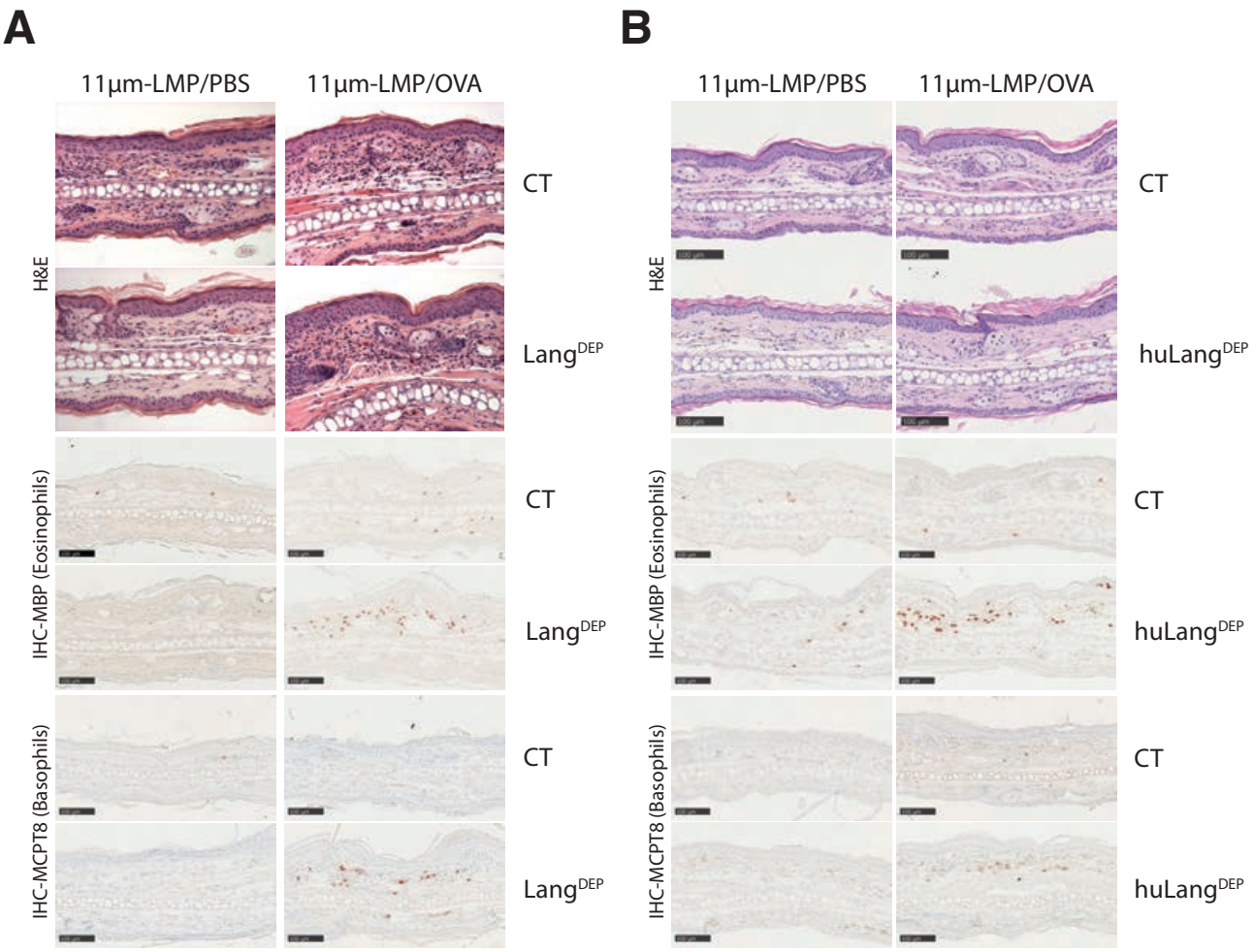
A
11µm-LMP/PBS
11µm-LMP/OVA
H&E
CT
Lang^DEP
IHC-MBP (Eosinophils)
CT
Lang^DEP
IHC-MCPT8 (Basophils)
CT
Lang^DEP
B
11µm-LMP/PBS
11µm-LMP/OVA
H&E
CT
huLang^DEP
IHC-MBP (Eosinophils)
CT
huLang^DEP
IHC-MCPT8 (Basophils)
CT
huLang^DEP

FIG E7.

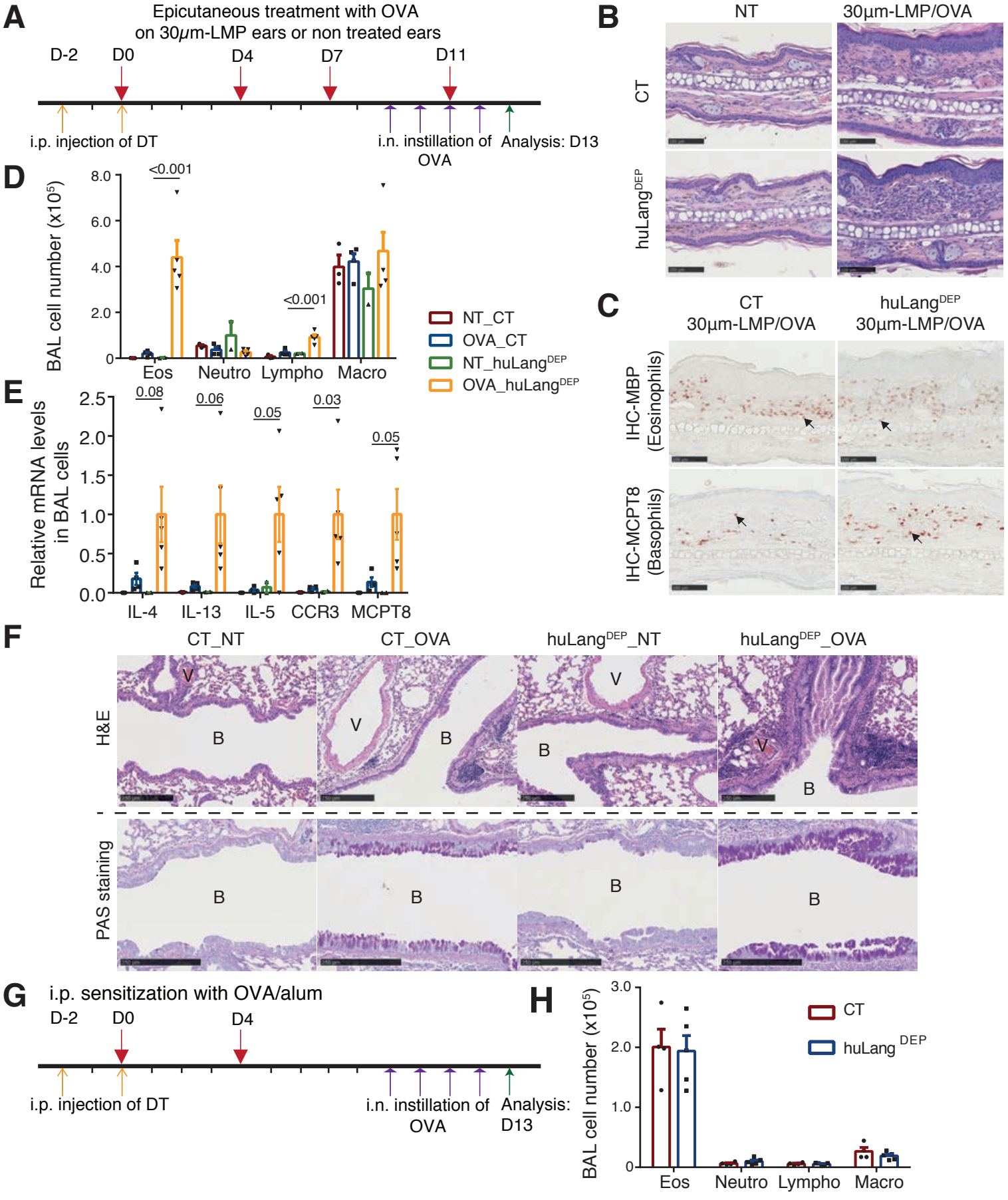
A
Epicutaneous treatment with OVA
on 30µm-LMP ears or non treated ears
D-2
D0
D4
D7
D11
i.p. injection of DT
i.n. instillation of OVA
Analysis: D13
B
NT
30µm-LMP/OVA
CT
huLangDEP
C
CT
30µm-LMP/OVA
huLangDEP
30µm-LMP/OVA
IHC-MBP (Eosinophils)
IHC-MCPT8 (Basophils)
D
BAL cell number (x10⁵)
<0.001
<0.001
Eos
Neutro
Lympho
Macro
NT_CT
OVA_CT
NT_huLangDEP
OVA_huLangDEP
E
Relative mRNA levels in BAL cells
0.08
0.06
0.05
0.03
0.05
IL-4
IL-13
IL-5
CCR3
MCPT8
F
CT_NT
CT_OVA
huLangDEP_NT
huLangDEP_OVA
H&E
PAS staining
V
B
G
i.p. sensitization with OVA/alum
D-2
D0
D4
i.p. injection of DT
i.n. instillation of OVA
Analysis: D13
H
BAL cell number (x10⁵)
CT
huLangDEP
Eos
Neutro
Lympho
Macro

FIG E8.

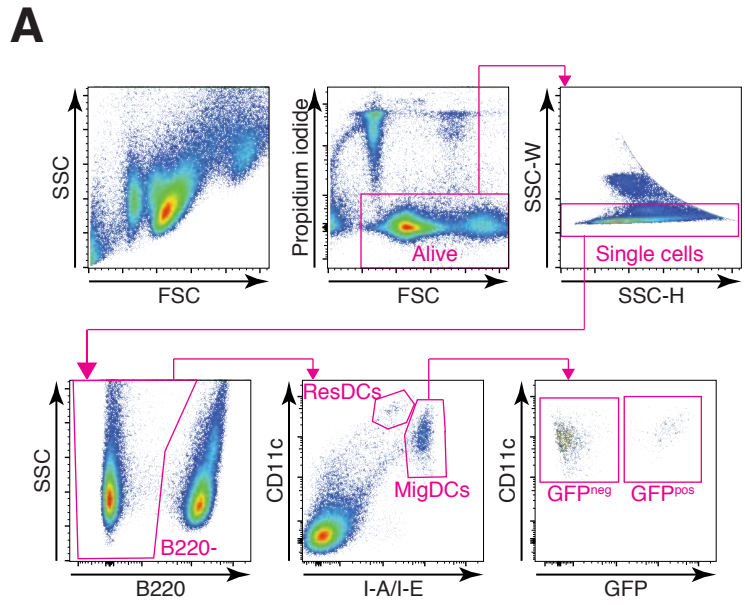
A
SSC
FSC
Propidium iodide
FSC
Alive
SSC-W
SSC-H
Single cells
SSC
B220
B220-
CD11c
I-A/I-E
ResDCs
MigDCs
CD11c
GFP
GFPneg
GFPpos

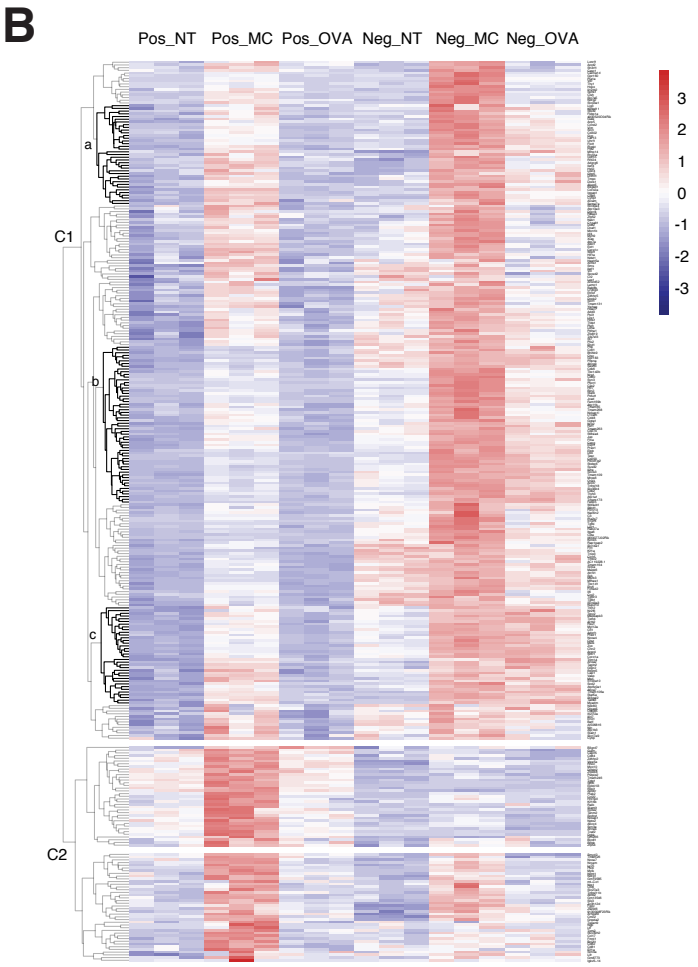
B
Pos_NT
Pos_MC
Pos_OVA
Neg_NT
Neg_MC
Neg_OVA
a
b
c
C1
C2
3
2
1
0
-1
-2
-3

FIG E9.

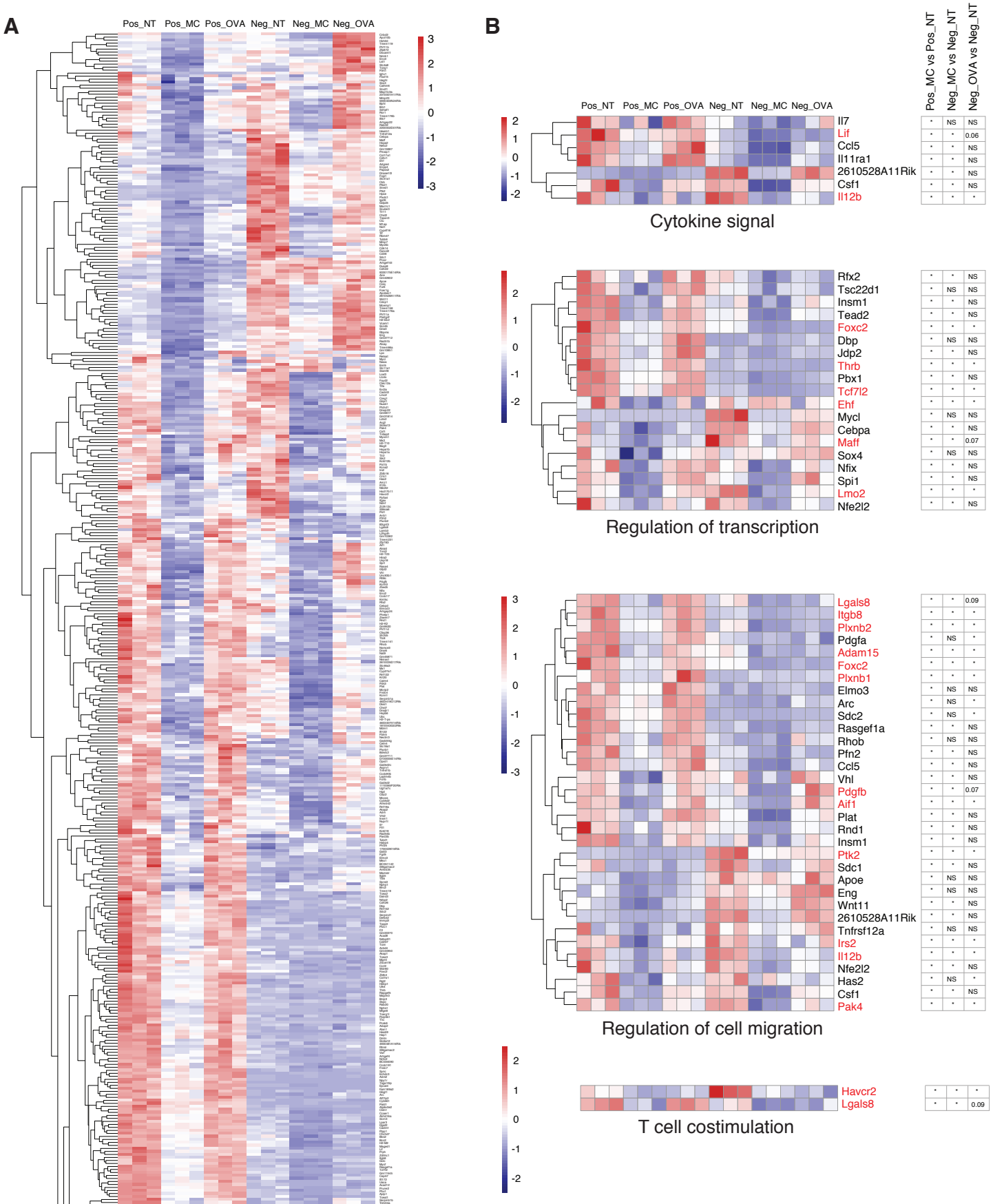
A
Pos_NT
Pos_MC
Pos_OVA
Neg_NT
Neg_MC
Neg_OVA
3
2
1
0
-1
-2
-3
B
Pos_NT
Pos_MC
Pos_OVA
Neg_NT
Neg_MC
Neg_OVA
Pos_MC vs Pos_NT
Neg_MC vs Neg_NT
Neg_OVA vs Neg_NT
Il7
Lif
Ccl5
Il11ra1
2610528A11Rik
Csf1
Il12b
Cytokine signal
Rfx2
Tsc22d1
Insm1
Tead2
Foxc2
Dbp
Jdp2
Thrb
Pbx1
Tcf7l2
Ehf
Mycl
Cebpa
Maff
Sox4
Nfix
Spi1
Lmo2
Nfe2l2
Regulation of transcription
Lgals8
Itgb8
Plxnb2
Pdgfa
Adam15
Foxc2
Plxnb1
Elmo3
Arc
Sdc2
Rasgef1a
Rhob
Pfn2
Ccl5
Vhl
Pdgfb
Aif1
Plat
Rnd1
Insm1
Ptk2
Sdc1
Apoe
Eng
Wnt11
2610528A11Rik
Tnfrsf12a
Irs2
Il12b
Nfe2l2
Has2
Csf1
Pak4
Regulation of cell migration
Havcr2
Lgals8
T cell costimulation

FIG E10.

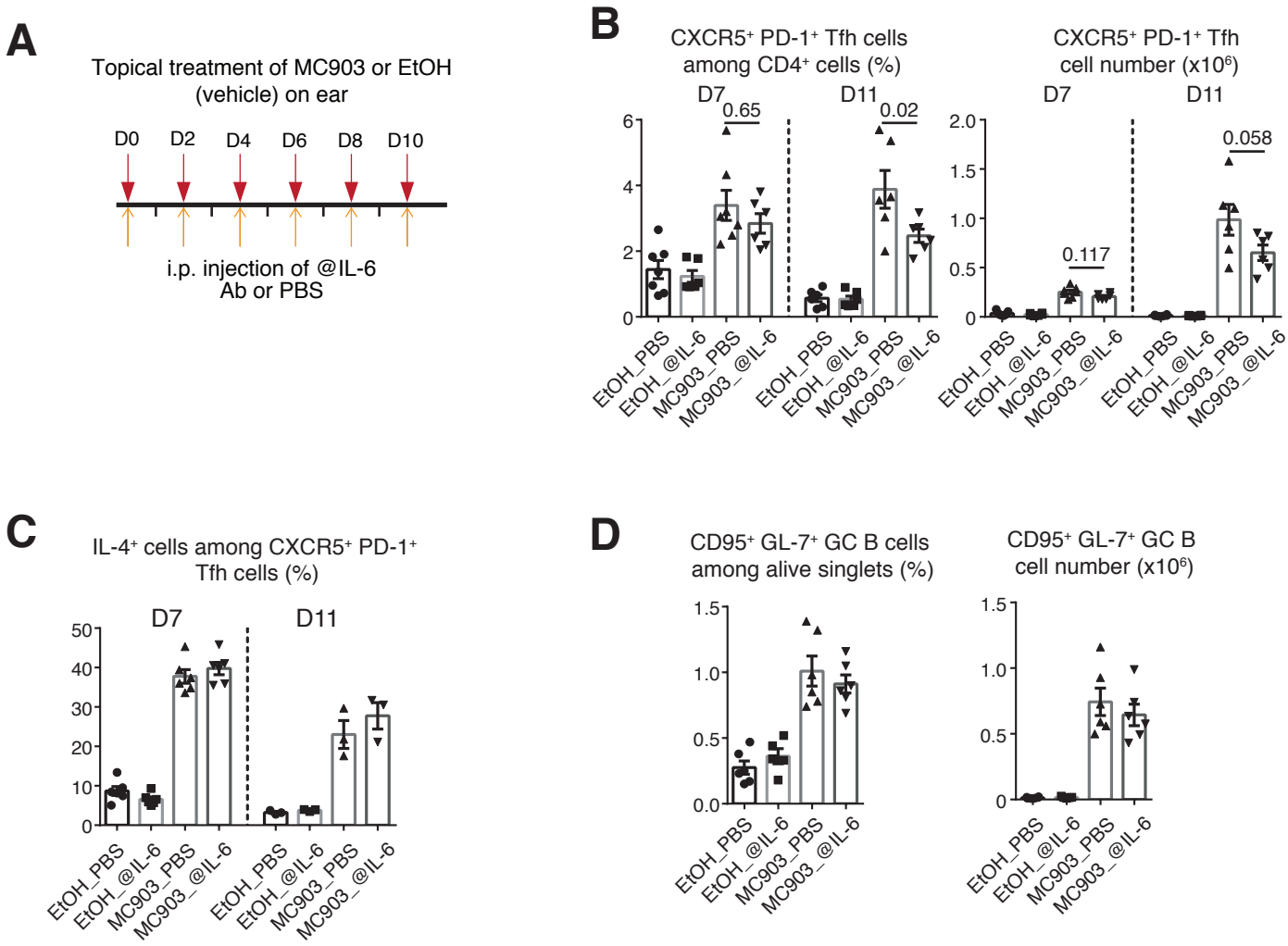
A
Topical treatment of MC903 or EtOH (vehicle) on ear
D0
D2
D4
D6
D8
D10
i.p. injection of @IL-6 Ab or PBS
B
CXCR5+ PD-1+ Tfh cells among CD4+ cells (%)
D7
D11
0.65
0.02
CXCR5+ PD-1+ Tfh cell number (x10^6)
0.117
0.058
EtOH_PBS
EtOH_@IL-6
MC903_PBS
MC903_@IL-6
C
IL-4+ cells among CXCR5+ PD-1+ Tfh cells (%)
D
CD95+ GL-7+ GC B cells among alive singlets (%)
CD95+ GL-7+ GC B cell number (x10^6)

FIG E11.

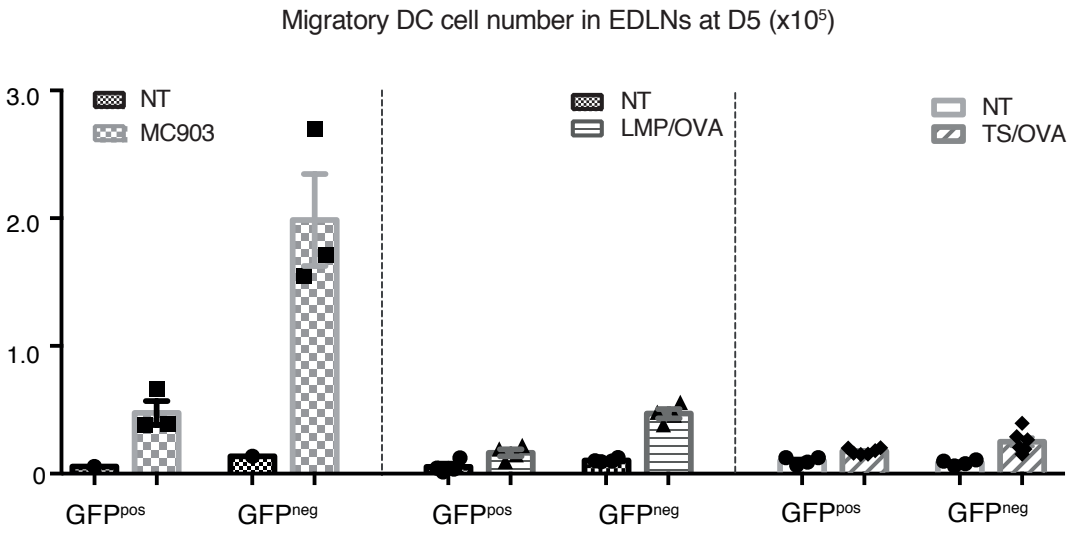
Migratory DC cell number in EDLNs at D5 (x10^5)
3.0
2.0
1.0
0
NT
MC903
NT
LMP/OVA
NT
TS/OVA
GFPpos
GFPneg
GFPpos
GFPneg
GFPpos
GFPneg

FIG E12.

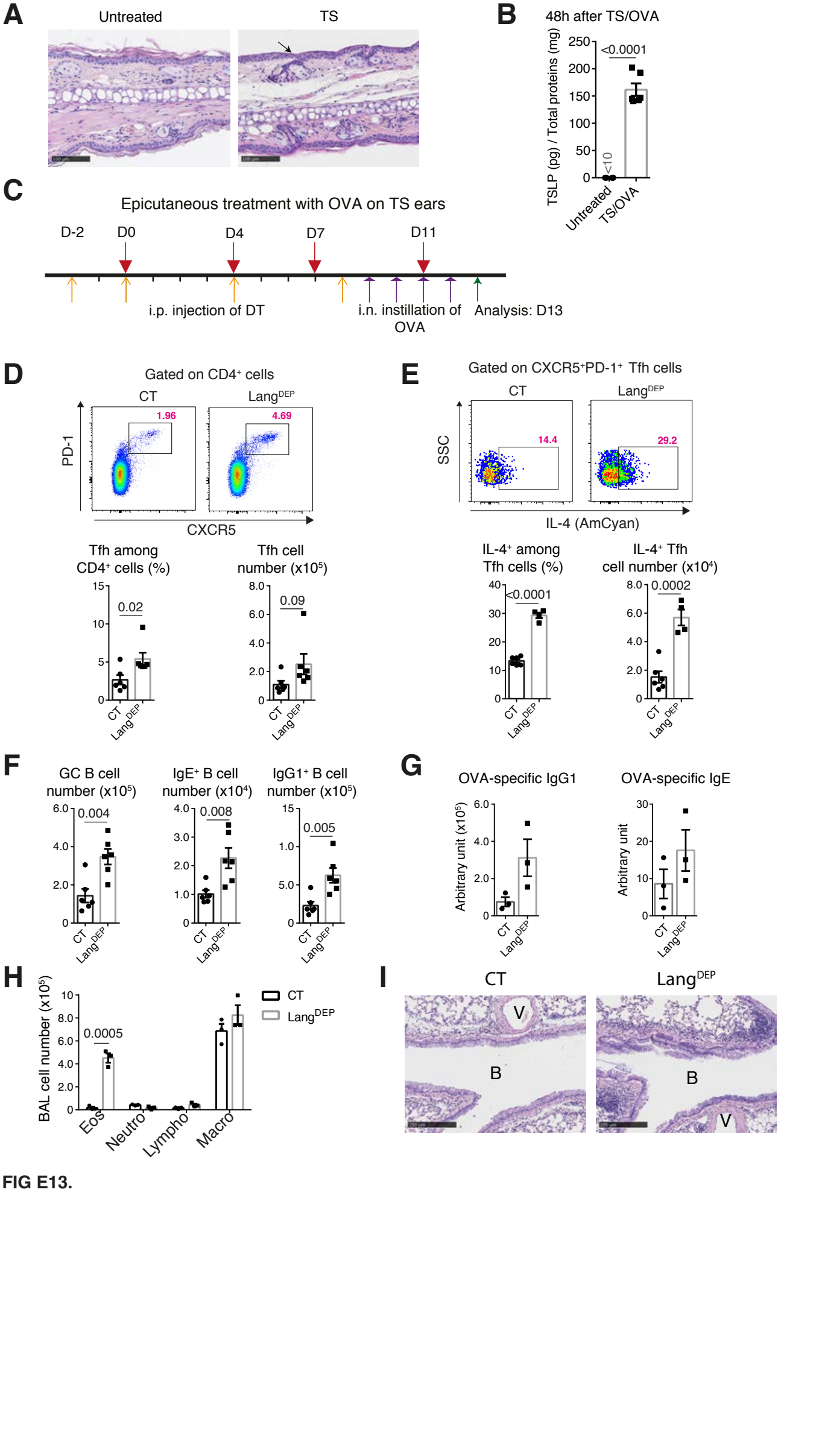
A
Untreated
TS
B
48h after TS/OVA
TSLP (pg) / Total proteins (mg)
<0.0001
<10
Untreated
TS/OVA
C
Epicutaneous treatment with OVA on TS ears
D-2
D0
D4
D7
D11
i.p. injection of DT
i.n. instillation of OVA
Analysis: D13
D
Gated on CD4+ cells
CT
Lang DEP
PD-1
CXCR5
1.96
4.69
Tfh among CD4+ cells (%)
0.02
Tfh cell number (x10^5)
0.09
E
Gated on CXCR5+PD-1+ Tfh cells
SSC
IL-4 (AmCyan)
14.4
29.2
IL-4+ among Tfh cells (%)
<0.0001
IL-4+ Tfh cell number (x10^4)
0.0002
F
GC B cell number (x10^5)
0.004
IgE+ B cell number (x10^4)
0.008
IgG1+ B cell number (x10^5)
0.005
G
OVA-specific IgG1
Arbitrary unit (x10^5)
OVA-specific IgE
Arbitrary unit
H
BAL cell number (x10^5)
0.0005
Eos
Neutro
Lympho
Macro
CT
Lang DEP
I
CT
Lang DEP
V
B

FIG E13.

Methods

Experimental mice. Balb/c mice were purchased from Charles River Laboratory. T*slp*$^{-/-}$ [1], 4C13R$^{Tg/0}$ [2], Langerin^{DTR} [3] and huLangerin^{DTR} [4] were as described and were all backcrossed to >99.9 % Balb/c genetic background. Lang^{GFP} reporter mice [3] were in C57BL/6J background. Breeding and maintenance were performed under institutional guidelines, and all of the animal experiments were approved by the animal care and ethics committee of animal experimentation of the IGBMC.

MC903 topical application. MC903 (Calcipotriol, Sigma) was dissolved in 100% ethanol and topically applied on mouse ears (2 nmol in 25 µl per ear) as previously described [5].

Epicutaneous OVA sensitization and airway challenge. Laser-assisted skin microporation (LMP) was performed using P.L.E.A.S.E.® research system (Pantec Biosolutions) on the dorsal side of mouse ears. For the depth of 30µm (30µm_LMP): 2 pulses per pore, with fluence of 7.5 J/cm2, pulse length of 75 µs, RepRate of 500 Hz and power of 1.0 W; for the depth of 11µm (11µm_LMP): 1 pulse per pore with fluence of 1,8 J/cm2, pulse length of 50 µs, RepRate of 500 Hz and power of 0.7 W. In all cases, the pore array size was set 14 mm and the pore density was set 15%. To induce epicutaneous OVA sensitization, 10 µl of sterile PBS solution containing 200 µg of OVA (Sigma-aldrich) were applied immediately on LMP ear skin at the time points indicated in experimental schemes in the Figures. In case of airway challenge, 25 µL of saline solution containing 50 µg of OVA was intranasally instilled.

Depletion of Langerin^{+} DCs or LCs in mice. Lang^{DTR} or huLang^{DTR} mice were intraperitoneally injected with diphtheria toxin (DT; Sigma-Aldrich) (1 µg per 25 g body weight) at the time points indicated in the experimental schemes in the Figures. The DT-injected wild-type littermate mice were used as controls.

Cell preparation for flow cytometry analyses. For cell preparation from ear-draining lymph nodes (EDLN) for Tfh/GC staining, EDLNs were dissociated with piston, passed through a 70µm strainer

(Falcon) and resuspended in PBS containing 0.5% BSA and 2mM EDTA. Cells were then centrifuged and resuspended in FACS buffer (PBS containing 1% FCS and 2mM EDTA), counted and used for FACS staining. In case of preparation of EDLN cells for DC staining, EDLNs were cut in small pieces and incubated 30 minutes at 37°C in 2mg/mL collagenase D (Roche), 0.25mg/mL DNase I (Sigma) and 2.5% foetal calf serum (Thermofisher) in PBS prior passing through the strainer.

For preparation of dermal cells, ears were split into ventral and dorsal halves and floated 1h at 37°C on a PBS solution containing 4mg/ml Dispase (Gibco). Dermis was subsequently separated from epidermis and incubated 1h at 37°C with 1mg/ml collagenase D, 0.25mg/ml DNase I and 2.5% of foetal calf serum in PBS. Cells were passed through a 70µm cell strainer and resuspended in PBS containing 0.5% BSA and 2mM EDTA. Cells were then centrifuged and resuspended in FACS buffer, counted and used for FACS staining.

Surface staining for flow cytometry analyses. Two million cells were used for antibody staining. Cells were first incubated with anti-CD16/CD32 (clone 93, eBioscience) to block unspecific binding, followed by surface staining with the following antibody panels : CD11c biotin (clone HL3), IgE biotin (clone R35-72), CD95 PE-Cy7 (clone Jo2), CD19 FITC (clone 1D3), CXCR5 biotin (clone 2G8), CD4 Alexa Fluor 700 (clone RM-5), CD4 BV421 (clone GK1.5), streptavidin BV605 were from BD Biosciences; CD8a PerCP-Cy5.5 (clone 53-6.7), B220 APC (clone RA3-6B2), GL-7 PE (clone GL-7), I-A/I-E PE (clone M5/114.15.2) and streptavidin APC were from eBioscience. PD-1 PE-Cy7 (clone RMP1-30), IgG1 PerCP-Cy5.5 (clone RMG1-1) were from Biolegend. Viability staining was performed by adding propidium iodide to a final concentration of 4 µg/mL prior to cell passing with the cytometer. Stained cells were analysed on a Fortessa or LSRII flow cytometer (BD Biosciences). Results were analysed using FlowJo (Treestar).

LN cell culture and antigen stimulation. To identify OVA-specific Tfh cells by activation-induced marker assay [6], one million of freshly isolated EDLN single cell suspensions were cultured in 96-well U-bottom plate in 200µl of medium (RPMI 1640 supplemented with 10% FCS, HEPES, 0.05mM 2-

mercaptoethanol, 100U/ml penicillin, 100U/ml streptomycin), stimulated with 500µg/ml of OVA or PBS (vehicle) for 18h. Anti-CD154 BV650 antibody (clone MR1, BD Biosciences) was added to all culture conditions. After the culture, cells were incubated with anti-CD16/CD32 (Clone 93, eBioscience) to block unspecific binding, and stained with viability dye 506 (eBioscience) and antibody panels: B220 FITC (clone RA3-6B2, Biolegend), CD4 BV421 (clone GK1.5, BD Biosciences), CXCR5 biotin (Clone 2G8, BD Biosciences), Streptavidin PE (eBioscience), PD-1 PE-Cy7 (clone RMP1-30, Biolegend), OX40 APC (clone OX86, eBiosience) and CD25 PerCP-Cy5.5 (clone PC61, BD Biosciences).

RNA sequencing. Migratory DCs from EDLNs were FACS-sorted with ARIA II (BD) (see Fig 8A for sorting strategies). RNA was extracted using RNeasy Micro Kit (Qiagen). RNA-seq was performed in IGBMC high-throughput mRNA sequencing facility. Full length cDNAs were generated from 1ng of total RNA using Clontech SMART-Seq v4 Ultra Low Input RNA kit for Sequencing (Takara Bio Europe, Saint Germain en Laye, France) according to manufacturer's instructions with 12 cycles of PCR for cDNA amplification by Seq-Amp polymerase. Six hundred pg of pre-amplified cDNA were then used as input for Tn5 transposon tagmentation by the Nextera XT DNA Library Preparation Kit (96 samples) (Illumina, San Diego, CA) followed by 12 cycles of library amplification. Following purification with Agencourt AMPure XP beads (Beckman-Coulter, Villepinte, France), the size and concentration of libraries were assessed by capillary electrophoreris. Libraries were sequenced as 50bp single-end reads on an Illumina HiSeq 4000 sequencer.

Reads were preprocessed in order to remove adapter, polyA and low-quality sequences (Phred quality score below 20). After this preprocessing, reads shorter than 40 bases were discarded for further analysis. These preprocessing steps were performed using cutadapt version 1.10. Reads were mapped onto the mm10 assembly of mouse genome using STAR version 2.5.3a. Read counts have been normalized across samples with the median-of-ratios method proposed by Anders and Huber [7], to make these counts comparable between samples. Comparisons of interest were performed using the method proposed by Love et al. [8] and implemented in the DESeq2 Bioconductor library version 1.16.1. P-values were adjusted for multiple testing using the Benjamini and Hochberg method. Gene expression

quantification was performed from uniquely aligned reads using htseq-count version 0.6.1p1, with annotations from Ensembl version 96 and "union" mode. The RNA-Seq data have been deposited in the NCBI's Gene Expression Omnibus (GEO) and are accessible as GSE149039.

Bronchoalveolar lavage (BAL) cell analyses. BAL was taken in anaesthetized mice by instilling and withdrawing 0.5 ml of saline solution (0.9% NaCl, 2.6mM EDTA) in the trachea. After six times lavages, BAL fluid was centrifuged, and BAL cells were counted using a Neubauer hemocytometer. $5x10^4$ BAL cells were cytospined and stained with Hemacolor kit (Merck) to identify macrophages, lymphocytes, neutrophils and eosinophils. After differential counting to obtain their frequencies, the number of each cell type was calculated according to the total BAL cell number and the frequency. For RT-qPCR analyses, RNA was extracted from BAL cells using NucleoSpin RNA XS kit (Macherey-Nagel), reverse transcribed by using random oligonucleotide hexamers and SuperScript IV Reverse Transcriptase (Invitrogen) and amplified by means of quantitative PCR with LightCycler 480 SYBR Green kit (Roche), according to the manufacturer's instructions. Relative RNA levels were calculated with hypoxanthine phosphoribosyl- transferase (HPRT) as an internal control. For analyses of each set of gene expression, an arbitrary unit of 1 was given to the samples with the highest level, and the remaining samples were plotted relative to this value. Sequences of qPCR primers are: Hprt (TGGATACAGGCCAGACTTTG ; GATTCAACTTGCGCTCATCTTA; 161 bp); Il4 (GGCATTTTGAACGAGGTCAC; AAATATGCGAAGCACCTTGG; 132 bp); Il5 (AGCACAGTGGTGAAAGAGACCTT; TCCAATGCATAGCTGGTGATTT; 117 bp); Il13 (GGAGCTGAGCAACATCACACA; GGTCCTGTAGATGGCATTGCA; 142 bp); Ccr3 (TAAAGGACTTAGCAAAATTCACCA; TGACCCCAGCTCTTTGATTC; 150 bp); Mcpt8 (GTGGGAAATCCCAGTGAGAA; TCCGAATCCAAGGCATAAAG; 160 bp).

Enzyme-linked immunosorbent assay (ELISA). To measure TSLP levels by ELISA, mouse skin was chopped and homogenized with a Mixer Mill MM301 (Retsch, Dusseldorf, Germany) in lysis buffer (25 mmol/L Tris pH 7.8, 2 mmol/L EDTA, 1 mmol/L dithiothreitol, 10% glycerol, and 1% Triton X-100)

supplemented with protease inhibitor cocktail (Roche). Protein concentrations of skin extract were quantified by using the Bio-Rad Protein Assay (Bio-Rad Laboratories, Hercules, Calif), and TSLP levels in skin extracts were determined with the DuoSet ELISA Development Kits (R&D Systems, Minneapolis, Minn).

To measure OVA-specific IgG1 and IgE in sera, microtiter plates were coated with OVA and then blocked with BSA. Serum samples were incubated in the coated plates overnight at 4°C followed by incubation with a biotinylated rat anti-mouse IgE (BD Biosciences; clone R35-118) or IgG1 (BD Biosciences; clone A85-1). Extravidin horseradish peroxidase (Sigma) and TMB (tetramethylbenzidine) Substrate Reagent Set (BD Biosciences) were used for detection. Levels of OVA-specific IgG1 and OVA-specific IgE were calculated relevant to a pre-prepared serum pool from OVA-sensitized and challenged mice and expressed as arbitrary units.

Histopathology. Mouse ears and lungs were fixed in 4% paraformaldehyde overnight at 4°C and embedded in paraffin. 5μm sections were stained with hematoxylin & eosin (H&E). For periodic Acid Schiff (PAS) staining, slides were incubated with 0.5% aqueous periodic acid (Alfa Aesar), washed with water and incubated 15 minutes in Schiff's reagent (Merck). Slides were counterstained with hematoxylin and differentiated with acid alcohol.

Immunohistochemistry (IHC). For IHC staining of major basic protein (MBP) and mast cell protease 8 (MCPT8), 5μm paraffin sections were treated with 0.6% H_2O_2 to block endogenous peroxidase activity before antigen retrieval with either Pepsin (for IHC of MBP; Life technologies) or citric buffer (10 mmol/L citric acid, pH 6; for IHC of MCPT8). Slides were then blocked with normal rabbit serum (Vector Laboratories) and incubated overnight with primary antibody (Rat anti-mouse MBP antibody (Mayo Clinic, Rochester); Rat anti-mouse TUG8 (Biolegend)). Slides were then incubated with biotinylated rabbit anti-rat IgG (dilution: 1/300) and treated with AB complex (Vector Laboratories). Staining was finally visualized with AEC high-sensitivity substrate chromogen solution (Dako) and counterstained with hematoxylin.

RNA in situ hybridization. Mouse ears were fixed in formalin and embedded in paraffin. RNA in situ hybridization was performed on freshly 5µm sections using RNAscope® 2.5 HD Reagent Kit-RED (Advanced Cell Diagnostics, Hayward, CA, USA) according to the manufacturer's instructions. Probe Mm-Tslp was used for detection of TSLP (Cat 432741).

Statistics. Data were analyzed using GraphPad Prism 6. Comparison of two samples was performed either by Student's two-tailed unpaired t-test with Welch's correction or the Mann–Whitney rank sum nonparametric test depending on results from the Kolmogorov–Smirnov test for normality. Comparison of more than two samples was performed by ordinary one-way ANOVA followed by Tukey's post-hoc test.

1 Li, M. *et al.* Induction of thymic stromal lymphopoietin expression in keratinocytes is necessary for generating an atopic dermatitis upon application of the active vitamin D3 analogue MC903 on mouse skin. *J Invest Dermatol* **129**, 498-502 (2009).

2 Roediger, B. *et al.* Cutaneous immunosurveillance and regulation of inflammation by group 2 innate lymphoid cells. *Nat Immunol* **14**, 564-573, doi:10.1038/ni.2584 (2013).

3 Kissenpfennig, A. *et al.* Dynamics and function of Langerhans cells in vivo: dermal dendritic cells colonize lymph node areas distinct from slower migrating Langerhans cells. *Immunity* **22**, 643-654 (2005).

4 Bobr, A. *et al.* Acute ablation of Langerhans cells enhances skin immune responses. *J Immunol* **185**, 4724-4728, doi:10.4049/jimmunol.1001802 (2010).

5 Leyva-Castillo, J. M. *et al.* Skin thymic stromal lymphopoietin initiates Th2 responses through an orchestrated immune cascade. *Nat Commun* **4**, 2847, doi:10.1038/ncomms3847 (2013).

6 Jiang, W. *et al.* Identification of murine antigen-specific T follicular helper cells using an activation-induced marker assay. *J Immunol Methods* **467**, 48-57, doi:10.1016/j.jim.2019.02.008 (2019).

7 Anders, S. & Huber, W. Differential expression analysis for sequence count data. *Genome Biol* **11**, R106, doi:10.1186/gb-2010-11-10-r106 (2010).

8 Love, M. I., Huber, W. & Anders, S. Moderated estimation of fold change and dispersion for RNA-seq data with DESeq2. *Genome Biol* **15**, 550, doi:10.1186/s13059-014-0550-8 (2014).